SALT SOLID DISPERSIONS: A FORMULATION STRATEGY TO ENHANCE DISSOLUTION RATE OF POORLY WATER-SOLUBLE IONIC DRUGS

by

ANASUYA A. GHOSH

A Dissertation submitted to the

Graduate School – New Brunswick

Rutgers, The State University of New Jersey

In partial fulfillment of the requirements

For the degree of

Doctor of Philosophy

Graduate Program in Pharmaceutical Sciences

Written under the direction of

Professor Tamara Minko, Ph.D.

And approved by

_____

_____

_____

_____

New Brunswick, New Jersey

October, 2012

ABSTRACT OF THE DISSERTATION

SALT SOLID DISPERSIONS: A FORMULATION STRATEGY TO ENHANCE DISSOLUTION RATE OF POORLY WATER-SOLUBLE IONIC DRUGS

By ANASUYA A. GHOSH

Dissertation Director:

Professor Tamara Minko

Improving oral bioavailability of poorly water-soluble drugs remains one of the most challenging aspects of drug development. Pharmaceutical salt formation is a widely accepted approach to improve dissolution rate of poorly water-soluble ionic drugs. Nevertheless, the salt formation process is often empirical and may not always lead to desired end product profile. Alternatively, pH-modifiers have been used as formulation components for such compounds. The purpose of this study is to explore the synergies between pH modulating ability offered by a salt form and the dissolution enhancement offered by an amorphous solid dispersion. The hypothesis of this study is that for a weakly basic drug, its solid dispersion with a hydrophilic polymer and a salt-forming acidic counterion should provide dissolution enhancement similar to that of a solid dispersion of its salt. Secondly, for a weakly basic drug if a salt form with a selected counterion cannot be synthesized, then solid dispersion of the drug, the non-salt forming

counterion and a hydrophilic polymer could also provide adequate dissolution enhancement. In the present investigation the dissolution enhancement of Cinnarizine, a weakly basic drug, is studied from its solid dispersions containing acidic counterions (organic acids) that have varying ability to form cinnarizine salts. The effect of adding ionic polymers as pH-modifiers is also investigated. Solid dispersions were prepared using melt extrusion technology. Molecular interactions between relevant functional groups of drug and pH-modifiers and the possibility of *in situ* salt formation during the melt extrusion process were explored. The results of this study systematically offer the benefits of adding acidic counterions during melt extrusion, should a classical salt formation technique fail. A predictive computational model was used to estimate human *in vivo* plasma profiles by using *in vitro* dissolution of the developed solid dispersions and the marketed product.

DEDICATION

To my wonderful parents,

My mother who by her simple thoughts and actions has been my anchor

My father who has always instilled perseverance in me

To Madhav, my husband and best friend,

Who has shown me life to be filled with infinite possibilities

To my precious daughters, Rhea and Risha,

Who by being a part of me have given me the reason to accomplish my goal

ACKNOWLEDGEMENTS

It is difficult to express in words the deep sense of gratitude that I have for my respected advisor, Dr. Tamara Minko. Her scientific curiosity, assertiveness at every critical step, generous encouragement and patience has made this thesis possible. She has become a role model for me not only as she is an excellent mentor but also as a successful career woman. I would like to thank her for teaching me to make every challenge an opportunity be it in the field of science or life.

I would like to thank my committee members Dr. Michniak and Dr. You for their time and suggestions which enabled me to advance my research. I am grateful to Dr. Erika Zannou, my committee member and a colleague at Novartis, for her guidance and her sound advice on how to handle difficult tasks.

To pursue my graduate studies part-time while having a full-time position in Novartis Pharmaceuticals has been one of the most arduous tasks for me. I am indebted to Dr. Yatindra Joshi, for providing me the opportunity to pursue graduate studies during my professional career. I am very thankful to Dr. Colleen Ruegger for her unflinching support throughout the tenure of my doctoral studies.

Colleagues from Dr. Minko's lab, Vatsal Shah, Dr. Min Zhang and Dr. Seema Betigeri have always been flexible to help me out at any time. I am grateful to Hui Pung for her patience and assistance in resolving any logistic issues to help my progress in the

program. My sincere thanks to many of my Novartis colleagues for their help. I am thankful to my friend, Sonali Bose, for all the moments of encouragement and laughter we have shared during our Ph.D. journey.

I am forever grateful to my parents, Dr. Ashok and Sutapa Ghosh, for their unconditional love, tenacious perusal and strong belief in me which helped me to finish my research. Thanks to my brother, Arka, who always makes me feel so capable. I thank my parents-in-law, Murthy and Girija Vasanthavada, for their constant motivation. Keshav, my brother-in-law and Sruthi, his wife but more like my sister, deserve a special thank you.

I am grateful to Ms. Marleen Rocca, as due to her presence I could spend countless evenings and weekends pursuing my studies with a peaceful mind that my daughters are in good hands.

I am very fortunate that I have good friends who have always supported me in every way!

My Ph.D. days have been even more exciting as I could share it with my loving husband. He has been a sounding board for my thoughts, a helping hand when I needed the most, and a source of cheer to bring back the smile.

To my bright stars, Rhea and Risha, thanks for everything that you had to do without Mommy being around. I am thrilled by the thought of spending so much more time now on with you two!

Last but not the least; I thank the good God for blessing me to achieve this dream.

TABLE OF CONTENTS

LIST OF TABLES

LIST OF FIGURES

1 INTRODUCTION

Over the last 15 years, despite increasing Research and Development (R&D) spend; overall R&D performance has not increased much. The number of new molecular entities (NMEs) approved by the Food and Drug Administration (FDA) fell from a high of 53 in 1996 to 36 in 2004, and to only 18 in 2010. Decline in NME approvals cannot be attributed only to the stringent hurdles set by FDA in the post-Vioxx era. The number of New Drug Applications (NDA) submitted by pharmaceutical companies has been a major contributor to poor drug approvals. Only 23 applications were submitted to the FDA in 2010, a number significantly down from 37 in 2009 and 45 back in 1998[1]. A variety of hypotheses have been floated by the industry experts to reason the obvious question: Why did the R&D productivity come down? Regardless of the reason, it has become clear that for pharmaceutical development to be productive, it has to churn out products that are even more potent, that have far fewer side effects and that demonstrate superior bioavailability.

To address the first two aspects: enhanced potency and safety, scientists have well leveraged recent advancements in the field of combinatorial and computational chemistry. Thousands of arrays of molecules are engineered and synthesized to evaluate for their site specificity and structure-activity in the biologic system[2,3]. But as a result, such molecules become lipophilic and consequently demonstrate very poor solubility in the gastro-intestinal (GI) fluids thereby making the third criteria of bioavailability, hard to achieve. Striking a good balance between making a drug molecule potent thereby

hydrophobic, and at the same time water-soluble (hydrophilic) in the pH of GI fluids has not been an easy task. Indeed, one report states that the overall attrition rate for developing a drug is about 10,000:1 – implying that for every 1 NME approved, some 10,000 entities are characterized during the chemical profiling in drug discovery[4]. A large fraction of attrition occurs at the interface between the drug discovery and product development groups. In the latter group, physico-chemical properties of drug substance are augmented to enhance drug dissolution and product stability. More than one-third of all the drugs listed in the U.S. Pharmacopoeia fall into the poorly water-soluble category[5], and the trend is not getting any better, making things difficult from a product development perspective. Majority of the drug molecules recently entering into the development pipeline have intrinsic solubility of less than 1 μg/mL when compared to 100 μg/mL a decade or so ago. In general, it is acknowledged that some 40% of molecules entering the pharmaceutical industry pipeline are poorly water-soluble, and that their limited oral absorption has often led to failures in clinical trials[6,7,8]. In order to deliver clinically effective and differentiated products, drug development scientists are grappling with multiple formulation approaches to design products with improved drug dissolution rate[9]. The underlying premise for such a strategy being that improving drug dissolution rate will lead to enhanced bioavailability and consequently a superior clinical performance [10].

Various techniques have been utilized to improve solubility and dissolution rate of poorly soluble drugs. Salt formation is the most common one, especially for “small molecules” (i.e., molecules with molecular weight less than 500Da) that have an ionizable group[11].

A pharmaceutical salt is a newly engineered molecule produced by chemically fusing two moieties: the active drug molecule, which is either weakly acidic (or basic), and a corresponding basic (or acid) counterion. Typically, counterions are small inorganic molecules (e.g., sodium, potassium, hydrochloride, phosphate ions) or small organic molecules (e.g., di- and tri-carboxylic acids to form citrate, tartarate, succinate, or other stronger ions such as mesylate, or edisylate). One theory for dissolution enhancement is that pharmaceutical salts adjust the pH of micro-environment during drug dissolution such that more of the drug dissolves in the diffusion layer surrounding drug particle, and hence more drug dissipates into the bulk medium. Counterions play a significant role in manipulating pH of diffusion layer to increase salt solubility and dissolution rate. For example, hydrochloride salt of a weakly basic anti-malarial drug almost doubled free base solubility in water. When organic salts of the same drug were prepared, it was found that lactate salt was some 200 times as soluble as the hydrochloride salt[12]. Differences in solubilities were attributed to differences in the pK_a of counterions. There are other similar examples cited in the literature where different counterions have altered solubilities to varying levels[13,14,15] and researchers have postulated that besides pK_a of counterions, melting point of the counterion, its size, and charge of the counterion explain the differences in solubility among various salts for a given drug[16]. It is hence not a straight forward "pick-and-go" exercise to select a counterion that offers high aqueous solubility. Further, different counterions used in salt formation may exhibit varying toxicity profile. Hence, it is essential to view counterion selection process more holistically to strike the right balance between safety and solubility. Furthermore, even if the right counterion is identified during miniature-scale screening studies, salt synthesis

in itself is a process that needs to be well designed and controlled. Any contamination or presence of foreign particles, abrasion in reactor vessels, etc., can potentially "seed" salt formation process leading to unwanted salt form. Furthermore, it is not uncommon to see that a salt achieves inferior dissolution rate and consequently bioavailability because of its conversion to the poorly soluble acidic or basic free form of the drug[17].

One formulation approach that has been evaluated for more than two decades, and one that circumvents hurdles seen with pharmaceutical salts, is solid dispersions[18]. In solid dispersions, the active ingredient is molecularly dispersed in a water-soluble polymer. During dissolution, as the polymer dissolves, it releases the drug as very fine particles. The higher surface area of the finely dispersed drug enhances its dissolution rate. In addition to polymers, surfactants and lipids have been used in solid dispersions to enhance bioavailability[19]. Increase in drug solubility and dissolution rate has also been attributed to enhanced wettability, reduced agglomeration, and formation of amorphous structure within the solid dispersion[20,21].

Although solid dispersions have proven valuable for poorly soluble drugs, they have demonstrated limited dissolution enhancement for pH-dependent soluble drugs[18.] While solid dispersion technology has been well studied in literature for over two decades, surprisingly, there is limited knowledge on the impact of incorporating organic acids as a pH modifier component in the solid dispersion of poorly soluble ionic drugs[22].

To summarize, on the one hand, pharmaceutical salts offer significant dissolution enhancement although the process of isolating desired salt is often empirical. Solid dispersions, on the other hand, offer dissolution enhancement by molecularly dispersing drug in a water-soluble polymer. However, there are limited reports in the literature on the use of solid dispersions for drugs that exhibit pH-dependent solubility. The purpose of this study is to explore synergies of the above two formulation approaches. Specifically, we believe that if a desired salt form of a weakly basic drug cannot be synthesized, then a molecular solid dispersion of the drug and acidic counterion should provide dissolution enhancement similar to that of a solid dispersion of its salt. The impact of adding pH-modifiers on the physical structure and dissolution performance of poorly soluble weakly basic drug: Cinnarizine, from its solid dispersion is examined.

Key questions that will be addressed are as follows:

a. What is the impact on dissolution rate by adding counterion, for example a weak organic acid, to solid dispersion of weakly basic drug and a neutral polymer?
b. Will the weak organic acid interact with the basic drug to form *in situ* salt during melt extrusion process?
c. How would the solubility and dissolution rate of such a salt solid dispersion compare with dissolution rate of the pure salt, if the salt is successfully isolated?
d. What are the critical factors for modulating the microenvironmental pH (i.e. solubility and acidity of the organic acid) in solid dispersions prepared using melt extrusion?
e. What is the effect of addition of ionic polymers as pH modifiers?

2 BACKGROUND AND SIGNIFICANCE

2.1 Theory of drug dissolution

For over decades, several different approaches have been used to improve dissolution rate of poorly soluble drugs. Formulation approaches can be broadly categorized as those that modify drug substance in the dosage form, either physically or chemically, to make it more soluble, and those that modify the environment surrounding the drug particles during dissolution. Whatever the approach be, the fundamental principles that guide dissolution process and help evolve formulation development, have been around for several decades now.

Back in 1897, Noyes and Whitney conducted the very first set of studies to understand physics of drug dissolution[23]. Many other researchers soon contributed to Noyes Whitney's findings to elucidate the mechanism of drug dissolution. Equation (1) and the illustration below describe the dissolution process.

$$\frac{dc}{dt} = \frac{D \cdot S \cdot (Cs - C_b)}{V \cdot h} \qquad \text{Eq 1}$$

in which, D the diffusion coefficient of the solute in solution, S the surface area of the exposed solid, h the thickness of the diffusion layer, Cs the intrinsic solubility of the solid and C_b the concentration of solute in bulk solution at time t. The dissolution rate is denoted as dc/dt with V being the volume of solution.

According to Nernst and Brunner diffusion layer model the outermost layer of the solid drug dissolves instantaneously into a thin layer of solvent to form a saturated solution, and the transfer of the dissolved compound to the bulk solution occurs by the diffusion of the drug molecules through this layer (Fig.2.1).

Noyes and Whiney suggested that the rate at which drug dissolves is directly dependent upon the differences between drug concentration at the dissolving surface and in the bulk. It is directly dependent upon the surface area of the dissolving particle, and is inversely dependent upon the thickness of diffusion layer surrounding the drug particle. Experimental evidence provided by Noyes-Whitney, and by others, has proved instrumental in designing improved pharmaceutical formulations for the past decades. Drug candidates have been either physically or chemically modified to improve their water solubility. Techniques include reducing drug particle size to increase surface area of the dissolving solid[24]; forming water-soluble pro-drugs by chemically conjugating drug molecule with a water-soluble moiety wherein parent drug is released after dissolution[25]; forming physical complex of drug and a water-soluble agent such as cyclodextrin; and forming a high-energy, highly soluble amorphous form of a crystalline drug[18]. The basic mechanism is to enhance drug solubility, which helps to increase drug concentration gradient between the drug surface and the bulk media and enhances dissolution rate.

Another key deduction from Noyes Whitney's model is the importance of the microenvironment layer surrounding the dissolving drug particle. Dissolution issues may

often arise due to poor wettability of drug; hostile pH conditions that prevent drug ionization and dissolution; super-saturation and precipitation of drug in microenvironment layer. To circumvent such issues, a wetting agent or a surfactant is sometimes added to the formula to enhance wetting in the micro-layer and increase drug dissolution. In other instances, co-solvents solubility enhancers aid to prevent drug crystallization in the micro-layer. But issues with wettability and micro-layer solubility are relatively uncommon when compared to pH related issues. Nearly two-thirds of all pharmaceutical active ingredients are electrolytic. Hence, ensuring pH in the microenvironment layer that is conducive to drug ionization, and consequently dissolution is important.

2.2 Pharmaceutical salts: Fundamental benefit

The concept of pharmaceutical salts for solid dosage form was demonstrated by Nelson as early as in the 1950s. He found that dissolution rates of salt forms of several weakly acidic compounds under GI pH conditions were much higher that those of their respective free acid forms[26]. He postulated that an increased dissolution rate was the result of the higher solubility of salt (compared to the free acid) into the pH-adjusted (alkali) micro-layer surrounding the drug. Many scientists later developed evidence to support the conception that pH in the microenvironment surrounding drug substance plays a main role during dissolution of an ionizable drug. Pharmaceutical salt formation is one of the widely accepted approaches that helps in regulating microenvironment pH and significantly enhances drug dissolution. Equilibrium solubility is defined as the

concentration of the dissolved drug in a saturated solution where the solute is in equilibrium with its solid phase at a given temperature. For non-ionizable drugs, the solubility is independent of solution pH. In other words, of the many factors that impact equilibrium solubility such as temperature, solid's crystal packing, its lattice energy, amorphous state of solid, etc., pH of solution is irrelevant. The solubility of an ionizable drugs, on the other hand is pH-dependent[27]. The ideal goal would then be to identify pH where equilibrium solubility of drug is the highest, and subsequently design a dosage form such that pH in the diffusion comes close to pH at which drug solubility, and consequently drug dissolution, is the highest. But how can one identify what that ideal pH is? Even if found, how can one manipulate the dosage form to mimic such a pH during drug dissolution?

2.2.1 pH-Solubility profile

Several techniques have been reported in the literature to measure equilibrium[28,29] solubility, and pH-solubility profiles of ionic drug[30]. One widely used method as summarized by Pudipeddi et. al. is the 'saturation shake-flask' method. In this method, saturated solutions of a free acid, base, or salt are prepared by shaking an excess of the solid with an appropriate volume of deionized water at a controlled temperature. Solubilities at various pH values are determined by stepwise titrations of the suspension with a relatively strong acid or alkali. After each addition, equilibrium is re-established by agitation. The pH of the suspension is measured, and the supernatant solution phase is separated from the excess solid by filtration or sedimentation. The supernatant is then

analyzed for the total solute concentration. The process is continued until the entire pH-solubility profile is obtained.

One drawback of saturation shake-flask method is that the ionic strength, i.e., the concentration of all ionized species, is not controlled. pH values can easily fluctuate as solid dissolves in the solution state and has to be closely monitored. As an alternate method, buffer solutions of a suitable ionic strength have been used to maintain desired pH conditions[31,32,33] and the solid is agitated to attain equilibrium. However, depending on the pH strength of dissolving solid, inadequate buffer capacity, and suppression of drug solubility due to ionic-strength effects have been noticed when buffers are used to control pH. Sometimes, salt formation may happen with the buffer species used. It is crucial to conduct analysis on the excess solid state to ensure that solubility is being measured with respect to the actual drug in free acid or base or salt form, and not to any polymorph or hydrated form. Typically, a calorimetric study or X-ray diffraction measurement should help identify the nature of the 'excess solid'.

2.2.2 Theory of pH-dependent solubility

Solubility of an electrolyte at a given pH is described by the sum of concentration of its ionized and un-ionized species. In 1923, Bronsted in Copenhagen and Lowry in London independently proposed parallel theories to define an acid and base. An acid is a substance that is capable of donating a proton, and a base is a substance that is capable of

accepting a proton from an acid. According to this theory, ionization of a weakly acidic drug substance [HA] in water may be written as:

$[HA] + H_2O \leftrightarrow H_3O^+ + [A^-]$ Eq 2

Similarly, for a weak base, the reaction may be expressed as:

$[B] + H_3O^+ \leftrightarrow [BH^+] + H_2O$ Eq 3 or

$[B] + H_2O \leftrightarrow OH- + BH+$ Eq 4

where HA is the weak acid, A^- is the dissolved, ionized state of weak acid. B is the weak base, BH^+ is the dissolved, ionized state of weak base. Brackets indicate concentration.

According to Bronsted-Lowry, HA reacts with water to donate a proton and release hydronium ion. As can be seen in Eq 2, if one adds more acid (or H_3O^+), the equilibrium shifts to the left, leaving larger fraction of the un-dissolved acid. In other words, solubility of weak acid reduces if acid is added to its supersaturated solution. Similarly, if more alkali is added, hydroxyl group [OH^-] from the alkali reacts with H_3O^+ and drives the equilibrium forward releasing more of the dissolved weak acid [A^-].

In the case of weakly basic drug, the process is the opposite. When acid is added, H_3O^+ reacts with solid [B] to drive the reaction forward and form solubilized [BH^+] at lower

pH values. Likewise, addition of alkali precipitates the weak base. The acidity of a weak acid or basicity of a weak base is the extent to which an acid gets dissociated. It may be derived from Eq 2 as:

$$K_a = [H_3O^+] [A^-] / [HA] \qquad \text{Eq 5}$$

Often, pK_a, which is the negative logarithmic value of K_a, is used to describe acid strength. pK_a has important implications in salt formation, as it is typically the value above which a weak acid gets ionized, and below which a weak base is ionized. Most of the strong acids have very low or negative pK_a values indicating that in the normal pH range, these acids are 100% ionized and release H_3O+ ions. Similarly, a strong base has very high pK_a values (or very low pK_b values), indicating that below such high pK_a value a base can readily accept proton.

Kramer and Flynn demonstrated that the pH-solubility profile of a basic drug (Fig.2.2) may be expressed by two independent curves, one where the free base is the saturation or equilibrium species and the other where the salt is the equilibrium species[34]. Directional trend in solubility in phase I can be expressed by reviewing Eq 3, where solubility of free base increases with increase in H_3O^+, or a decrease in pH. Solubility curve may be expressed by the following equation:

$$S_{T,\,base}\,(pH>pH_{max}) = [B]_s + [BH^+] = [B]_s(1+ H_3O^+/K_a) \qquad \text{Eq 6}$$

where S_T is the total solubility of ionized and un-ionized species, pH_{max} is the pH where total solubility is the highest, and $[B]_s$ is the solubility of equilibrium free base.

Solubility curve in phase II for the salt can the expressed as:

$$S_{T,\,salt}\ (pH<pH_{max}) = [BH+]_s + [B] = [BH+]_s(1+ Ka/H_3O+) \qquad \text{Eq 7}$$

The two independent curves (Eq 6 and Eq 7) intersect at a common pH value, which is the pH of maximum solubility. If the solid phase that is in equilibrium with solution is analyzed, it would be free base at $pH > pH_{max}$, and would be a salt at $pH < pH_{max}$. In other words, if the pH of a saturated solution with excess solid free base is lowered to values below its pKa and pH_{max}, the solid phase will convert to the salt. As pointed by Serajuddin ATM[11], the pH will not drop below pH_{max} until enough acid is added to convert the entire excess free solid base into salt. Implications of the above are clear. For a salt formation to occur, the counterion must be such that the pH of combined solution should drop to values below pH_{max}. To form salt of a weak base, if the counterion is so weak that pH cannot be lowered to below pH_{max}, then salt formation will not occur. As shown in Fig.2.3, the converse is true for the conversion of a free acid to the salt in that the counterion must be sufficiently basic that pH is greater that the pH_{max} value[35].

Based on the interdependencies between pH, the extent of ionization, and salt formation, it is generally regarded that for a salt formation to occur between a weak base and an acidic counterion, pK_a of the acid should ideally be at least two units below the pK_a of the

weak base. In such an event, the acidic counterion exhibits sufficient strength to lower pH values below pH_{max}, thereby ionizing the weak base and enabling salt formation.

But simply selecting a counterion that has pK_a two units below free base pK_a does not guarantee salt formation. While pH-dependent solubility profile is a pre-requisite for salt formation, there are numerous reports in the literature demonstrating that salt formation is a complex chemical process dependent upon multiple factors that affect nucleation and crystallization of appropriate salt[36,37].

Although multiple different counterions are available for salt formation, the actual frequency of their use for salt formation is disproportionately skewed to only a hand-full of counterions. Bowker and Stahl compared the frequency of usage of salt formers reported in 1977 by Berge et.al. and in 1998 by Stahl et.al.[14]. As seen from Table 2.1 and 2.2, the pattern in usage of salt formers is surprisingly similar even after 20 years of progress in development of pharmaceutical salts. This draws for an interesting observation. On the one hand, more than two-thirds of all pharmaceutical compounds have ionizable groups; a vast majority of them have pH dependent solubility, indicating a strong potential to form salts with variety of agents. Yet, on the other hand, despite the abundance of counterions as well as free acids and free bases, almost 50% of all salts of weak bases are reported to be hydrochloride salt; and more than 50% of all salts of weak acids are reported to be sodium salts. Such a disproportionate distribution of salts underscores that salt selection and formation is not a straight forward process. The fact that there is a long tail in distribution, i.e., that all other salt formers have <10%

prominence suggests that that many of the salt candidates could not (a) be successfully isolated as a stable crystalline salt; and/or (b) pass the rigorous levels of physic-chemical testing during product development.

2.2.3 Salt screening and synthesis

Salt preparation techniques have made significant progress over the recent years with teams of chemists from discovery to chemical process development working to optimize process parameters to isolate desired salt form in a controllable and scalable manner. In order to maximize the number of leads, scientists first work on miniature scale using microplate technique for salt screening. As described by Bowker and Stahl[16], usually, a small amount (50 mg) of sample is dissolved in suitable volatile solvent and a fixed volume of this stock solution, representing 0.5 mg of drug substance, is added into each of micro-plate well. Then, stock solution of each potential salt former is prepared and a few microliters of each are added in specific molar proportion sequentially to each well. Eventually, all wells in the micro-plate are filled with solutions of samples and counterions. Different, potential crystallizing anti-solvents are then added along the y-axis to systematically precipitate salts. Sometimes, crystallization can be promoted by evaporation of any excess solvent in some wells using a slow stream of dry nitrogen gas. The wells are inspected at periodic intervals for the appearance of crystals using an inverted microscope or other suitable technique. Once the combinations of counterion and solvent(s) are identified, studies at incrementally larger scale (usually 10-50 mg to up

to 500 mg) can be initiated to confirm suitability and viability of crystalline salts produced.

Conducting experiments in micro-plates offer multiple benefits in terms of higher speed, ability to evaluate multiple solvent systems with convenience, greater efficiency, while saving cost and improving productivity. Use of organic solvent also helps to lower dielectric constant of the solvent system, thereby reducing solubility of salt, and enabling salt crystallization and isolation from solvents.

There are however, a few drawbacks to this technique. Firstly, failure to produce salt on a miniature scale in the solvent system combination chosen may not be indicative that salt cannot be formed at larger scale. So, many potential salt formers may be filtered out early on. Secondly, due to kinetic nature of salt formation, multiple factors including rate of solvent addition, nucleation and crystal growth, rate of evaporation play a role in forming crystalline salt - a micro-plate may not be able to mimic large scale condition. Finally, pH shifts and extent of ionization seen in organic solvents upon addition of counterion may be different from shifts seen in aqueous conditions, and that it may impair ability of a potential salt former to react with a drug. On the contrary, sometimes, because of the reduced solubility of salt in organic solvents, salts that would not have formed in aqueous conditions may be isolated. This may be misleading because such salts might de-protonate into its free unionized form when in contact with aqueous media, thereby rendering the salt of less use. Nonetheless, above described micro-well plate method is widely used and major pharmaceutical companies have invested heavily in automating

salt selection process. Once a salt form is successfully isolated in crystalline form, its manufacturing is scaled-up to a few gram levels. Depending on the amount of material available for testing, a battery of tests is conducted before declaring a candidate ready for further development[38]. Fig.2.4 highlights some of the frequently conducted tests to characterize salt form.

2.3 Pharmaceutical solid dispersions

In the last 10-15 years, the number of poorly soluble drugs synthesized through combinatorial and computational chemistry has been on the rise. Majority of the drug molecules recently entering pharmaceutical pipeline have intrinsic solubility of less than 1 μg/mL when compared to 100 μg/mL of the yesteryears. Pharmaceutical salts in general have multiple hurdles to overcome as described in the section 2.2.

As early as in 1961, Sekiguchi et. al. demonstrated that eutectic mixtures of sulfathiazole had superior absorption in humans when compared to ordinary sulfathiazole[39]. Later again in 1964, they showed fused conglomerates of chloramphenicol and urea to have superior absorptions in rabbits[40]. The authors attributed enhanced drug absorption to the formation of eutectic mixtures of drug with water-soluble carriers. Once the carrier dissolved, it released the drug as fine particles that led to its faster absorption. Goldberg et. al., later in 1966 attributed increase in gastrointestinal absorption to increase in drug dissolution rate from solid dispersions. They demonstrated that solid solution and eutectic mixtures of acetaminophen-urea, and griseofulvin-succinic acid showed higher

dissolution rate and absorption profiles compared to their respective physical mixtures[41,42]. The authors argued that certain fraction of drug was molecularly dispersed in the carrier, while other portions were embedded as pockets of amorphous material. Building on these findings, Chiou and Reigelman in 1971 described solid dispersions as the dispersion of one or more active ingredients in an inert excipient or matrix, where the active ingredients could exist in finely crystalline, solubilized, or amorphous states[43]. It is generally believed that solid dispersion can enhance the dissolution rate of a poorly soluble drug through one or combination of the following factors:

a. Increased surface area: a drug exists either as very fine crystalline particles or molecular dispersion in a solid dispersion. Therefore, the surface area of the drug is significantly increased as compared to the conventional formulation.

b. Surface modification through intimate contact with hydrophilic carriers such that the drug wettability is improved

c. Increased solubility through formation of solid solution wherein due to the molecularly dispersed form of the drug the step of drug dissolution is bypassed.

Pharmaceutically approved solid dispersion carriers include polyethylene glycol (PEG), polyvinylpyrrolidone (PVP) and its copolymers, cellulose derivatives, acryl ate polymers, sugars and its derivatives, emulsifiers, organic acids and its derivatives[19]. Although solid dispersions offer great potential for enhancing the bioavailability of BCS Class II

compounds, decades of research have only resulted in a few marketed products. These include Griseofulvin-PEG dispersion (Gris-PEG®, Novartis), Nabilone-PVP dispersion (Cesamet®, Lilly) and Troglitazone formulation (marketed by Parke-Davis as Rezulin®). In the recent years, several breakthroughs in solid dispersion technology, including dosage form design, development, and manufacturing have shaped the landscape to cope as a drug delivery technology for poorly soluble drugs. With the growing interest in utilizing hot-melt extrusion technology for manufacturing solid dispersion dosage forms, the success is highlighted by the development of Kaletra® tablets (Abbott)[18].

2.4 Hot melt extrusion: An emerging drug delivery technology

Although hot melt extrusion (HME) has been a mainstay technology in the plastics industry for over 70 years, research and manufacturing within the pharmaceutical industry over the past 2 decades have propelled HME as an alternative 'platform' for developing solid dosage forms of numerous poorly soluble compounds[44]. In the HME process, the active component is embedded in a carrier system, usually comprised of one or more thermoplastic polymers[45], low melting waxes[46], sugar alcohols[47] or starch[48]. Molten polymers or waxes used in extrusion process can function as thermal binders and act as drug depots and/or drug release retardants on cooling and solidification. Other functional excipients such as plasticizers[49], fillers[50], pH and release modifiers[51], stabilizers[52], surfactants[53], antioxidants[54] and processing aids can also be included in the HME process. Intense mixing and agitation imposed by the rotating screws cause de-aggregation of suspended drug particles in the molten polymer, resulting in a more

uniform dispersion, a solid solution or a combination of the two in the final product. The physical state of the active moiety will have a significant effect on processing, drug release properties and the stability of the drug in the final extrudates.

Different working principles of extrusion exist, whereas the screw extrusion is mainly applied in pharmaceutical processing[55]. A screw extruder provides high shear stress and intense mixing and can therefore handle high drug loads. These machines exist as single screw or twin screw extruders. The single screw extruder is the most widely used extrusion system and has an advantage of a high pressure build-up and generation of mechanical energy to induce specific modifications of the product. It is common for the extrusion screw to be characterized by the length/diameter (L/D) ratio, which typically ranges from 20 to 40:1. Typical pilot plant extruders have diameters ranging 18–30 mm, whereas production machines are much larger with diameters typically exceeding 50 mm. Irrespective of the complexity of the machine, the extruder must be capable of rotating the screw(s) at a selected speed while compensating for the torque generated from the material being extruded.

The versatility of a twin-screw extruder (process modification and optimization) and the ability to accommodate various pharmaceutical formulations makes this set-up much more favorable. In relation to machine design, rotation of the screws inside the extruder barrel may either co-rotate (same direction) or counter-rotate (opposite direction); both directions are equivalent from a processing perspective. Another significant design variable is whether the two screws are intermeshing or non-intermeshing, the former is

preferred because of the greater degree of conveying achievable and the shorter residence times. Additionally, the configuration of the screws themselves may be varied using forward conveying elements, reverse conveying elements, kneading blocks and other designs to achieve particular mixing characteristics.

Twin-screw extrusion offers the pharmaceutical formulator a rapid, continuous process that has much better mixing capability than single screw extrusion. Moreover, twin-screw extrusion provides a more stable melting process, shorter residence times and significantly greater output[56]. Industrially, twin-screw extrusion has become extremely favorable because of process practicality and the ability to combine separate batch operations into a single continuous process, thus increasing manufacturing efficiency.

2.5 Choice of Model Compound: Cinnarizine

Cinnarizine (1-(Diphenylmethyl)-4-(3-phenyl-2-propenyl)-piperazine is a piperazine derivative which was first synthesized by Dr. Paul. A.J. Janssen in 1955.

The structure is as follows[57] :

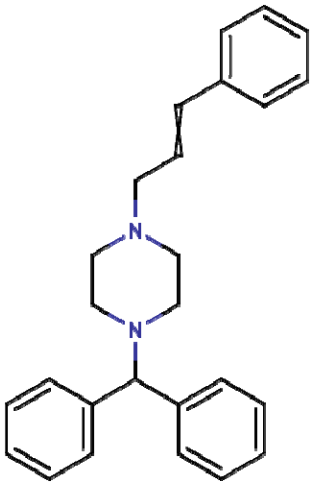

It displays antihistaminic, antiserotoninergic, antidopaminergic and calcium blocking activities. *In vitro* and *in vivo* studies indicate that cinnarizine can inhibit the contraction of vascular smooth muscle by blocking calcium channels, improve the cerebral and coronary circulation, reduce blood viscosity and increase erythrocyte deformability.

These various mechanisms of action allow for a wide range of therapeutic effects[58,59,60]. Currently, an oral formulation of cinnarizine, Stugeron® 25 mg, is available in clinical practice for the treatment of cerebral thrombosis, cerebral arteriosclerosis, subarachnoid hemorrhage and some other diseases caused by poor peripheral circulation.

After oral administration, cinnarizine exhibits variable dissolution and low bioavailability as a consequence of its poor aqueous solubility and scarce wettability [61]. Many different formulation approaches have been studied to improve the physicochemical and

biopharmaceutical properties of cinnarizine such as fast dissolving tablets, self-emulsifying drug delivery systems, floating microspheres, enteric microparticles and lipid emulsions [62,63,64]. There is only one report of a dispersion of cinnarizine in Gelucire® 53/10 by Gines et. al, wherein only 10% cinnarizine loading was achieved as a amorphous dispersion[65].

Thus formulating a delivery system for cinnarizine, a representative molecule of the class of poorly soluble ionic compounds, which will help to increase its solubility in physiological relevant media and thus consequently improve its absorption, is necessary. Herein, we have investigated the salt forming potential of cinnarizine and compared its dissolution enhancement to its pH modified-solid dispersion formulation manufactured using hot melt extrusion technology. Finally, computational tools are utilized to predict *in vivo* absorption enhancement using the experimental *in vitro* dissolution profiles.

2.6 Predicting oral drug absorption

Whether or not a drug will be absorbed after oral administration depends on events depicted in Fig.2.5, their importance relative to each other and the rates at which they occur. Release and absorption must occur within the available transit time that the drug spends in the gastrointestinal tract before reaching its absorptive sites, as well as its residence time at the site of absorption.

Important factors affecting oral drug absorption are:

1. Solubility and dissolution
2. Stability of the drug in luminal fluids (e.g. decomposition and complexation)
3. Transport through the gut wall in both directions
4. Possibility of first-pass metabolism in gut and/or in liver

Predicting oral drug absorption has several important applications in the pharmaceutical industry[66,67]. First, when applied in the drug discovery area, it could be used to screen for new chemical entities which can be administered orally. This is a major advantage for drug administration, since the oral route is a convenient way of administering drugs, well accepted by patients. Second, in early preclinical development, dosage forms must be developed for toxicological and pharmacological screening in animals. Since it is usually most convenient to dose the animals orally, a formulation suitable for this route must be developed. At this stage, it is important to know if the drug will be absorbed after oral administration in the species of interest and also, assuming this is the case, it would also be important to select a dosage form which can generate acceptable bioavailability over a wide range of dosing levels. For these reasons, it is important to be able to predict oral absorption not only in humans but also in the animal species used in preclinical studies. Prior to entry into human study, a decision has to be taken about the route of administration in Phase I activities. If the oral route is to be used, a suitable dosage form must be developed. Again, this dosage form should function well over a wide range of dosing levels since Phase I studies involve dose escalation from an initial dose (estimated to be free of toxicologic implications) through to dosing levels that are expected to generate pharmacological effects. Estimating absorption as a function of dose for the

dosage form selected may point to the need of developing more than one dosage form to complete the studies and/or to better interpret the data generated. Once the dose for the proof-of-principle (Phase II) clinical studies has been fixed, the dosage form often undergoes optimization. Here, prediction of absorption as a function of dosage form design can be used to streamline the development process. Since the goal is often to arrive at the final formulation concept prior to starting the wider clinical trials (Phase III testing), efficient methods for optimizing the formulation at this point in the process are particularly prized. Once the Phase III studies are started, it may still be necessary to make changes to the formulation in order to meet scale-up demands and clinical needs, and in this case a bioequivalence (BE) study is used to determine if the formulation change will alter the pharmacokinetic (PK) profile and thus potentially the therapeutic effect of the drug. Being able to predict the outcome of the BE study de-risks the clinical development process by helping steer away from formulation changes which may jeopardize comparability of results in various clinical trials. If additionally absorption can be estimated correctly in important subpopulations, such as, children, the elderly, populations of different ethnic backgrounds, this will assist in developing suitable formulations and even dosing schedules for these subpopulations. Last but not least, should post-approval changes be made to the formulation to achieve different doses, different dosing intervals, better stability characteristics, etc. or to bring a generic formulation onto the market, being able to predict the influence of these changes on the plasma profile is of paramount importance to the success of the program. Therefore, for all of the reasons described, it is highly desirable to be able to predict oral drug performance on an *a priori* basis.

2.6.1 Computational absorption simulation models

The first PK model published in scientific literature was designed by Teorell in 1937 [68]. The paper described a physiologically based model, but since no analytic solution could be developed to solve the model structure, the approach was not further evolved. Parallel attempts to simulate release from the dosage form using dissolution testing equipment in the 1950s and 1960s, pharmacokineticists were describing oral drug absorption with an absorption rate constant, typically first order, which was incorporated into a simplified compartmental description of the body[69,70]. The PK approach essentially dealt with the gastrointestinal (GI) tract as a black box and usually made little attempt to sift out the relative contributions of release from the dosage form, decomposition in the gut lumen and GI transit, permeability and first pass metabolism to the overall absorption process. As pharmaceutical scientists became more aware of the impact of events in the GI tract on absorption, attempts were made to relate these factors to one another[71]. It was also recognized that the contributions of the different factors might vary among drug products and some rudimentary attempts were made, for example, to simulate the effect of particle size on drug absorption using compartmental modeling[72]. The classical PK approach to describing drug absorption is to deconvolute the plasma profile and arrive at an absorption rate constant. The kinetics is usually approximated as first order for immediate release (IR) formulations but may be zero order or mixed order for modified release (MR) formulations. Analytical solutions based on deconvolution are available for determining the rate of absorption into a one compartment open PK model or a two

compartment open model. The first uses the Wagner–Nelson equation[73], while the second relies on the Loo–Riegelman analysis[74].

However, sometimes absorption does not follow simple first or zero order kinetics and variations on the above approaches were developed to describe, for example, delayed absorption after administration of an enteric coated tablet by invoking a lag time, pulsatile release *via* two consecutive first order input steps[75] and combinations of lag times with consecutive first order input steps to describe double peak phenomena[76].

In the 1980s, an allometric approach was used to develop WinNonlin® (Pharsight, USA), which today is the benchmark program for PK analysis. This program enables the user to enter plasma level results, determine which PK model best fits the data and then derives the corresponding PK parameters using numeric algorithms, including an empirical description of the absorption kinetics. In drug development, classical approaches to modeling drug absorption are especially useful for establishing *in vitro–in vivo* relationships (IVIVR). These enable the pharmaceutical scientist to understand how changes in the formulation will likey affect the plasma profile on the basis of dissolution test results, rather than having to perform a PK study each time. Up until recently, the primary application of IVIVR was to products with MR and many examples of IVIVR for such products can be found in the literature. The most common method of constructing an IVIVR is to deconvolute the plasma profile and plot the fraction absorbed against the fraction released over the entire release profile. The method was first proposed by Gerhard Levy and is commonly referred to as the Levy Plot[77]. It is also

recognized by various regulatory agencies as a Level A correlation[78]. If the post-absorptive kinetics is established, it is also possible to build a simulated plasma profile using the *in vitro* release data using convolution techniques[79].

2.6.2 Compartmental Models

These models assume the GI tract as one compartment or a series of compartments with linear transfer kinetics, and each compartment is well mixed with a uniform concentration. These can be linked to pharmacokinetic models to predict plasma concentration-time profiles of drugs.

CAT Model

The basic equation for the CAT model is described as follows

$dY_n/dt = K_t Y_{n-1} – K_t Y_n – K_a Y_n$ where, n=1,2,.....,7.

where, Y_n is the percent of dose at the n^{th} compartment, n is the number of total compartments, K_t is the transit rate constant, and K_a is the absorption rate constant.

The original assumptions for this model include passive absorption, instantaneous dissolution, linear transfer kinetics for each segment, and minor absorption from the stomach and colon[84]. This model was originally developed to predict oral drug absorption for nondegradable and highly soluble drugs. Nevertheless, this model was shown to capture the dependence of the fraction of dose absorbed on the effective permeability for

various drugs with different absorption characteristics[80]. The CAT model could also be linked directly to pharmacokinetic models to predict plasma concentration-time profiles. By incorporating Michaelis–Menten kinetics for carrier/transporter-mediated absorption, gastric emptying rate constant, and compartment-dependent degradation rate constant into the model, the CAT model was extended for predicting dose-dependent drug absorption with degradation in the small intestine, such as for cefatrizine[81]. Moreover, the CAT model was extended to simulate the fraction of dose absorbed in controlled release dosage forms by including a compartment that represents the controlled-release dosage form[84]. By taking gastric emptying and dissolution into consideration, the CAT model was also used to predict the fraction of dose absorbed for poorly absorptive drugs such as digoxin, griseofulvin, and panadiplon, and to determine the cause of poor oral absorption (dissolution-, solubility-, or permeability-limited absorption) [82].

Based on the CAT model, a very similar approach was developed by Kortejarvi *et al.* [83] by considering the process of gastric emptying, drug dissolution, and drug intestinal transit within the GI tract. This model was constructed using Stella software for investigating the effects of different factors including formulation types, physiology of the GI tract, dissolution, absorption, and elimination on biowaiver criteria evaluation. The investigators concluded that, based on the simulation, about half of BCS I drugs have a higher risk to fail a bioequivalence study than BCS III drugs do. The above statement can be valid for some BCS I drugs with rapid absorption and elimination *vs.* BCS III drugs when excipients have no impact on GI transit time and permeability.

Advanced CAT (ACAT) model

The ACAT model is an extension of the original CAT model which was developed by Yu and Amidon[84]. This model (Fig.2.6) includes linear transfer kinetics and nonlinear metabolism/transport kinetics, six states of drug component (unreleased, undissolved, dissolved, degraded, metabolized, and absorbed), nine compartments (stomach, seven segments of small intestine, and colon), and three states of excreted material (unreleased, undissolved, and dissolved) [85]. The CAT model does not account for dissolution rate, the pH dependence of solubility, controlled release, absorption in the stomach or colon, metabolism in gut or liver, degradation in the lumen, changes in the absorption surface area, transporter densities, efflux protein densities, and other regional factors within the intestinal tract.

- For drugs with low permeability or solubility, absorption may not be complete in the small intestine and the CAT model can be made more accurate by treating the colon as an additional absorbing compartment.
- For drugs with moderate to low permeability, for most immediate release and controlled release formulations, colonic absorption can be significant.
- For drugs with high permeability and high solubility, colonic absorption is a negligible fraction of the total absorption of the immediate release formulations.

For example, the ACAT model successfully predicted oral absorption for drugs undergoing first-pass hepatic metabolism (propranolol), first-pass intestinal and hepatic

metabolism (midazolam), efflux transport (digoxin), and first-pass metabolism plus efflux transport (saquinavir)[86]. Furthermore, this model demonstrated the potential to predict food–drug interactions (e.g., grapefruit juice with CYP3A substrates) and drug–drug interactions (e.g., rifampin with P-gp substrate digoxin) during oral drug absorption. However, some features that have an impact on drug absorption, such as local structure of gut enterocytes, cytoplasmic protein binding, segregation of blood flow to the intestine, and the heterogeneous expression and activities of drug metabolizing enzymes and transporters along the GI tract were not included in the original ACAT model[85].

2.6.3 Gastroplus™

In our case, we have utilized simulation software such as Gastroplus™ (Simulations Plus, Inc., Lancaster, CA, USA) which helps in predicting bioavailability by estimating biopharmaceutical properties and simulating gastrointestinal absorption and metabolism by extending the advanced compartmental absorption and transit (ACAT) model to account for nonlinear saturable processes. It has been used to simulate the *in vivo* absorption profile of drugs by using *in vitro* dissolution data for establishing *in vivo-in vitro* correlation. With an integration of drug physicochemical properties and physiological parameters, Gastroplus™ has been used to aid in justifying biowaivers for selected BCS II compounds[87]. Moreover, the impact of different formulation factors such as solubility, particle size, and size distribution on oral drug absorption were also predicted by Gastroplus.

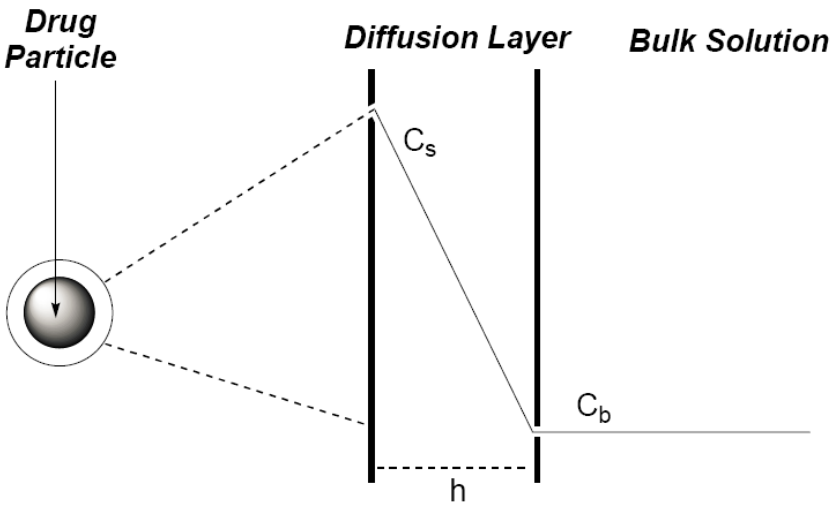

Figure 2.1 Schematic presentation of diffusion-controlled model. The Nernst-Brunner equation postulates the existence of a diffusion layer (an unstirred layer) adhering the dissolving solid surface. C_b is the concentration of the solute in the bulk media at time t cannot exceed C_s, since the concentration gradient (C_s-C_b) approaches zero as C_b increases with time (23).

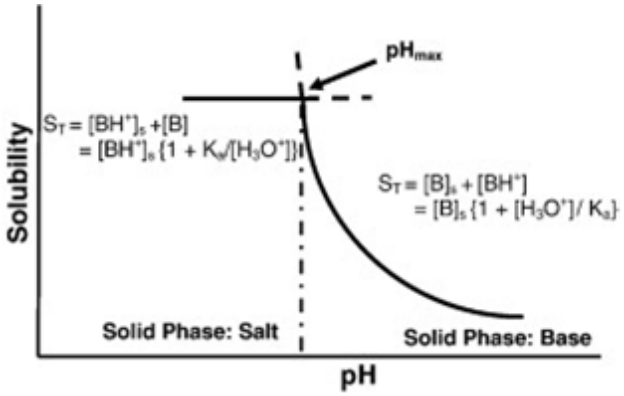

Figure 2.2 Schematic representation of the pH–solubility profile of a basic drug indicating that the solubilities may be expressed by two independent curves and that the point where two curves meet is the pH_{max} (11).

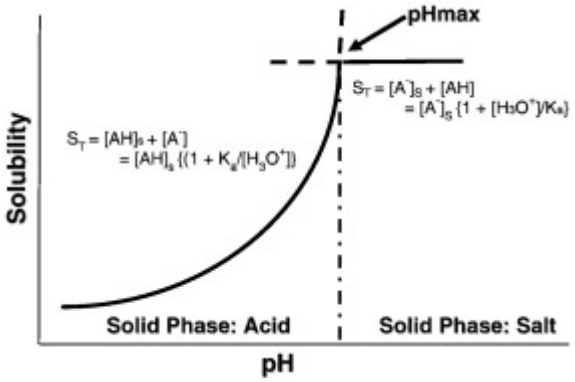

Figure 2.3 Schematic representation of the pH–solubility profile of an acidic drug indicating that the solubilities may be expressed by two independent curves and that the point where two curves meet is the pH_{max} (11).

Salt former	Approximate frequency (%)	
	Stahl (1998)	Berge *et al.* (1977)
Sodium	58	62
Calcium	12	10.5
Potassium	5	10.8
Magnesium	4.5	1.3
Meglumine	2.5	2.3
Ammonium	2	<0.3
Aluminium	1.5	0.7
Zinc	1	2.9
Piperazine	1	<0.3
Tromethamine	1	<0.3
Lithium	1	1.6
Choline	0.5	0.3
Diethylamine	0.5	<0.3
4-Phenyl-cyclohexylamine	0.5	<0.3
Benzathine	0.5	0.7

Table 2.1 Frequency of use of 15 most commonly used cationic salt formers (16)

Salt former	Approximate frequency (%)	
	Stahl (1998)	Berge *et al.* (1977)
Hydrochloride/chloride	49	43
Sulfate	6	7.5
Hydrobromide/bromide	5	2
Tartrate	3	3.5
Mesylate	3	2
Maleate	3	3
Citrate	3	3
Phosphate	2.5	3.2
Acetate	2	1.3
Embonate (pamoate)	1.5	1
Hydroiodide/iodide	1	2
Nitrate	1	0.6
Lactate	1	0.8
Methylsulphate	1	0.9
Fumarate	1	0.3

Table 2.2 Frequency of use of 15 most commonly used anionic salt formers (16)

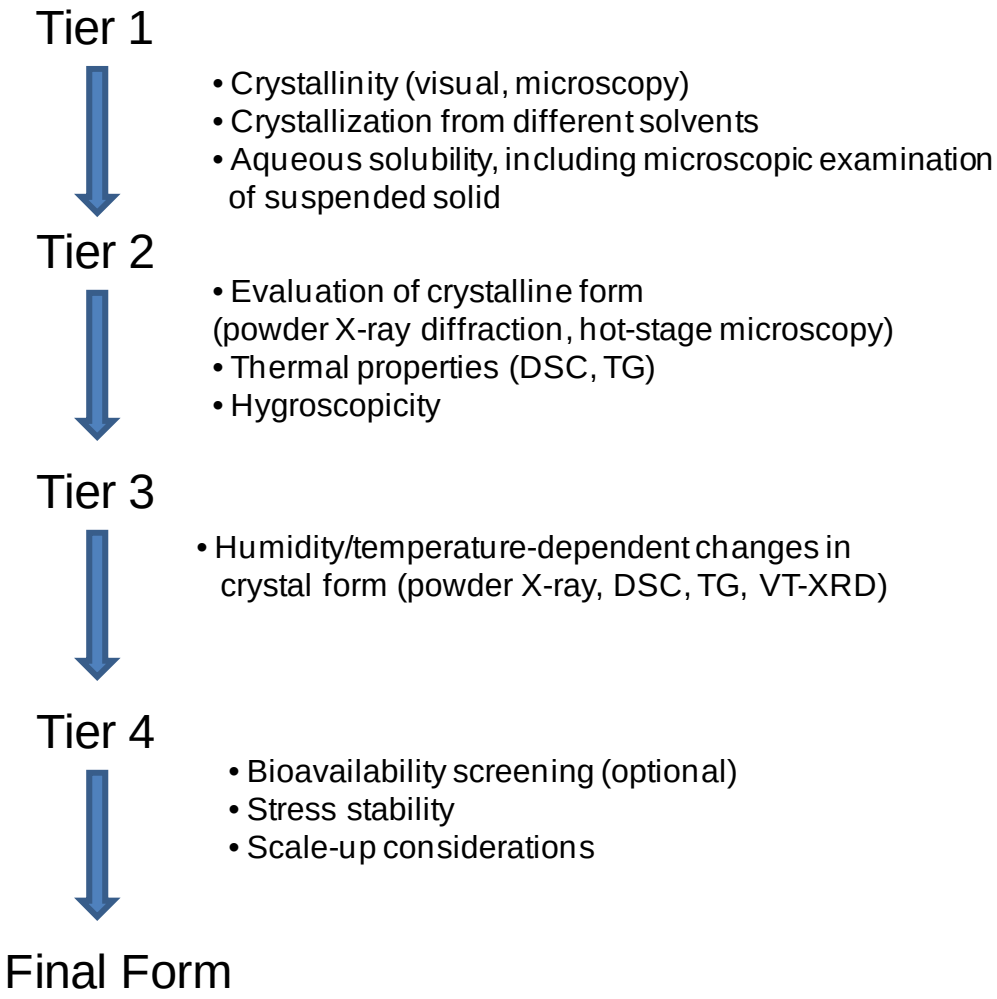

Figure 2.4 Schematic representation of a multi-tier approach for the selection of optimal salt form of a drug (39).

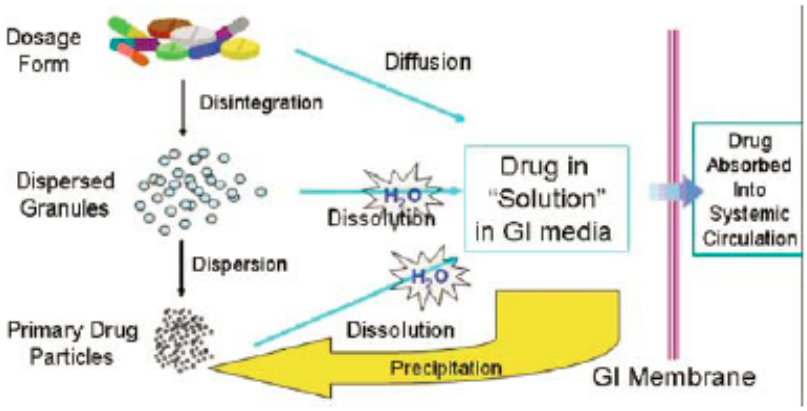

Figure 2.5 The kinetics of disintegration, dissolution, diffusion, precipitation after oral administration of a formulation until drug absorption into the systemic circulation (Reference: Hageman, AAPS Workshop on Optimization of Drug-like properties during lead optimization, September 19-22, 2004).

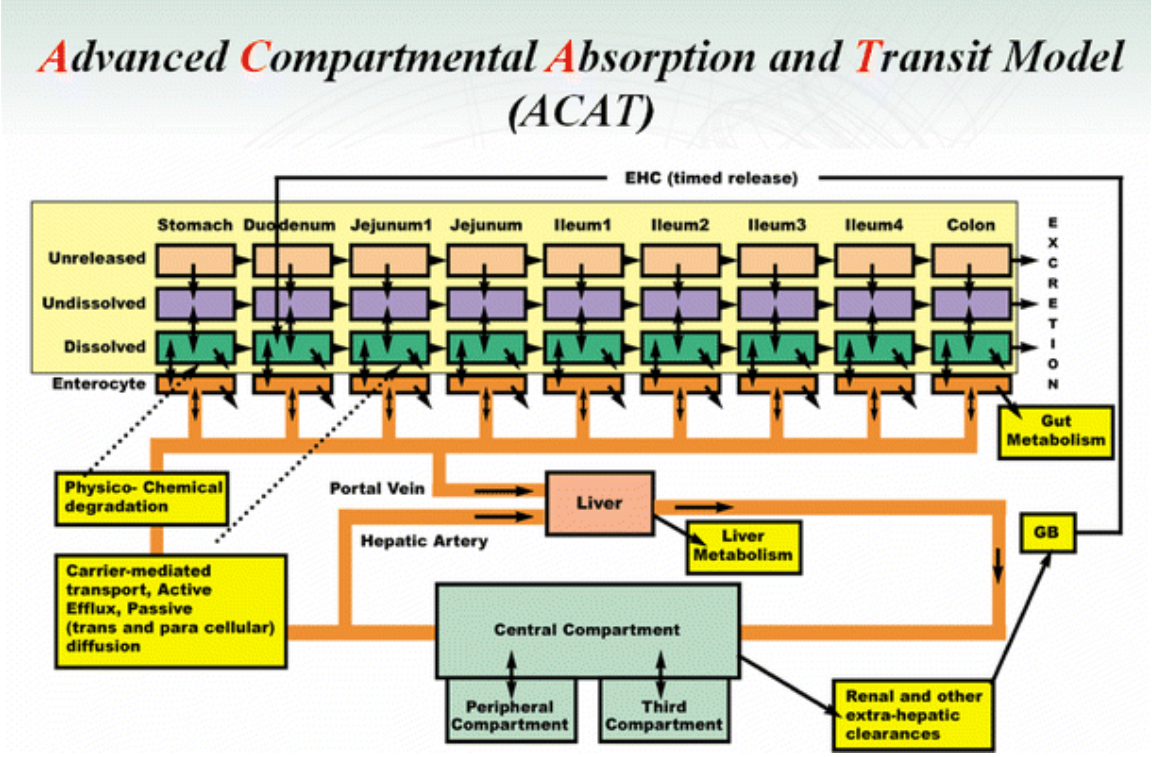

Figure 2.6 Schematic of the ACAT model. The original CAT model with seven compartments was modified to include compartment-dependent physiological parameters and the colon. One to three compartment pharmacokinetic models were also included to estimate concentration-time plasma profiles (86).

3 SPECIFIC AIMS

Specific Aim 1: To synthesize salts of a poorly soluble weak base, Cinnarizine, using weakly acidic di-carboxylic acids.

Salt screening and selection is a well established approach in early development of new molecular entities for facilitating compound dissolution in aqueous environment of gastrointestinal tract and consequently increasing the oral bioavailability[11]. The pH solubility profile and the pK_a of the weak base are important for counterion selection. The probability of the salt formation for a weak base with an acidic counterion is high if the pK_a of the weak base is at least 2 pH units higher than the pK_a of the weak acid counterion. Though an inorganic ion such as hydrochloride is the most frequently encountered species in pharmaceutical salts, it is susceptible to common ion effect due to the presence of chloride ions in the gastric media which limits the hydrochloride salt solubility due to conversion to its free base form[17]. It has also been observed that the choice of organic solvents or aqueous solvents as reaction media could significantly influence compound ionization by causing a shift in relative pK_a; inhibiting salt formation[38]. This study will evaluate the salt forming potential of a weak base, cinnarizine, with organic weak acids with different pK_a as counterions. Purely non-aqueous solvent systems and a mixture of aqueous and non-aqueous solvent systems will be evaluated to favor salt formation. The identified crystalline salt forms will be scaled-up. Analytical tools will be used to characterize the salt form and confirm its stoichiometry.

Specific Aim 2: To develop pH-modifying solid dispersion systems of a poorly soluble weak base, Cinnarizine, and perform a mechanistic study to evaluate their *in vitro* dissolution enhancement potential.

Pharmaceutical salts are one of the widely accepted approaches to improve dissolution rate of poorly soluble ionic drugs. However, the salt formation process is often empirical[18]. The primary goal of this study is to develop a formulation approach for poorly soluble ionic drugs that combines the benefit of pH modulation (by incorporating pH modifiers) with the solubility enhancement achieved by solid dispersions, to design pH-modifying solid dispersions. The hypothesis of this study is that if a desired salt form of a weakly basic drug cannot be synthesized, then a molecular solid dispersion of the drug and acidic counterion should provide dissolution enhancement similar to that of a solid dispersion of its salt. Cinnarizine free base (CNZ-fb), a piperazine derivative, is selected as a model drug due to its poor aqueous solubility (2 μg/ml) and its potential to form salts. Melt extrusion technology will be used to manufacture Kollidon VA64 based amorphous dispersions of CNZ-fb, CNZ-fb plus acidic counterions and CNZ salt form. Release of CNZ will be determined in pH 4.5 acetate buffer which provides non-sink conditions for dissolution of 25mg dose equivalent of CNZ-fb. The possibility of acid-base interactions between CNZ-fb and acidic counterion during melt extrusion will be investigated using Raman spectroscopy.

Specific Aim 3: To compare *in silico* pharmacokinetic performance based on *in vitro* dissolution of the weak base, Cinnarizine, from the designed solid dispersions and a marketed product.

Predictive modeling tools such as Gastroplus™ have been used successfully to predict oral drug absorption for poorly soluble drugs. Simulation of the *in vivo* absorption profiles of drugs by using *in vitro* dissolution data for establishing *in vitro – in vivo* correlations is becoming a common practice during different phases of drug product development[66]. This study objective is to compare the designed solid dispersions to a marketed product of the selected weak base. In doing so, a physiologically relevant pH (pH=6.8) where the rate of solubility would drive the absorption for a weak base is selected to generate dissolution profiles for all the formulations. Published human oral plasma concentration data of marketed CNZ tablets is used to build an absorption model and predictions for *in vivo* pharmacokinetic performance of the designed solid dispersions is achieved based on experimental *in vitro* dissolution profiles.

Specific Aim 4: To study the effect of incorporating ionic polymers (enteric) and organic acids (dicarboxylic and hydroxy) on the dissolution enhancement from solid dispersion of the selected weak base.

The impact on dissolution rate of weakly basic drug in solid dispersion formulation containing organic acids or ionic polymers as pH modifiers prepared using melt extrusion has not been studied. We propose to systematically evaluate the formulation of such solid

dispersions of CNZ-fb and understand the mechanisms governing the dissolution rate enhancement. Multiple organic acids will be selected with varying degree of aqueous solubility, acidity levels and potential for inter-molecular interactions based on their chemical structures. Two ionic polymers with different functional backbones will be selected to evaluate the impact of increasing molecular weight of the pH-modifiers on release rate of cinnarizine from such solid dispersions. Moreover, the effect of physiologically relevant pH conditions on dissolution of cinnarizine from such solid dispersions will be examined. These findings will help to optimize the formulation design and develop pH-independent formulations for poorly water-soluble ionic drugs.

4 A COMPARATIVE EVALUATION OF DISSOLUTION ENHANCEMENT OF A WEAKLY BASIC DRUG FROM ITS SALT SOLID DISPERSION AND AMORPHOUS DISPERSIONS CONTAINING ACIDIC COUNTERIONS

4.1 Introduction

It is no secret that pharmaceutical scientists are grappling to maximize R&D productivity. The number of poorly water-soluble drug molecules entering pharmaceutical development pipeline has been staggering and rising over the past decade[88,89]. Often, inter-disciplinary teams of scientists work in parallel to evaluate different technologies that enhance bioavailability of poorly soluble drugs and to launch products faster to market. One of the techniques widely published in the literature and routinely practiced to enhance dissolution rate of poorly soluble ionic drugs is salt formation[11]. An ideal salt should be easily synthesized with high purity, have favorable physicochemical properties, and have low irritancy and toxicity[38].

Pharmaceutical salts are made up of two components: the drug itself, which exhibits pH-dependent solubility; and a counterion, which is typically an acidic or basic small molecule. Drugs that are weakly basic ionize, and dissolve, when pH of surrounding media is below drug pK_a. During dissolution process, it is believed that the acidic counterion from the salt lowers pH in the microenvironment layer of the drug particle, a phenomenon that leads to increased drug solubility and dissolution[27]. The reverse is true

for salt of a weakly acidic drug, where the basic counterion increases pH in the surrounding layer and increases dissolution of the acidic drug.

Although salt formation has been used widely for decades, the salt formation process for a new chemical entity is not often predictable and remains empirical to a large extent. Serajuddin et al., have highlighted criteria to consider when forming and selecting pharmaceutical salts[38]. Chemists evaluate a battery of counterions and multiple combinations of solvents to isolate crystalline salts, but the process is not always a trial-free one. It is not uncommon to see a sticky residue in the bottom of a flask, o r an amorphous substance, or powder mixture of drug substance and the counterion. Such salt candidates are terminated on the grounds of poor develop-ability. In a recent review, published by Stahl et al.,[90] among the 15 most common acid and base salt formers, hydrochloride and sodium salts are the most dominant. However, for hydrochloride salts there is always the risk of poor dissolution rate due to the common ion effect from the intestinal fluids. Despite the potential for conversion to a hydrochloride salt, nonhydrochloride salts are still preferred in dosage form development due to their kinetic advantages during dissolution[91].

Alternatively, a formulation strategy that often circumvents hurdles seen with pharmaceutical salts, are solid dispersions. Solid dispersion is a molecular dispersion of drug in a polymer matrix which, because of their enhanced surface area, increases the dissolution rate and effectively the bioavailability of poorly water-soluble drugs[18,92]. Specifically, pH-modified solid dispersion represents a recent attempt taken to improve

solubilization of poorly water soluble drugs with pH dependent solubility. Inclusion of an acidifier or alkalizer (counterion) into the solid dispersion containing weakly basic drug or weakly acidic drug, respectively, creates a corresponding acidic or basic microenvironment in the dissolving layer. This enhancement of drug dissolution has been attributed to the release rate of the pH modifier from the solid dispersion prepared using solvent evaporation method[93].

The purpose of this study is to explore the synergies between pH modulating ability offered by a salt form and the dissolution enhancement offered by an amorphous solid dispersion prepared using hot melt extrusion. The hypothesis of this study is that if a desired salt form of a weakly basic drug cannot be synthesized, then a molecular solid dispersion of the drug and acidic counterion should provide dissolution enhancement similar to that of a solid dispersion of its salt. To test the hypothesis, a systematic study was designed to evaluate the dissolution enhancement potential of a multi-component solid dispersion system of a weakly basic compound containing acidic salt forming or non-salt forming counterions. Cinnarizine, a piperazine derivative, was selected as a model drug due to its poor aqueous solubility (2 μg/mL) and its potential to form salts. Hitherto, an oral formulation of cinnarizine is available in clinical practice; it exhibits variable dissolution and low bioavailability as a consequence of its scarce wettability and pH dependent solubility[94,95]. Weak acid counterions such as maleic and succinic acid with pK_a 1.9 and pK_a 4.2 respectively, were chosen from the class of organic dicarboxylic acids to evaluate their salt forming potential with cinnarizine. Fig.4.1 illustrates the schematics of the study. While the concept of inclusion of pH-modifiers in solid

dispersion is not new, this study attempts to systematically offer the benefits of adding acidic counterions during melt extrusion, should a classical salt formation technique fail. All dissolution studies were conducted in non-sink condition to differentiate the formulations. Cinnarizine salt solid dispersion was used as a positive control. We also investigated the mechanisms for dissolution enhancement of such pH-modified solid dispersions including the possibility of ionic interactions and *in situ* salt formation during melt extrusion.

4.2 Material and Methods

4.2.1 Materials

Cinnarizine free base (CNZ-fb), ($C_{26}H_{28}N_2$; pK_a 1.9 and 7.5), was purchased from Sigma Aldrich (St. Louis, MO) and was used as the model compound due to its low aqueous solubility (2 µg/ml in purified water, 0.01 mg/ml in pH 4.5 acetate buffer), and its demonstrated ability to form salts with selected organic acids[96]. Maleic acid ($C_4H_4O_4$; pK_a 1.9 and 6.1) and Succinic acid ($C_4H_6O_4$; pK_a 4.2 and 5.6) were purchased from Sigma Aldrich Chemical Co., (St. Louis, MO), and were used as acidic counterions. Kollidon® VA64, a water-soluble non-ionic polymer with poly-vinylpyrrolidone-co-vinyl acetate backbone (M_w ~ 55000 g/mol) was obtained from BASF Chemicals (Budd Lake, NJ). Organic solvents used in salt synthesis were purchased from Sigma-Aldrich Co. LLC., (St. Louis, MO). All materials were used as received.

4.2.2 Synthesis of cinnarizine salt

Potential for CNZ-fb to form salts with various weak acids has been previously evaluated, albeit on a miniature scale[96]. In this study, ability for CNZ-fb to form salt with maleic acid or succinic acid on lab scale was tested. 400mg of CNZ-fb was added to 14 mL of 50:50 acetone: water. To this mixture, 126mg of either maleic acid or succinic acid was added to create an equimolar mixture (0.54 mmol) of CNZ-fb and of acid. Solution flask was placed in EasyMax™ Synthesis Workstation (Mettler Toledo Inc., Columbus, OH) and was subjected to heat-cool cycles under constant stirring. Temperature was ramped-up at 5 ºC/min from 5 ºC to 35 ºC, held steady for 10 min, and ramped-down at 0.5 ºC/min to 5 ºC, where it was held for 20 min. Such a cycle was repeated 15 times, to allow for precipitation and maximize yield. At the end of temperature cycle, product was kept at 5 ºC until the precipitated solid was filtered out under vacuum. Solid residue was then dried overnight in a vacuum oven (< 50 mbar) at 50 ºC. Dried solid was characterized using polarized light microscopy, X-ray diffraction and calorimetry. Salt synthesis was scaled-up from 500 mg to 6 g, and to 25 g using 1 L reactor of HP AutoMATE® (HEL Inc., Lawrenceville, NJ). Yield of the cinnarizine salt was greater than 85% in all cases.

4.2.3 Determination of salt stoichiometry

4.2.3.1 Solution NMR

NMR spectra were recorded at room temperature using a Bruker DPV 400 MHz spectrometer equipped with a 3 mm QNP probe. DMSO was used as sample solvent. Chemical shifts were referenced to the respective DMSO-d6@ 2.5 ppm. The 1D proton spectrum was recorded in 128 scans.

4.2.3.2 Ion chromatography

A Dionex ICS-2000 system with a Famos autosampler controlled by Chromeleon software (Dionex, Sunnyvale, CA) was used for the quantitative anion analysis as described by Reilly J. et al.[97] An ionpac AG19 pre-column (50x4mm) with an Ionpac AS19 column (250x4mm) was used for this study. The KOH eluent was adjusted by the use of an eluent generator cartridge. Chromatograms were recorded using conductivity detection. A linear gradient was performed with the mobile phase flow rate of 1.4 mL/min with the column temperature set at 30 ºC and injection volume of 25 µL. A suppressor type ASRS_4mm was used with a constant current of 243 mA. A four component anion test standard consisting of acetate, chloride, trifluoroacetate and sulfate (0.5 mg/mL) was used for anion system quality control check. Salt stoichiometry helped to assess salt correction factor which was used to prepare solid dispersions of CNZ-fb with stoichiometric equivalents of organic acids, and for dissolution studies.

4.2.4 Solid state characterization of CNZ-fb, its salts and solid dispersions

4.2.4.1 X-ray powder diffraction (XRPD)

Powder X-ray diffraction analysis was performed on Bruker D8 Advance, controlled by diffrac plus X-ray diffraction (XRD) commander software (Bruker AXS Inc., Madison, WI). The sample was prepared by spreading powder sample on a polymethyl methacrylate (PMMA) specimen holder rings from Bruker (AXS Inc., Madison, WI) and was scanned from 2 to 40 degrees at the rate of 2 degrees/min with 0.02 degrees step size and 0.6 s/step at 40 KV and 40 mA. The divergence and anti-scattering slits were set to 1 degree and the stage rotated at 30 rpm. Data analysis was performed using EVA Part 11 version 14.0.0.0 software.

4.2.4.2 Thermal analysis

Modulated Differential scanning calorimeter (mDSC) Q1000® TA Instruments (New Castle, DE) was used to assess structural properties of the salt and solid dispersion systems. High purity indium and sapphire were used frequently to calibrate the heat flow and heat capacity of the instrument. All systems were placed in standard aluminum pans and crimped with lids containing three pin-holes. Salts were heated at 10 °C/min to determine melting point, and solid dispersions were heated at 1 °C/min with modulation of 0.5 °C every 50 sec to determine glass transitions. Refrigerated Cooling System (RCS) was used for controlled cooling.

4.2.4.3 Thermogravimetric analysis (TGA)

Thermal stability of CNZ free base and salts were assessed using a thermogravimetric analyzer (TGA) with a TA5300® controller. TGA analysis was carried out by heating samples at 10 ºC/min in an open pan under air from room temperature to 240 ºC. TGA helped to determine a maximum processing temperature for melt extrusion studies.

4.2.4.4 Raman spectroscopy

Raman spectra of crystalline CNZ-fb, CNZ salts and solid dispersions were collected using Raman RXN1™ (Kaiser Optical systems, Inc., Ann Arbor, MI) analyzer equipped with an Invictus® 785-nm He-Ne external-cavity-stabilized diode laser. The samples were scanned using PhAT probe. The stokes-shifted Raman scatter was dispersed using a 600 groove/min grating onto a peltier-cooled charged-coupled device (CCD, Andor Technology PLC, South Windsor, CT) to capture the spectrum.

4.2.5 Determination of pH-solubility profile

pH-solubility profiles of CNZ-fb and CNZ maleate were established at 25 ºC using shake-flask method. Buffer solutions with pH ranging from pH 2 to pH 9 were used. Excess solid was added to 2 mL of each buffer solution vial. Suspensions were placed in Synscreen and Neslab instrument and shaken for more than 1 week to attain equilibrium. Vials were checked periodically to ensure presence of excess solids. pH values were measured prior to the study and pH shifts were adjusted using 0.1N HCl or 0.1N NaOH. At the end of equilibration period, final pH of the suspensions was recorded and aliquots

were filtered using 0.45 µm filter. Filtrate was analyzed using HPLC. Absorbance linearity was established in concentration range from 1 mg/mL to 0.00001 mg/mL using CNZ-fb.

4.2.6 Preparation of solid dispersion using melt extrusion

Melt extrusion was conducted using a bench-top ThermoHaake minilab extruder (Minilab 557-2200, Thermoelectron, Newington, NH). Extruder consists of two co-rotating screws that allows for mixing and transporting the material. Prior to extrusion, physical mixtures of CNZ-fb (20% w/w) and Kollidon® VA64 (80% w/w), with and without maleic acid or succinic acid were prepared using blend/screen/blend process. 20% w/w drug loading was found to be optimal for extrusion studies. When acid counterion was used, polymer levels were adjusted and drug loading was kept constant at 20%. Extrusions were performed using 20 g batch size that allowed for a steady-state process. All ingredients were weighed and blended for 150 revolutions, passed through a 1 mm screen, and re-blended for 300 revolutions. Prior to each extrusion, torque levels were calibrated. Physical mixtures were fed manually into the extruder at a consistent rate. Screw speed was set at 150 rpm, and extrusion was conducted above the glass transition temperature (T_g) of Kollidon® VA 64 and the melting point of CNZ-fb (120 °C), and ranged from 125 ºC to 145 ºC, depending on the composition. First one gram of extrudates was always discarded. Extrudates were allowed to cool to room temperature, milled, sieved through 0.5 mm screen, and placed in air-tight containers at 5 ºC until further analysis. Milled

extrudates were assayed using HPLC method to assess thermal degradation, if any, from melt extrusion.

4.2.7 *In Vitro* Dissolution Study

Dissolution studies were performed in 500 mL of pH 4.5 acetate buffer, USP using USP basket apparatus (Varian™, Cary, NC). Basket speed was set to 100 rpm; and the dissolution study temperature was maintained at 37±0.5 ºC. Size 3, pink, opaque hard gelatin capsules were filled with solid dispersions containing 25 mg equivalents of CNZ-fb. At this concentration, the system was not in sink conditions making the dissolution method discriminatory. pH of bulk media did not change at the end of dissolution. 10 mL aliquots were siphoned at pre-defined time-points (10, 20, 30 and 45 min), and passed through 0.45 μm PVDF filter. 600 μL of filtered aliquot was added to 400 μL of acetonitrile and analyzed using HPLC. Dissolution for each formulation was performed in triplicates.

4.2.8 HPLC analysis

Concentrations of CNZ-fb in the samples were determined using Waters 2695 Separations Module with a Waters 2487 dual λ absorbance detector HPLC system at a wavelength of 254 nm using a Waters Xterra MS C8, 3.5 μm, 4.6 x 50 mm column (Waters Corporation, Milford, MA). All measurements were performed at an injection volume of 10 μL using a mobile phase mixture of acetonitrile (50%) in water (50%) with

0.1% TFA pumped at a flow rate of 1 ml/min, and at temperature of 30 ºC using a column oven. These conditions resulted in an elution time of around 1.5 min for CNZ. Calibration curves were constructed using standard solutions of known concentrations. Chromeleon™ software (Dionex Corporation, Sunnyvale, CA) was used to integrate the peak areas.

4.2.9 Optical Microscopy

Morphology of the CNZ-fb, CNZ maleate and CNZ-succinic acid precipitate was observed using Clemex Intelligent Microscope JS-2000 (Clemex Technologies, Quebec, Canada) using 10X magnification.

4.2.10 Statistical analysis

Data obtained were analyzed using descriptive statistics, single factor analysis of variance (ANOVA) and presented as mean value ± the standard deviation (SD) from three independent measurements in separate experiments. The comparison among groups was performed by the independent sample Student's *t* tests. The differences between variants were considered significant as the value for $P < 0.05$.

4.3 Results and Discussion

4.3.1 Cinnarizine salt formation

Interestingly, CNZ-fb interacts very differently with the two acidic counterions: maleic acid and succinic acid. Fig.4.2 and Fig.4.3 compares the DSC scans and XRPD patterns, respectively, for CNZ-fb and its precipitates with maleic and succinic acid. CNZ-fb showed a single melting endotherm at 118.6 ºC; and CNZ-maleate demonstrated a significantly higher melting point of 181.5 ºC (Fig.4.2), which is different from melting point of neat maleic acid (140 °C, not shown). Moreover, X-ray patterns of CNZ-maleate (Fig.4.3), showed a unique crystalline pattern, indicating formation of a new solid structure between CNZ-fb and maleic acid. In the case of CNZ-fb and succinic acid system, DSC scan showed only a single melting endotherm at 119.6 °C that corresponds to melting point of CNZ-fb. The X-ray pattern in Fig.4.3 revealed similarities between CNZ-fb and CNZ-succinic acid co-precipitate. Based on the above data, it is confirmed that while CNZ-fb formed a salt with maleic acid, no salt was formed between CNZ-fb and succinic acid under the tested experimental conditions.

Our study confirmed results observed by Tarsa et. al.[96] where the authors conducted high-throughput salt screening in multiple solvent systems to assess counterions that formed salts with CNZ-fb. The authors showed that while maleic acid formed salt with CNZ-fb, succinic acid did not. The fact that some counterions do not form salt using conventional salt formation techniques is not surprising. As a rule of thumb, for salt formation to occur

between free base and acidic counterion, pK_a of the base should ideally be at least 2 units above the pK_a of the acidic counterion. In the present case, CNZ pK_a value (pK_a 7.5) is far greater than that of maleic acid (pK_a 1.9) and that of succinic acid (pK_a 4.2 and 5.6). The authors demonstrated that even the choice of solvent system for salt screening studies plays an important role in crystalline salt hits. For poorly water-soluble drugs, addition of aqueous content in the solvent system improved the rate of crystalline hits for salt formation. As seen in our study, a 50:50 acetone: water solvent system was better than 100% acetone or 80:20 acetone : water for forming the crystalline CNZ maleate salt.

Even upon scale-up of CNZ maleate from 6 g to 20 g, a clean melt at 183 ºC was observed. XRD patterns also confirmed formation of a consistent form of crystalline CNZ maleate salt, as seen in Fig.4.4.

Fig.4.5, Fig. 4.6, Fig.4.7 shows morphology and particle size of the crystals for CNZ-fb, CNZ maleate and CNZ succinic acid precipitate, respectively using optical and confocal microscopy. While CNZ succinic acid system showed a mix of very fine particles and crystalline rods with mean size similar to that of CNZ-fb, CNZ maleate particles were larger and had different packing thereby visually conforming formation of new crystals in CNZ maleate.

As a next step to test our hypothesis, solid dispersion systems containing molar equivalent levels of maleic acid and CNZ-fb were prepared, and their dissolution performance were compared with CNZ maleate solid dispersion. In order to determine

required levels of maleic acid for solid dispersion preparation, stoichiometry of CNZ maleate was determined using ion chromatography and solution NMR. As seen in Fig.4.8 and Fig.4.9, ^{1}H NMR and ion chromatography determined stoichiometry values maleate anion to be 1.0 and 0.98, respectively.

^{1}HNMR 1D spectra specifically showed that multiplet peak at 6.5 ppm is the olefinic proton of cinnamyl moiety (HPhC=CH) near phenyl group while the multiplet peak at 6.3 ppm is the proton next to it (HPhC=CH-CH_2). The singlet at 6.0 ppm is formed by the 2 hydrogen atoms of maleic acid olefinic moiety (OOCHC=CHCOO) due to symmetry in its structure. Two peaks at 4.5 ppm and 3.9 ppm represents the methine proton (Ph_2CH-N), and at the two NCH_2 protons, respectively. The protons on the piperazine formed peaks at 3.5-2 ppm (including DMSO peaks). Peaks at 7.2-7.7 ppm represent 15 aromatic protons (3 Phenyl group). Based on peak integration of cinnamyl olefin proton as standard (unit 1), and the olefinic protons of maleic acid, base: acid ratio is determined to be 1:1. Based on the determined 1:1 stoichiometric ratio, the calculated salt correction factor of 1.31 was used for manufacturing solid dispersions with the maleate salt. In other words, for every gram of CNZ-fb, 0.63 gram of maleic acid was added to establish molar equivalence.

4.3.2 pH-solubility profile

Fig.4.10 shows the pH-solubility profile of CNZ-fb and CNZ maleate salt. pH-solubility values along with final pH at the end of solubility study are reported in Table 4.1. A few different observations can be made from the pH-solubility profile.

Firstly, as expected, the pH-solubility curve for CNZ-fb was flat at higher pH values and spiked up as the pH lowered. The curve reached an inflection point at around pH_{max} of 3. At pH values less than 3, the solubility was lowered to 0.6 mg/ml presumably due to interactions with HCl ion and conversion to the more stable HCl salt. Salt conversion at very low pH values and consequent reduction in solubility and dissolution has been reported in the literature[98].

Secondly, above the pH_{max}, solubility values at any given pH, were found to be similar regardless of whether free base or maleate salt was used. This was expected because at higher pH values, free base is in equilibrium and has the lowest solubility[99]. Below the pH_{max}, different solubility values have often been reported at a given pH when different salt forms are used. Such a phenomenon is attributed to (a) super-saturation and difficulty in nuclei formation and crystallization from salt solution, or (b) genuine differences between salt solubility when different salts are used, or (c) preferential *in situ* conversion of salt to lead to the less soluble, more stable salt form.

Finally, although the initial pH values were spread over the entire pH range from 2 to 9, the final pH values, in the case of free base, were still nearly identical to the initial ones. On the other hand, when maleate salt was used as the starting material, final pH values never exceeded 5.5, because of strong buffer capacity offered by maleate component of the salt (Table 4.1). Such a behavior once again underscores the impact of counterions during dissolution by modulating pH in the micro-layer. Implications of such a finding may be significant in designing of a dosage form. For example, if pH of dissolution media is equal to 6.8, it is quite likely that maleic acid would keep pH in the micro-layer at around 5.5 and thereby would offer higher dissolution profile compared to that from free base alone. Indeed, similar effect of pH modifiers on micro-layer during dissolution profile has been documented in the literature[100,101,102].

As seen from Fig.4.10, at pH values above 3, solubility dropped steeply. As pH increased greater than 4.5, the dissolution rate for free base reduced. Under intestinal pH conditions (pH=6.8), dissolution rate for free base will be much lower than that of its salt forms. On the other hand, at lower pH values (pH=2), dissolution profile for free base would be similar to that of salt form. In order to have sufficient discriminatory power, pH=4.5 was chosen as the dissolution media.

4.3.3 Hot melt extrusion of solid dispersion formulation

Thermogravimetric analysis for CNZ free base (Fig.4.11) showed that CNZ melted at 120 ºC, with decomposition initiating at 171.5 ºC, as indicated by the weight loss. CNZ

maleate salt melted with decomposition starting at around 185 ºC. The binary solid dispersions (CNZ-fb + polymer) were extruded at 125 ºC. For the ternary solid dispersions (CNZ-fb + polymer + acidic counterion) including the matrix with succinic acid (M.P. 187 ºC), it was possible to extrude at lower temperatures (140 ºC) without introducing any plasticizers, which can be attributed to the good miscibility of the succinic acid in the selected polymer matrix. At a constant screw speed of 150 rpm, the torque values for all extrusions were < 25 N cm. A visual micrograph of the glassy nature of the extrudate is shown in Fig.4.12. All extrudes had cinnarizine content of at least 95% as assayed using HPLC.

4. 3.4 Dissolution studies

As seen from Fig.4.13, only 3% CNZ-fb dissolved within 45 min while 12.6% of CNZ maleate was dissolved in pH 4.5. Interestingly, as seen from Fig.4.14, the release rate of CNZ from succinic acid precipitate was significantly lower than that from maleate salt. Perhaps because succinic acid did not form a salt, and consequently was not bound to CNZ in a crystal lattice, it may have preferentially dissolved leaving behind CNZ as a free base. That may explain why release rates from succinic acid system were almost identical to those for the free base.

Additional key observations to be made from Fig.4.13 and Fig.4.14 are as follows. Firstly, there was 6-fold increase in CNZ-fb release rate from its amorphous SD with Kollidon® VA64 when compared to CNZ-fb alone. Such an increased dissolution

behavior is in-line with the well documented finding that amorphous solid dispersions enhance dissolution of poorly soluble drugs[43,103].

Secondly, SD of CNZ-fb containing acidic counterions (i.e. maleic acid or succinic acid) had a significantly faster dissolution rate when compared to the dissolution rate from SD of CNZ-fb + polymer, or from their corresponding physical mixtures, or from CNZ maleate salt. Moreover as seen from Fig.4.13, with increase in the amount of maleic acid (i.e. ratio of CNZ-fb: maleic acid of 1:0.3 and 1:1) in its SD, dissolution rate increased reaching as high as 40% release at 45 min, in comparison to 19% at 45 min from SD containing no acidic counterion. Such a pattern in dissolution enhancement is presumably attributed to maleic acid's ability to reduce pH in the microenvironment layer around CNZ-fb and promoting its dissolution rate. Dissolution rate from SD of CNZ maleate+ polymer (31% at 45 min) and from SD of CNZ-fb + maleic acid (1:0.3) + polymer (27% at 45 min) were similar when molar equivalent amount of maleic acid was used for SD preparation (Fig.4.13). This suggests that upon melt extrusion, the resulting structure of SD, and consequently mechanism of drug dissolution, is similar irrespective of the starting material because components are fused and intimately mixed during melt extrusion.

Thirdly, and more interestingly, drug release from SD of CNZ-fb + succinic acid (1:1) + polymer (Fig.4.14) was significantly higher (56% at 45 min) when compared with that from SD of CNZ-fb + maleic acid (1:1) + polymer (40% at 45 min). In other words, although succinic acid did not form a salt under experimental conditions with CNZ-fb,

the SD with succinic acid (pK_a 4.2 being above the pH_{max}) as a component showed superior dissolution rate when compared to SD with maleic acid (pK_a 1.9 being below the pH_{max}).

All solid dispersion systems were amorphous and exhibited a single dominant phase as indicated by a glass transition temperature (T_g) upon heating (Fig.4.16). It is also interesting to note that for the SD of CNZ-fb + maleic acid (1:0.3 ratio) + polymer the Tg is the same as the SD of CNZ maleate + polymer denoting that both systems are similar and in the same state of miscibility. Compared to that of CNZ-fb alone (Tg ~ 8.9°C), the SD system with or without the acidic counterions helps to shift the Tg to a higher temperature making it a more stable system (Fig.4.15). X-ray patterns confirmed absence of crystallinity (Fig.4.17). Consequently, physical form of the dispersion itself could not have played a significant role in this phenomenon. To test the impact of microenvironment pH, 10% slurry was prepared using deionized water and its pH was measured as a proxy; a practice that is used frequently in the industry[104]. pH values for succinic acid containing slurry was 2.5 versus that for maleic acid system was 1.8, both being below the pH_{max} of the free base. This confirms the role of the acidic counterions in reducing the micro-pH, thereby promoting the dissolution rate of CNZ-fb.

Another important area of the study is the solubility of the acidic counterion itself. If the acid is poorly soluble, it will remain in the micro-layer for a longer time, thereby prolonging the pH effect in promoting drug dissolution. There are evidences in the literature where acidifiers with different aqueous solubility have shown differences in

drug dissolution rate from tablets[105,93]. Because water solubility of succinic acid (58 mg/mL) is less than that of maleic acid (788 mg/mL) by 13-fold, solubility differences could play a potential role in dissolution rate differences seen between their extrudates.

Another possibility is the formation of complexation or ionic interaction between maleic acid or succinic acid and CNZ-fb during melt extrusion. This could thus be an additional mechanism for the improved dissolution rate seen with the SD with the acidic counterions. If such an interaction were occurring, then superior dissolution from SD of CNZ-fb + succinic acid + polymer could be postulated due to the superior solubility of CNZ-succinate salt versus CNZ-maleate. Because CNZ-succinate could not be isolated during salt screening experiments, it was not possible to determine its solubility. But there is evidence to suggest that below pH_{max} of free base, salts can have different solubility values[98]. At pH above pH_{max}, solubility at any given pH should of course be identical regardless whether a salt or a free base was used. One missing piece of the puzzle therefore, was to determine whether salt formation or some kind of complex formation occurred between the acidic counterion and CNZ-fb during melt extrusion.

4.3.5 Investigation of inter-molecular interactions

Raman spectroscopy and Fourier Transform Infrared (FT-IR) spectroscopy belong to the class of vibrational spectroscopy; and have been used quite extensively to study inter molecular interactions in pharmaceutical solids[106,107,108]. Because Raman spectra does not suffer from the large water sorption effects found with FT-IR technique, it can be

employed as a powerful tool to study the components in solid state (e.g. amorphous or crystalline; free solids or bonded) [109]. The use of Raman spectroscopy to reveal acid-base reaction or complex formation in solid dispersions has been highlighted in the literature[110,111,112,113].

In order to evaluate whether CNZ-fb could interact with acidic counterions during melt extrusion, the spectrum of CNZ-fb was compared with that of CNZ maleate and all solid dispersions and their respective physical mixtures. Table 4.2 provides specific wave numbers that illustrate spectral shifts between the different SDs and physical mixtures. CNZ-fb and CNZ maleate were used as positive controls. Single component spectras of maleic acid, succinic acid and Kollidon® VA64 were used as controls.

The characteristic region in the Raman spectra which highlights the spectral shifts between CNZ-fb and CNZ maleate is shown in Figure 4.18 a,b,c,d. Shift from 1655 and 1596 cm^{-1} for the CNZ-fb to 1666 and 1599 cm^{-1} for CNZ maleate is attributed to the stretching of the deprotonated carbonyl (C=O) group of the maleic acid in CNZ maleate. Also, other prominent spectral differences attributed to stretching vibrations included split of 1309 cm^{-1} in free base to 1300 cm^{-1} in CNZ maleate; and shift from 1204 cm^{-1} to 1211 cm^{-1}. These characteristic absorptions in the finger print region CNZ-fb and CNZ salt were used as a reference to understand the state of CNZ in solid dispersions. Relative to the crystalline systems, spectra of the amorphous solid was broader and less resolved; a characteristic that typically reflects the random nature of an amorphous system.

As expected, Raman spectra of CNZ maleate mapped well with that of a physical mixture of (CNZ maleate + polymer). Similarly, spectra of CNZ-fb mapped with spectra of physical mixture of (CNZ-fb+ maleic acid+ polymer). Interestingly, the spectrum of physical mixture (CNZ-fb + maleic acid+ polymer) was different from that of SD prepared at the same molar composition. In fact, SD of (CNZ-fb + maleic acid + polymer) had characteristic peaks that mapped to that of CNZ maleate salt. Moreover as seen from Fig.4.19 a,b,c absorption peaks of SD of (CNZ-fb + maleic acid + polymer) were similar to peaks exhibited by SD of (CNZ maleate + polymer). These findings suggest that CNZ-fb may have reacted with maleic acid during the melt extrusion process to form an *in situ* salt. It is likely that due to the greater molecular mobility in the fused state, the glassy polymer Kollidon® VA64 may have served as a "solvent" to facilitate proton transfer between maleic acid and the nitrogen in piperazine moiety of CNZ-fb to form an *in situ* CNZ maleate. Polyelectrolyte complexes of acidic drug naproxen and basic polymethacrylate powder blends during melt extrusion have been reported[114].

In the case of succinic acid containing system, Raman spectra of physical mixture of the components was strikingly different from that of its solid dispersion, indicating inter-molecular interactions. Because CNZ succinate could not be isolated, its spectra could not be used as a reference. However, upon closer examination, the characteristic peaks from SD of (CNZ-fb + succinic acid) mapped well with those exhibited by CNZ maleate (Table 4.2), suggesting that same set of nitrogen groups in the piperazine ring of CNZ-fb were involved in formation of CNZ salt with succinic acid as well during melt extrusion.

Analyses of Raman spectra help explain why SD of (CNZ-fb + maleic acid + polymer) exhibited faster dissolution rate over SD of (CNZ-fb + polymer). With the possibility of an *in situ* salt formation during extrusion, there is a likelihood that the CNZ succinate salt formed in the SD of (CNZ-fb + succinic acid + polymer) due to its higher solubility than the CNZ maleate salt formed in the SD of (CNZ-fb + maleic acid + polymer) shows a higher dissolution rate.

4.4 Conclusions

This study demonstrated that the addition of an organic dicarboxylic acid such as maleic acid to a solid dispersion system of CNZ-fb and Kollidon® VA64 (neutral polymer) helped to increase CNZ-fb dissolution rate when compared to its dissolution from the cinnarizine maleate salt solid dispersion. Further investigation revealed that inter molecular interactions between maleic acid and CNZ-fb could lead to *in situ* salt formation due to interaction between maleic acid, CNZ-fb and Kollidon® VA64 in the molten state where sufficient molecular mobility may exist, and the polymer may serve as a suitable vehicle for proton transfer. Secondly, it was demonstrated that for the acidic counterion such as succinic acid, which failed to form a crystalline salt under experimental conditions with cinnarizine, a solid dispersion of cinnarizine, neutral polymer and succinic acid showed the highest dissolution rate for cinnarizine. Thirdly, microenvironment pH in the diffusion layer plays an important role in influencing dissolution rate of ionic drugs. In addition, other physicochemical properties of the pH modifier including its solubility and its ability to complex with the active ingredient

should be closely evaluated. Finally, there is generally an opportunity for development scientists to evaluate techniques such as melt extrusion to re-deploy counterions that were terminated following salt screening. A counterion like succinic acid would have been terminated early-on using traditional salt screening techniques; while it was in fact the one that offered the best dissolution rate.

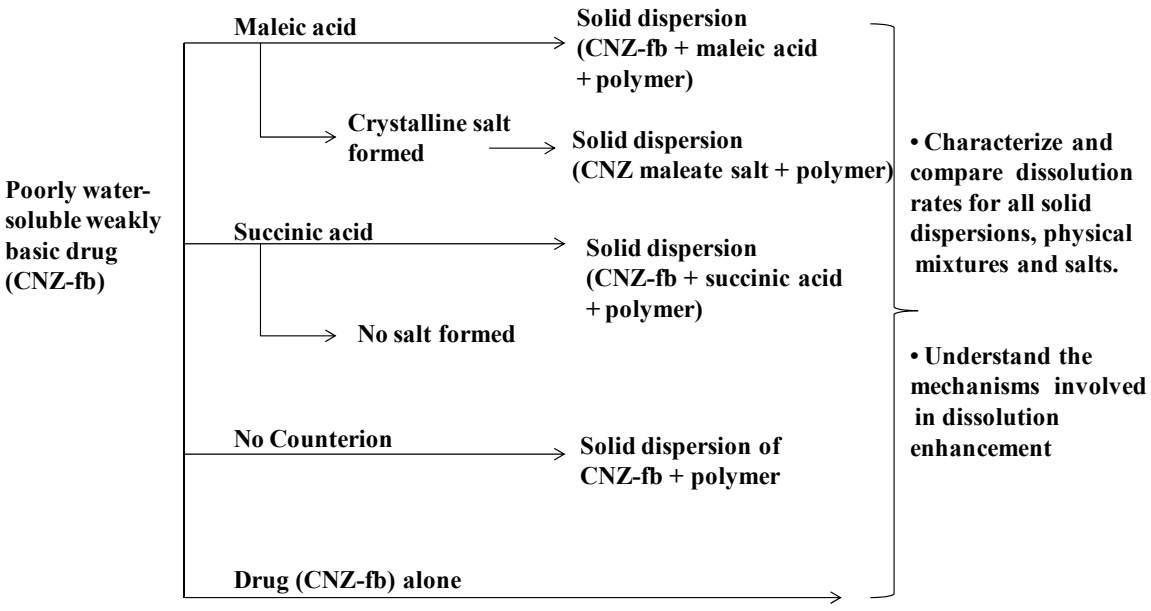

Figure 4.1 Schematic of a mechanistic study to evaluate the effect of acidic counterions in modulating dissolution rates of a poorly soluble weakly basic drug - Cinnarizine.

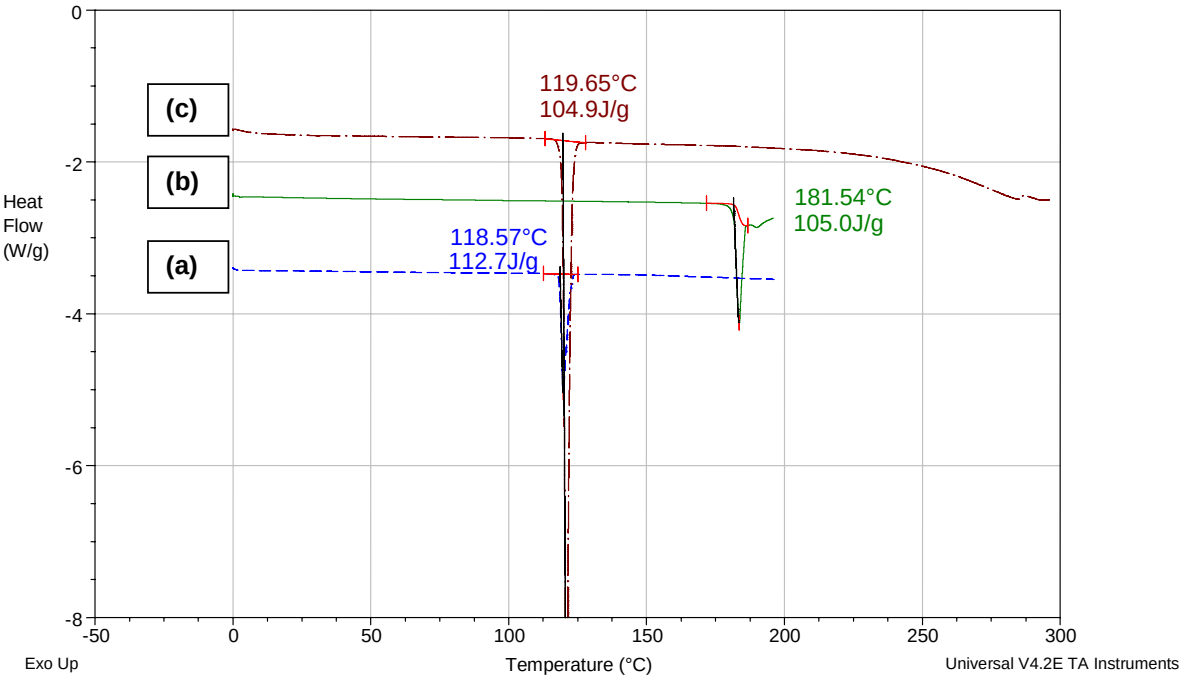

Figure 4.2 Modulated DSC overlay of cinnarizine free base (a), cinnarizine maleate (b) and precipitate of cinnarizine and succinic acid (c).

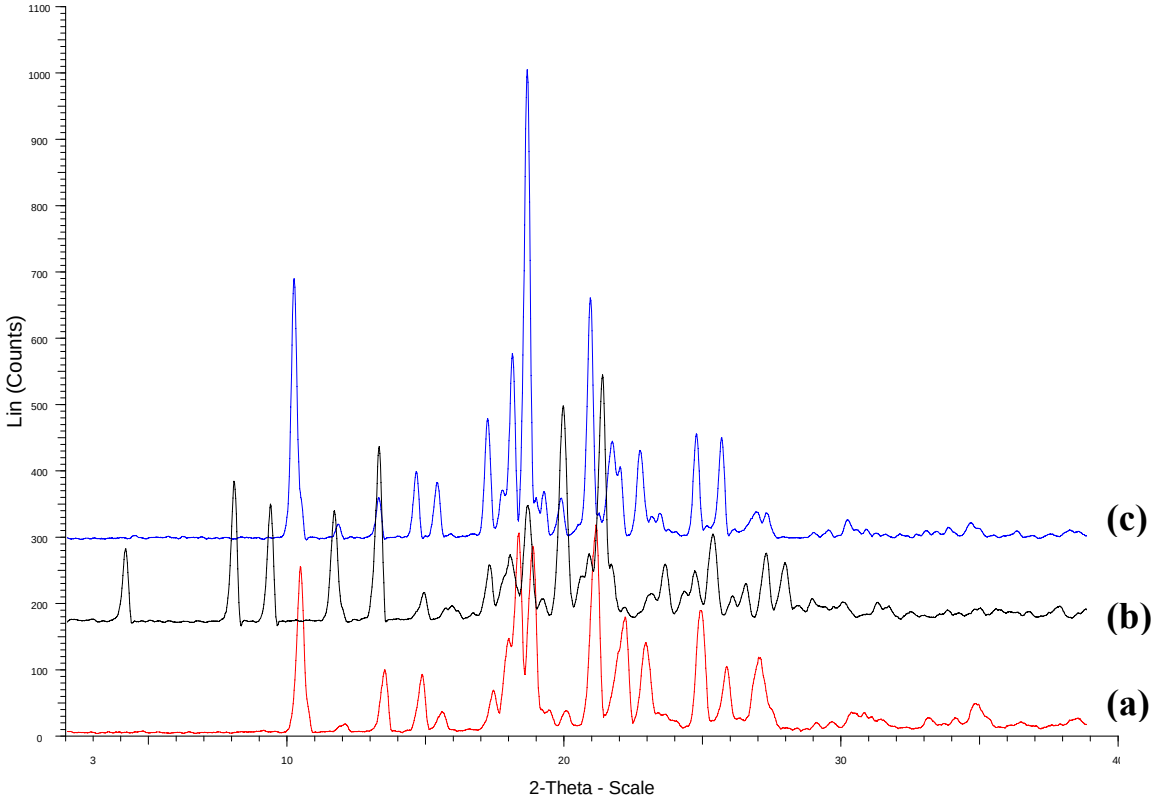

Figure 4.3 X-ray diffraction overlay of cinnarizine free base (a), cinnarizine maleate (b) and precipitate of cinnarizine and succinic acid (c) showing differences between the free base and maleate salt pattern and similarities between the free base and succinic acid precipitate.

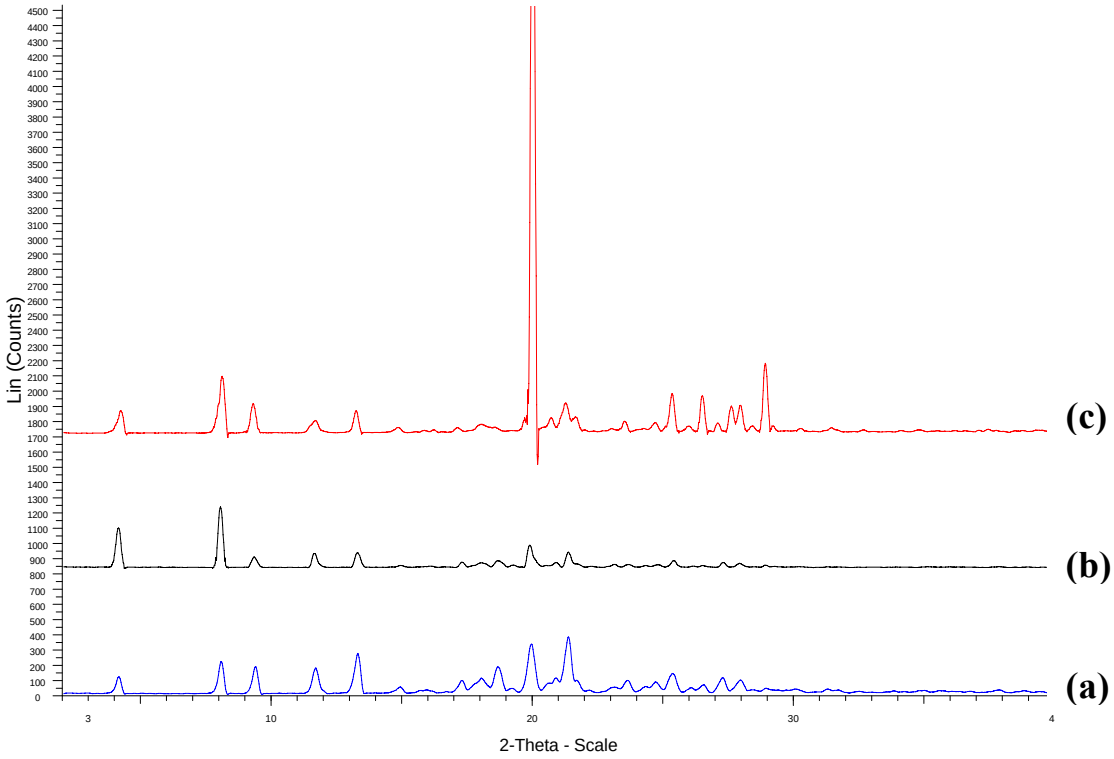

Figure 4.4 X-ray diffraction overlay of cinnarizine maleate synthesized at different scales (a) batch size 525mg (b) batch size 6gms (c) batch size 20gms showing similar crystal packing.

(a)

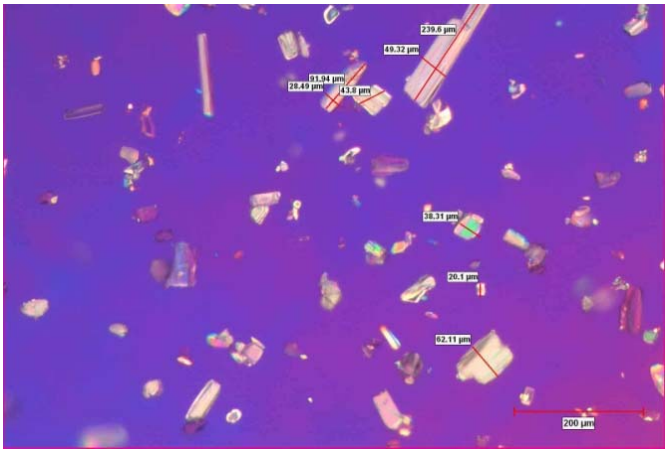

(b)

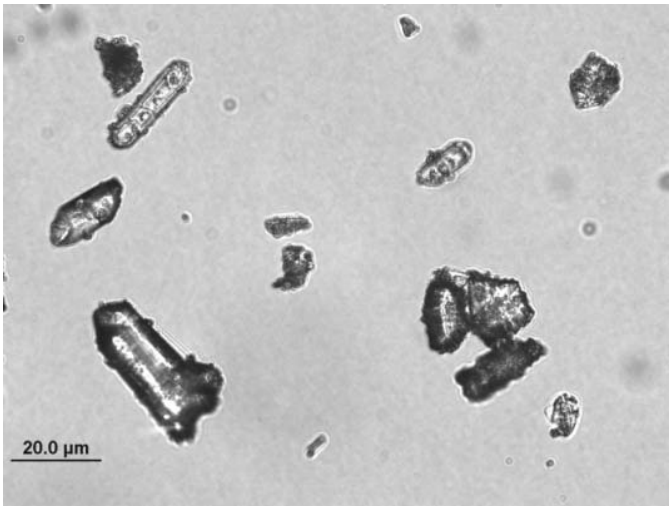

Figure 4.5 Optical microscopic image (a) and confocal microscopy image (b) showing flat elongated morphology of crystalline CNZ-fb.

(a)

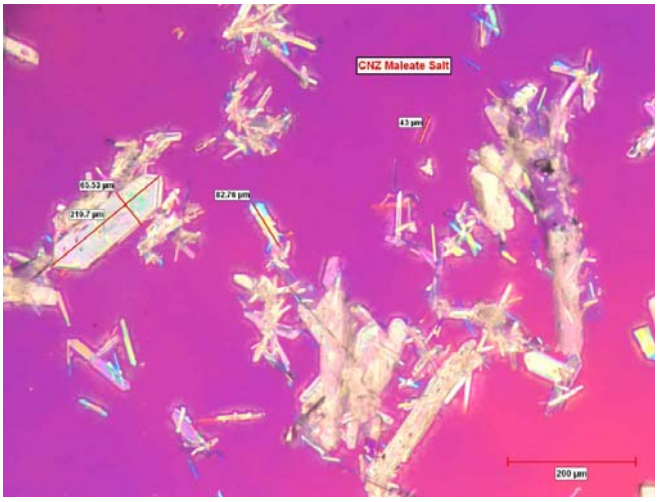

(b)

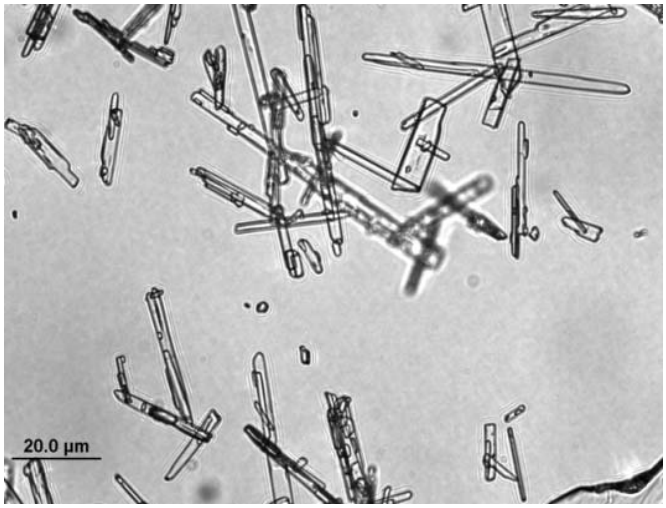

Figure 4.6 Optical microscopic image (a) and confocal microscopy image (b) showing highly crystalline elongated needles of the synthesized CNZ maleate salt.

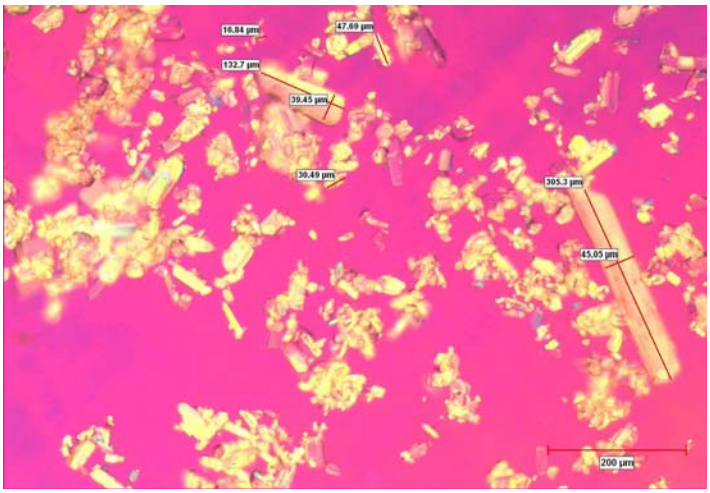

Figure 4.7 Optical microscopic image of the precipitate of CNZ-fb and succinic acid showing the presence of CNZ-fb with the flat elongated crystal morphology.

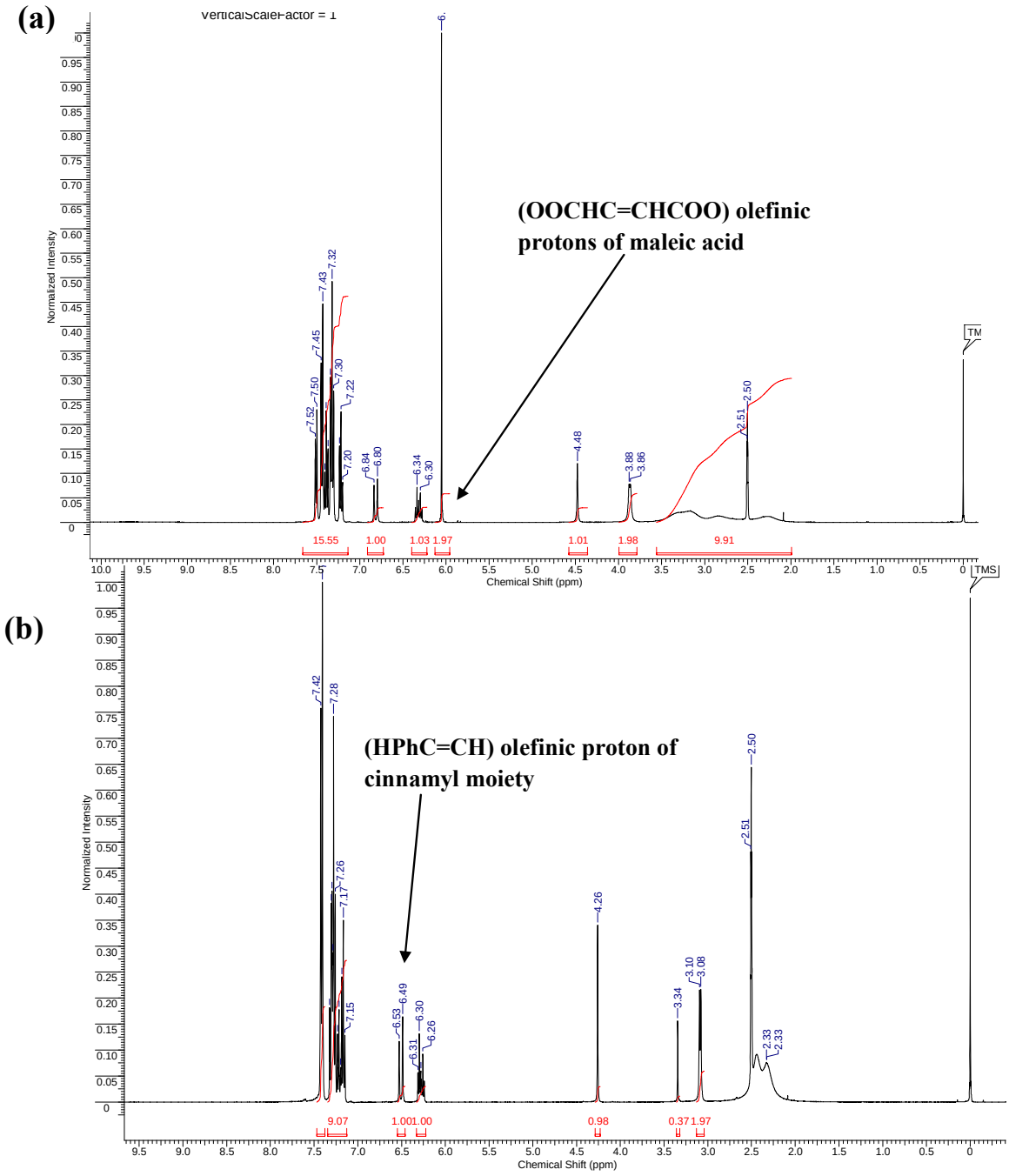

Figure 4.8 ^{1}H NMR spectra of (a) cinnarizine maleate salt and (b) cinnarizine free base indicating the presence of salt and 1:1 stoichiometry.

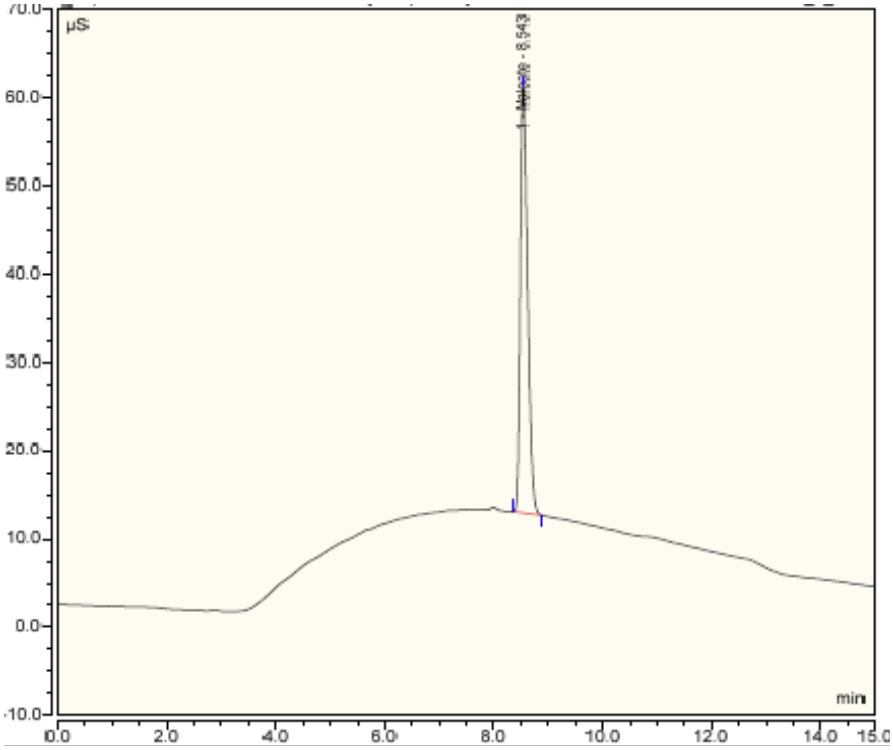

Peak Name	Retention Time (min)	Area (uS*min)	Amount	R-squared	# Cal points	mmol ion	mmol Cpmd	eq of anion
Maleate	**8.54**	**7.443**	**0.2395**	**0.994**	**3**	**0.0021**	**0.0021**	**0.98**

Figure 4.9 Quantification of the maleate counterion in cinnarizine maleate using anion exchange chromatography. Analysis shows 0.98 equivalents of anion present in the salt.

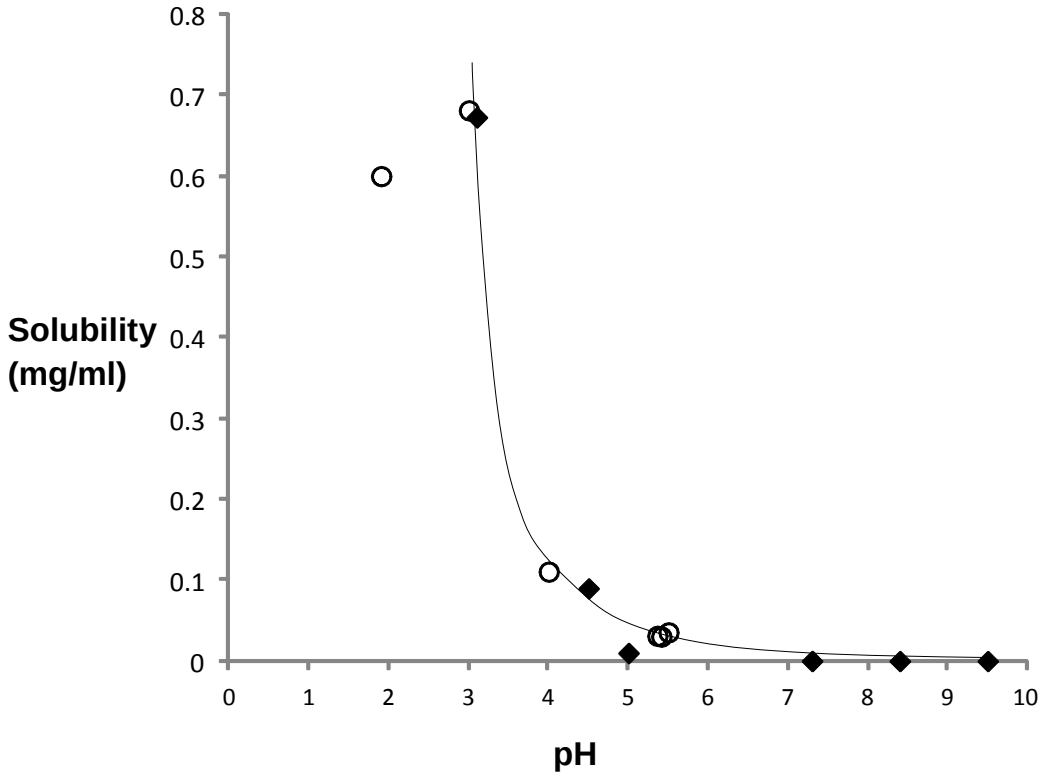

Figure 4.10 pH-solubility profile of cinnarizine free base (♦) and its maleate salt (○) at 25ºC.

	Adjusted initial pH	Final pH
Cinnarizine free base	2.01	3.1
	4.51	5
	6.89	7.3
	7.95	8.4
	8.92	9.5
	Water (6.37)	Water (7.7)
Cinnarizine Maleate	1.99	1.9
	4.51	4
	6.76	5.5
	8.1	5.41
	9.0	5.36
	Water (5.5)	Water (4.2)

Table 4.1 Summary of the shift in pH values from the initial adjusted pH to the final pH measured at the end of equilibration during solubility measurement for CNZ free base and its maleate salt at 25ºC.

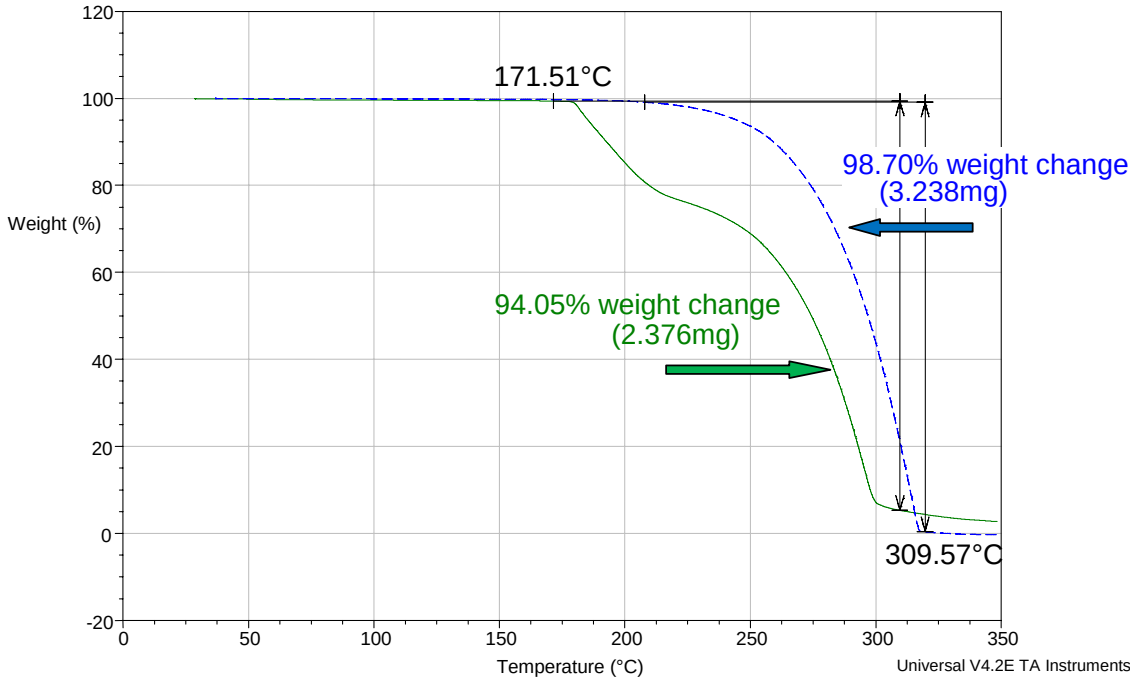

Figure 4.11 Thermogravimetric analysis overlay of cinnarizine free base (blue) and cinnarizine maleate (green) indicating the onset temperature for decomposition.

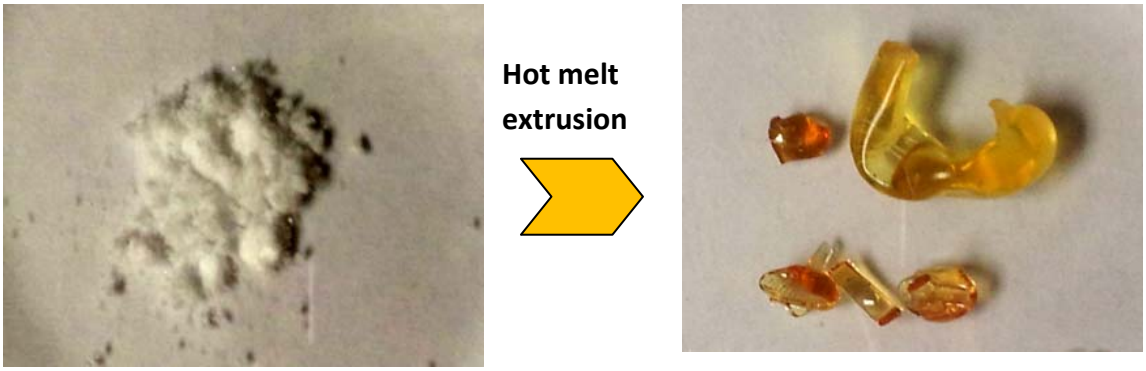

Figure 4.12 Formation of glassy solid dispersion on hot melt extrusion of powder mixtures of CNZ-fb, Kollidon®VA64 with or without maleic or succinic acid.

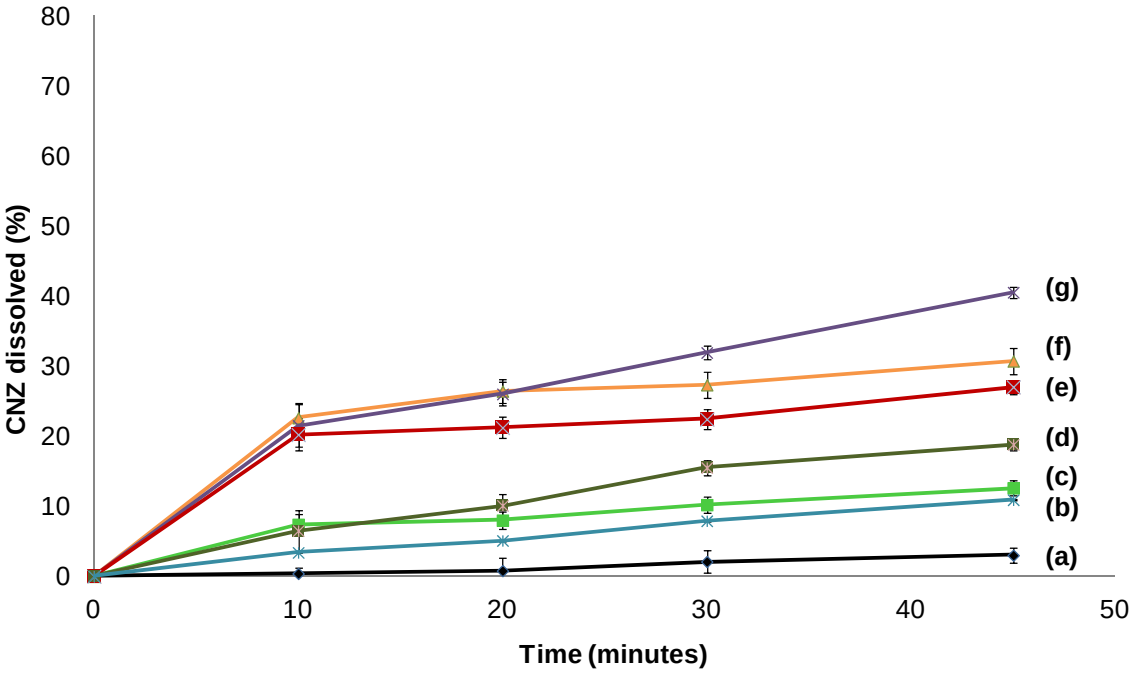

Figure 4.13 Comparison of dissolution rates for capsules containing equivalent to 25 mg CNZ-fb in pH 4.5 acetate buffer using USP Apparatus 1. **(a)** CNZ-fb, **(b)** physical mixture of CNZ-fb+ maleic acid + polymer, **(c)** CNZ maleate salt, **(d)** SD of CNZ-fb + polymer, **(e)** SD of CNZ-fb + maleic acid (in ratio 1:0.3) + polymer, **(f)** SD of CNZ maleate + polymer, **(g)** SD of CNZ-fb + maleic acid (in ratio 1:1) + polymer. Data points are expressed as mean± S.D (n=3).

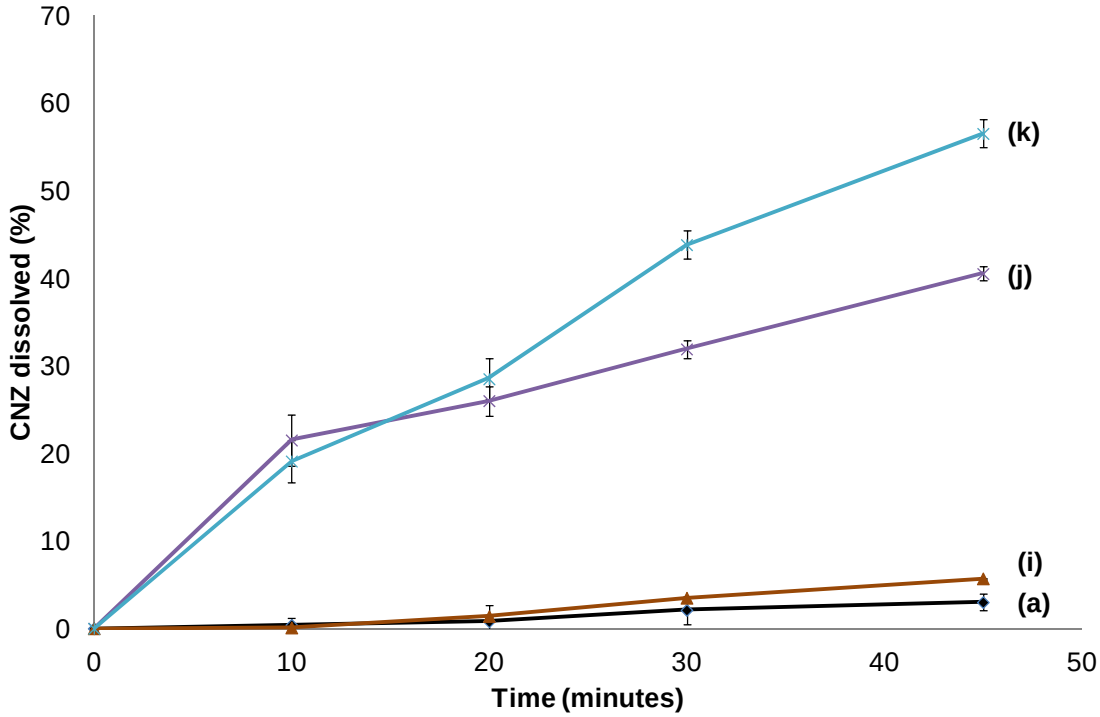

Figure 4.14 Comparison of dissolution rates of CNZ-fb in SD with maleic acid and SD with succinic acid in pH=4.5 acetate buffer using USP Apparatus 1. **(a)** CNZ-fb, **(i)** CNZ-fb and succinic acid precipitate, **(j)** SD of CNZ-fb + maleic acid (in ratio 1:1) + polymer, **(k)** SD of CNZ-fb + succinic acid (in ratio 1:1) + polymer. Data points are expressed as mean± S.D (n=3).

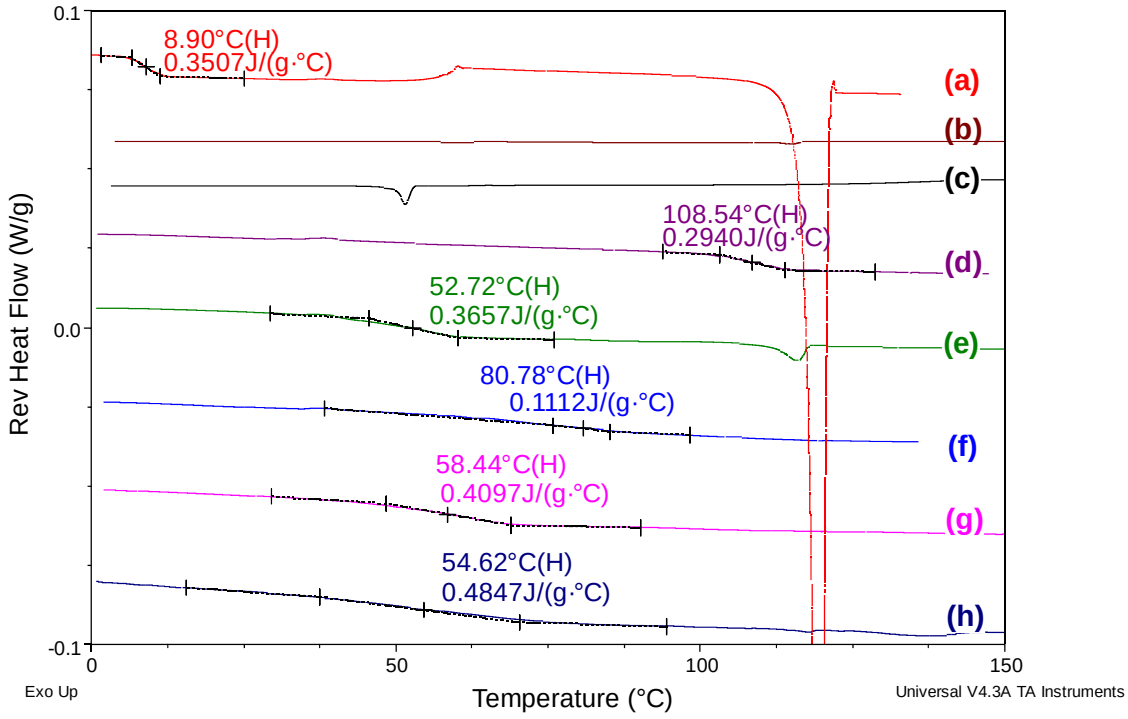

Figure 4.15 Modulated DSC overlays of the solid dispersion systems (a) CNZ-fb (b) Succinic acid (c) Maleic acid (d) Kollidon®VA64 (polymer) (e) CNZ maleate salt (f) Physical mixture of CNZ-fb + polymer (g) Physical mixture of CNZ-fb + maleic acid (1:1 ratio) + polymer (h) Physical mixture of CNZ-fb + succinic acid (1:1 ratio) + polymer, showing the Tg (glass transition temperatures) of the single components and physical mixtures of systems with and without acidic counterions.

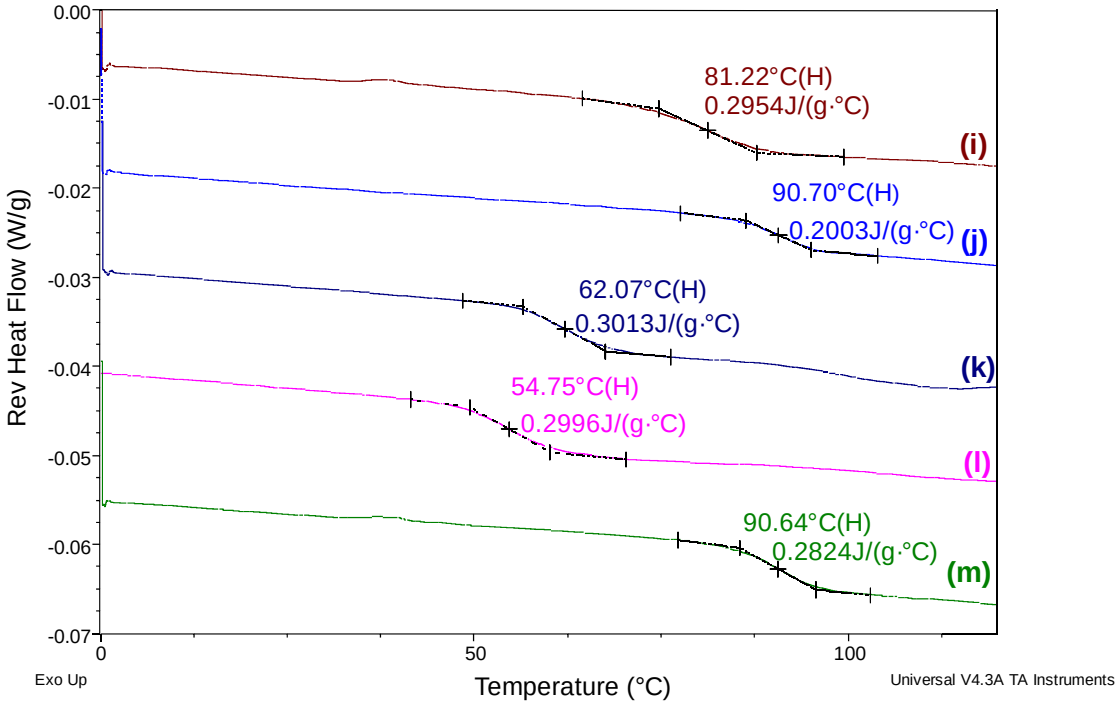

Figure 4.16 Modulated DSC overlays of the solid dispersion systems (i) SD of CNZ-fb + + polymer (j) SD of CNZ-fb + maleic acid (1:0.3 ratio) + polymer (k) SD of CNZ-fb + maleic acid (1:1 ratio) + polymer (l) SD of CNZ-fb + succinic acid (1:1 ratio) + polymer (m) SD of CNZ maleate + polymer, showing amorphous nature with shifts in Tg (glass transition temperatures) for systems with and without acidic counterions.

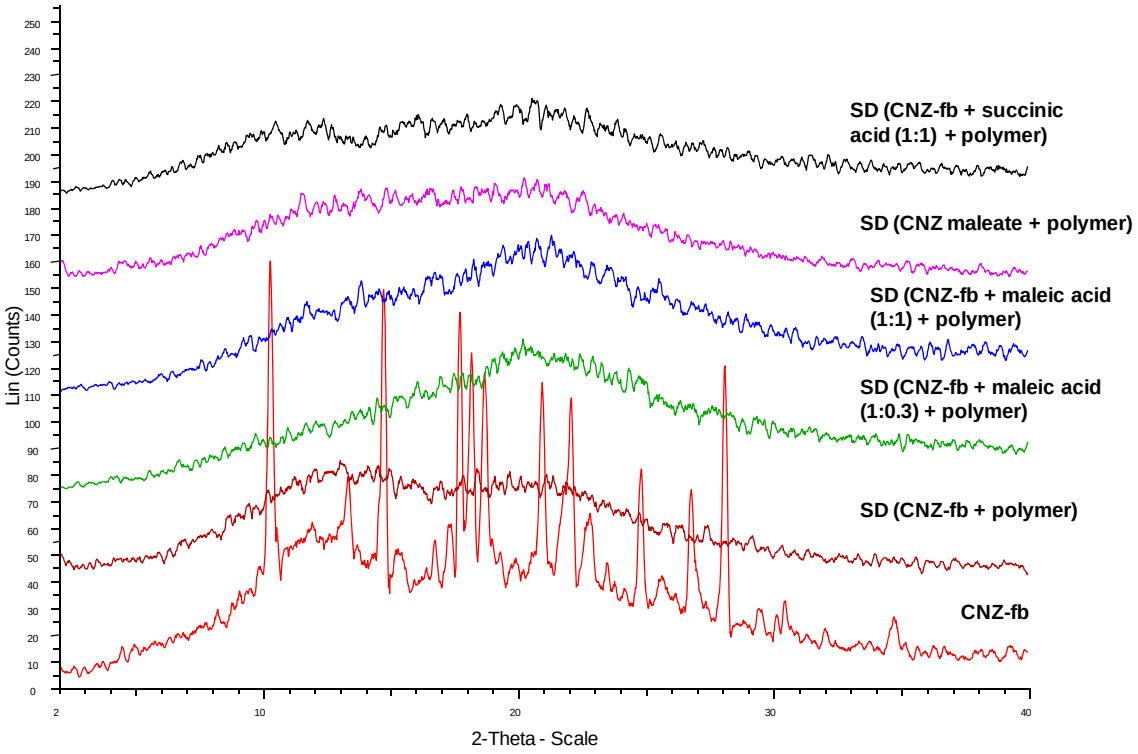

Figure 4.17 X-ray diffraction pattern overlays of the manufactured solid dispersions with maleic acid or succinic acid showing the lack of crystallinity compared to CNZ-fb.

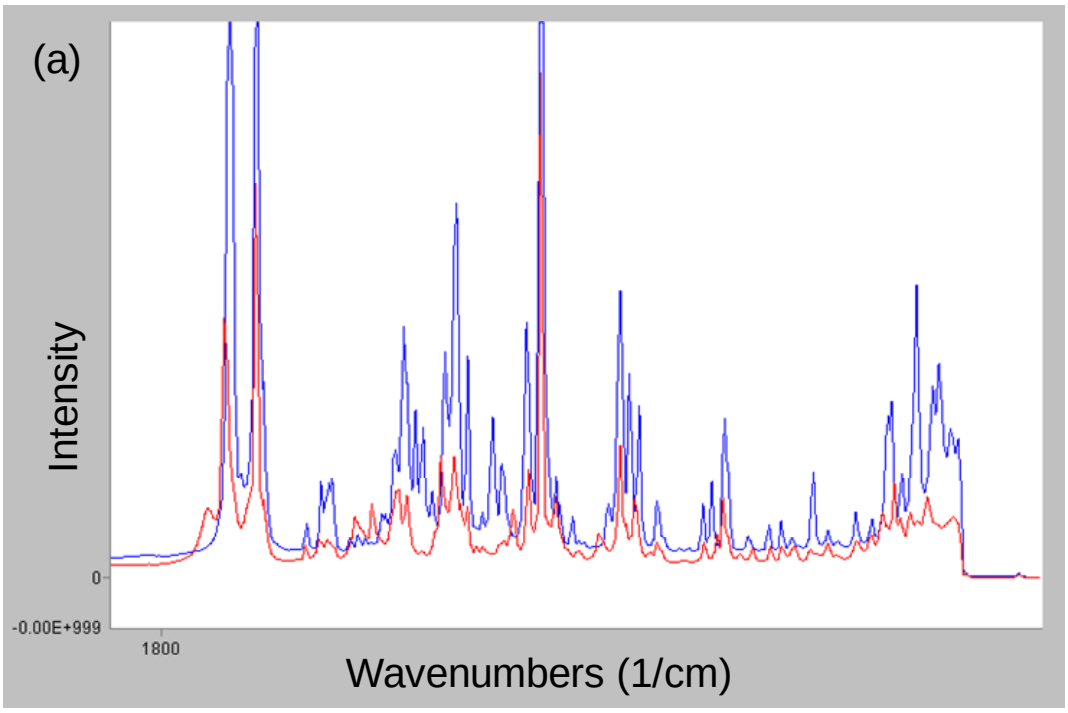

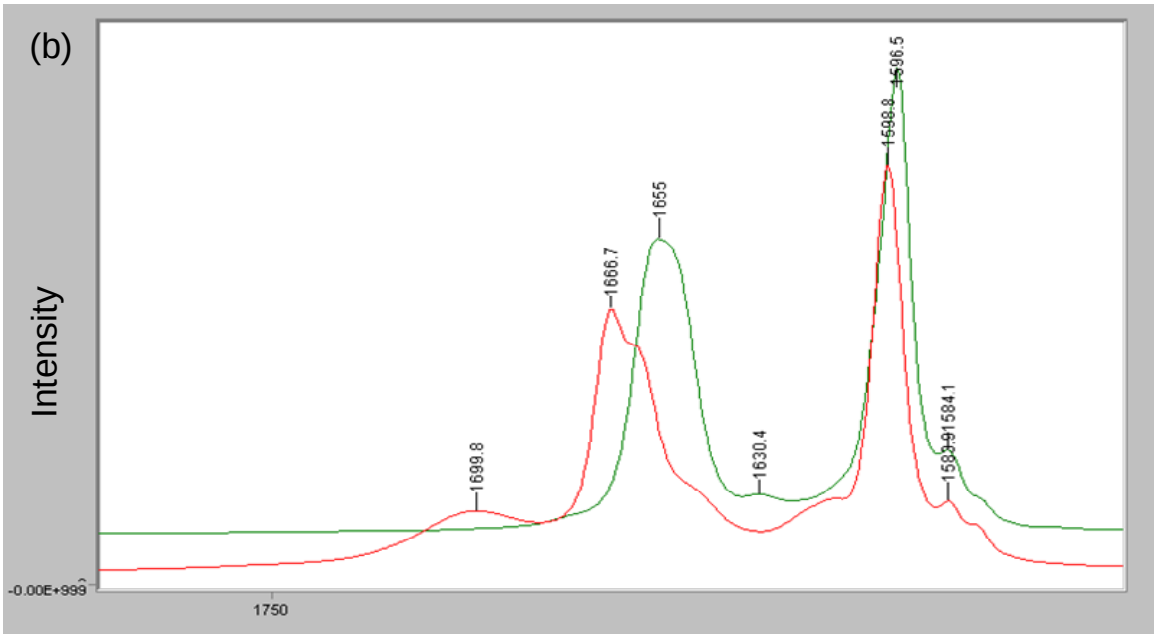

Wavenumbers (1/cm)

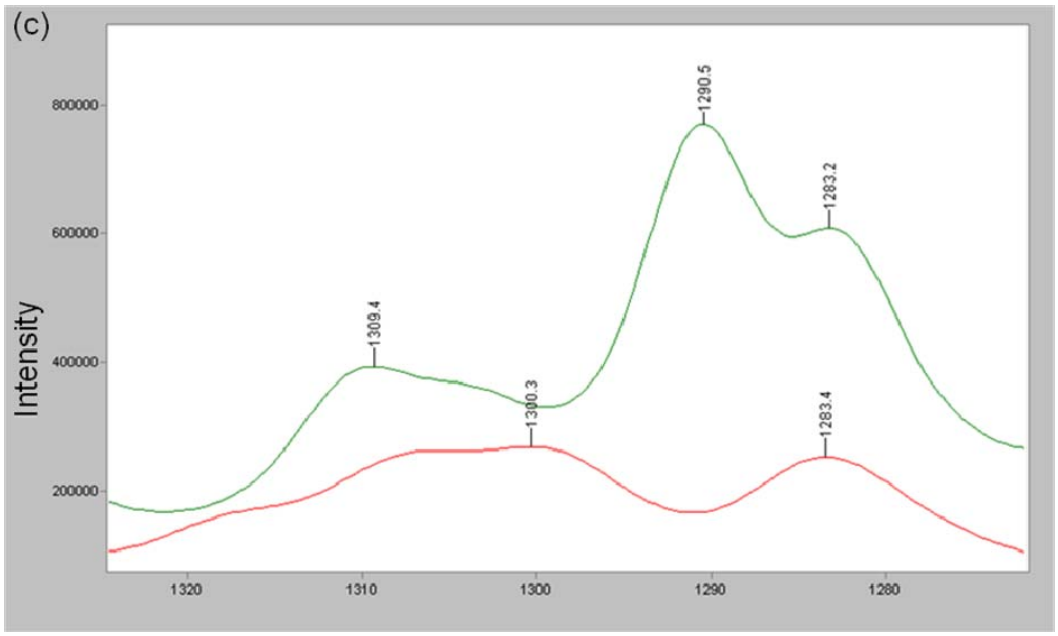
(c)
Intensity
800000
600000
400000
200000
1309.4
1300.3
1290.5
1283.2
1283.4
1320
1310
1300
1290
1280
Wavenumbers (1/cm)

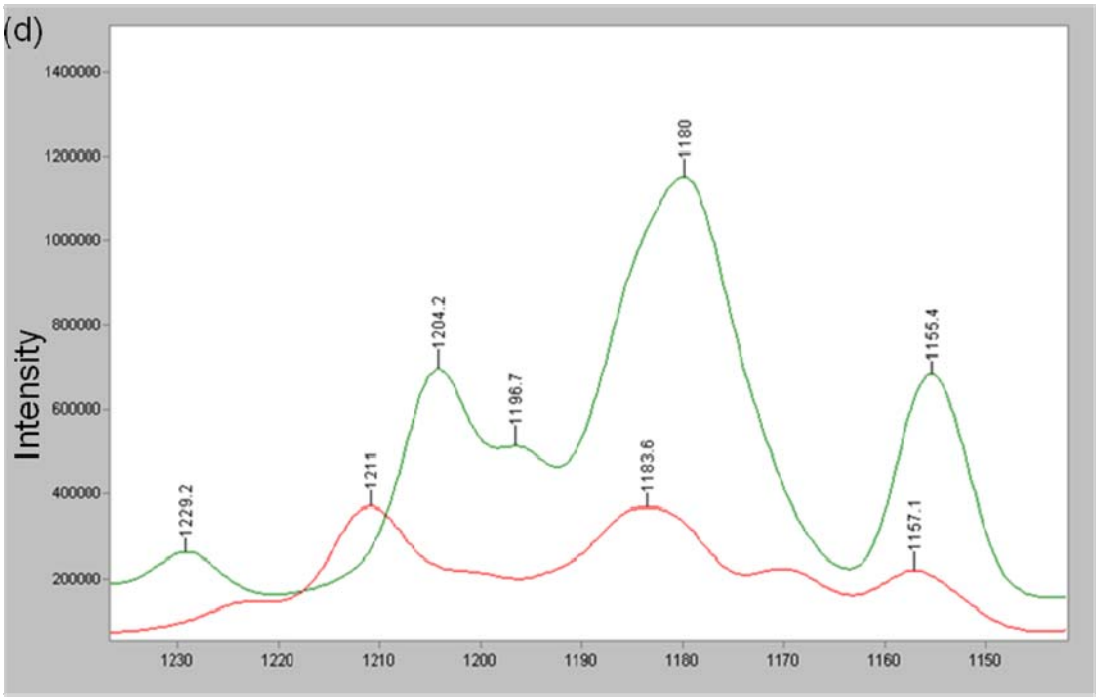
(d)
Intensity
1400000
1200000
1000000
800000
600000
400000
200000
1229.2
1211
1204.2
1196.7
1183.6
1180
1157.1
1155.4
1230
1220
1210
1200
1190
1180
1170
1160
1150
Wavenumbers (1/cm)

Figure 4.18 Overlay of the Raman spectra for CNZ-fb (green) and cinnarizine maleate salt (red) in Figure 4.18(a) with the shifts in frequencies in the range of 750 to 1800 cm^{-1} detailed in Figures 4.18(b),(c),(d).

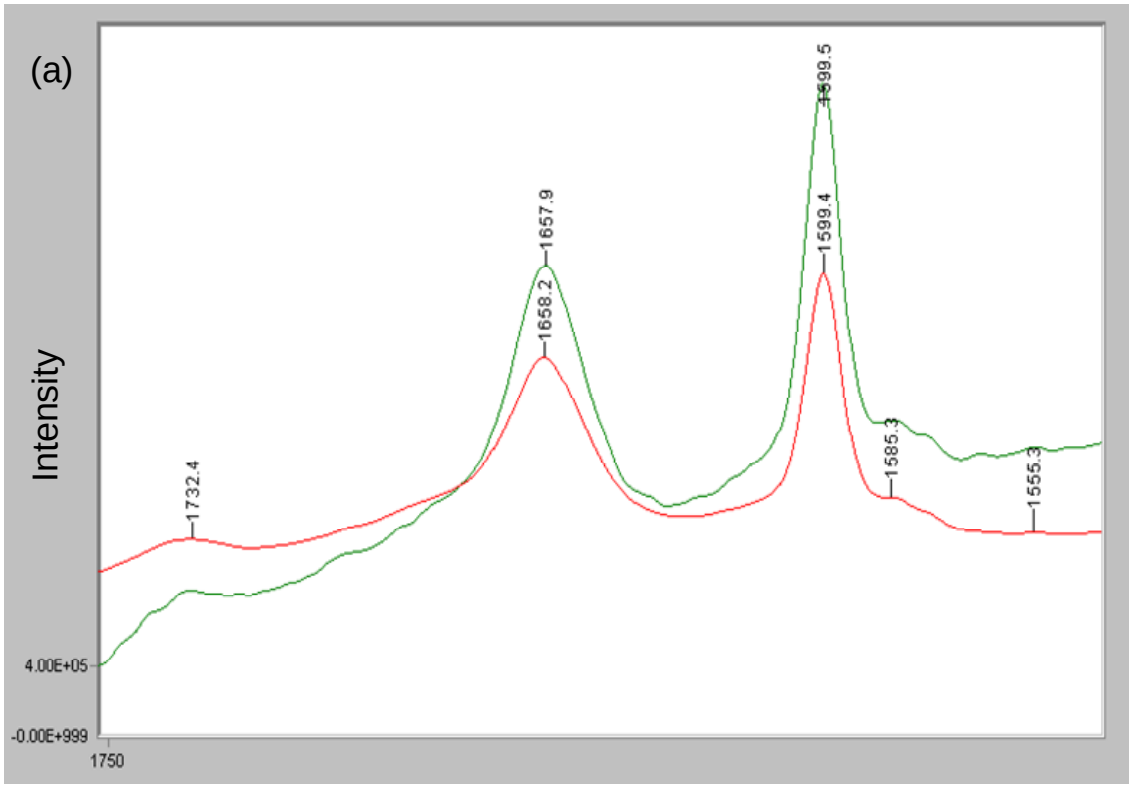

Wavenumbers (1/cm)

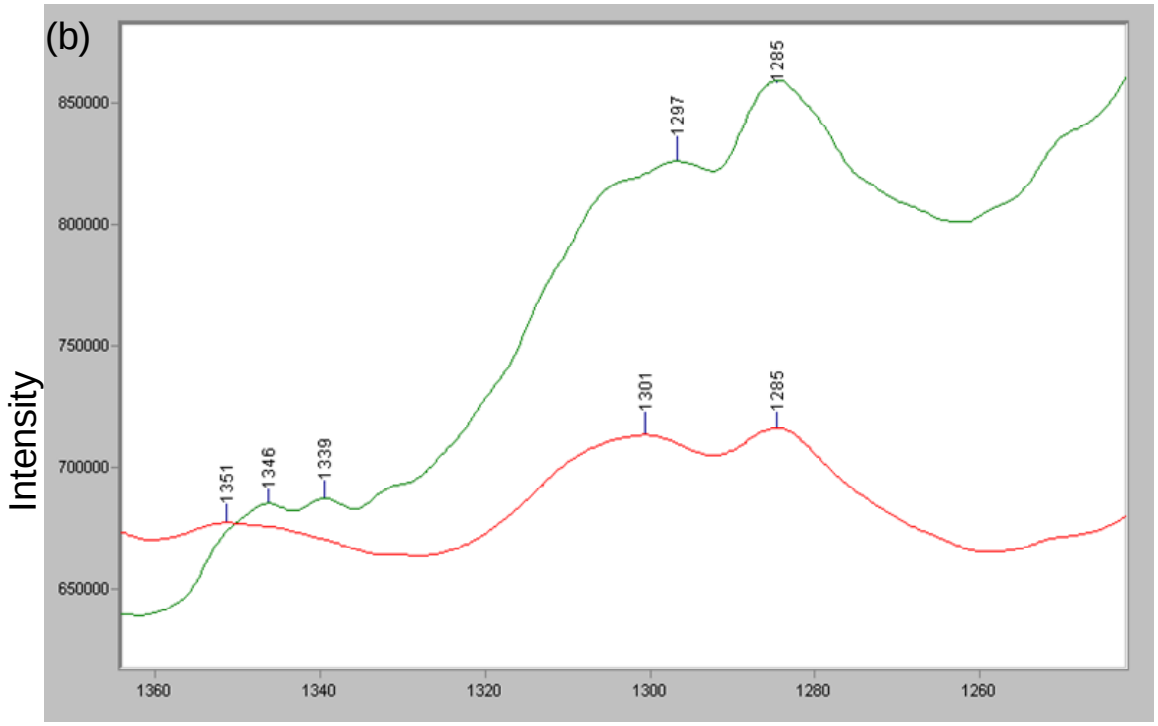

Wavenumbers (1/cm)

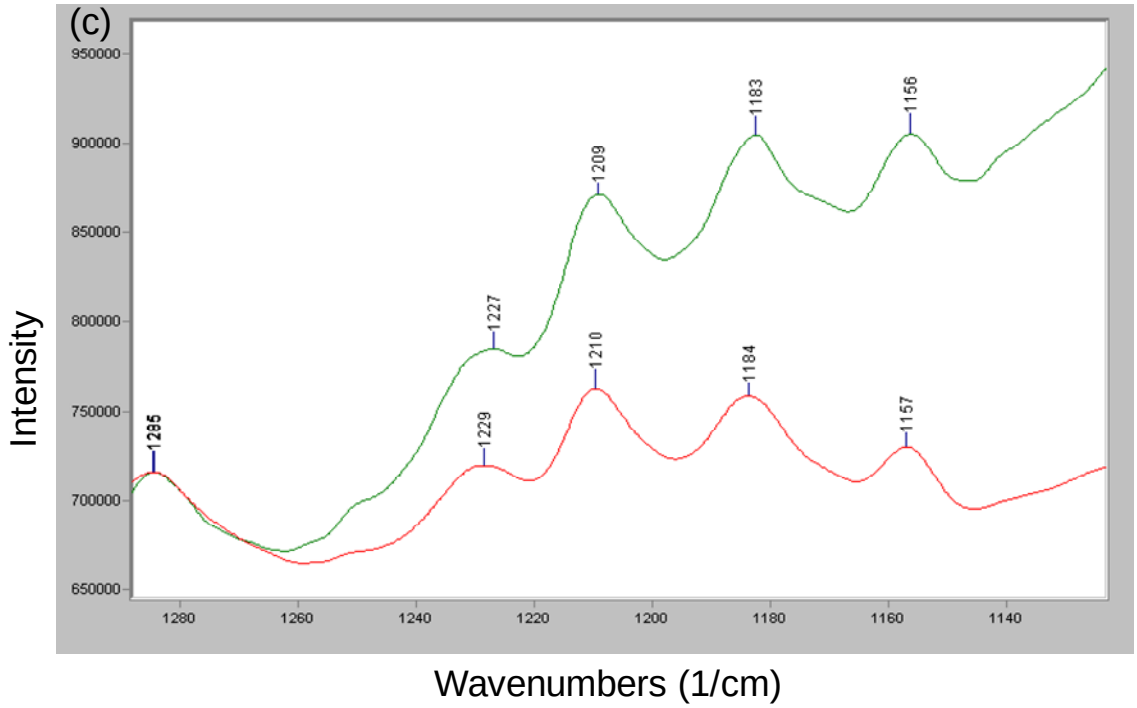

Figure 4.19 Mapping of Raman spectra for SD (CNZ-fb + maleic acid + polymer) (green) and SD (CNZ maleate + polymer) (red) showing the similarities in shifts for the relevant frequencies in the range of 750 to 1800 cm^{-1} compared to that with the CNZ maleate salt as shown in Figures 4.19 (a),(b),(c).

a)	CNZ-fb	PM of CNZ-fb +maleic acid + polymer	CNZ maleate	PM of CNZ maleate +polymer	SD of CNZ-fb + polymer	SD (CNZ-fb +maleic acid + polymer)	SD of CNZ maleate +polymer	SD of CNZ-fb+ maleic acid (1:1 ratio) + polymer
Wave-number (1/cm)	1655	1654.9	1666.7	1659	1654.4	1657.9	1658.2	1658.2
	1596.9	1597.1	1598.6	1599.0	1597.1	1599.3	1599.4	1599.4
	1309.8	1310.7	1300.3	1300.6	1277.9	1284.7	1284.6	1284.7
					1310.1	1300.7	1299.8	1300.2
	1204.2	1204.9	1211.0	1211.2	1205.1	1209.9	1209.1	1209.8

b)	CNZ-fb	PM of CNZ-fb +succinic acid (1:1 ratio) + polymer	SD of CNZ-fb+ succinic acid (1:1 ratio) + polymer
Wave-number (1/cm)	1654.6	1655.9	1658.0
	1596.9	1597.1	1599.5
	1309.8	1310.8	1301.1
	1204.2	1204.8	1210.4

Table 4.2 Summary of the shifts in frequencies from the Raman spectra of the different formulations. (a) shows the characteristic peaks of CNZ-fb (green) present in physical mixtures (PM) and SD without maleic/succinic acid. Peaks of CNZ when present as a maleate salt (red) are detected in the SD (CNZ-fb+ maleic acid+ polymer) and SD (CNZ maleate salt + polymer). (b) shows the differences between the PM and SD with succinic acid as counterion. The characteristic peaks of the CNZ as a salt form (blue) are also observed in the SD with succinic acid.

5 GASTROPLUS™ PREDICTIONS OF *IN VIVO* PK PERFORMANCE OF CINNARIZINE FROM ITS *IN VITRO* DISSOLUTION PROFILE OF THE DEVELOPED SOLID DISPERSIONS AND ITS MARKETED PRODUCT

5.1 Introduction

The initial step in oral drug absorption is disintegration and dissolution from the dosage form. These processes can be affected by many factors, including the physicochemical properties of the drug, formulation design, particle size, physiological pH, and presence of food[115]. For highly soluble drugs (BCS Class I and III), dissolution is not the rate-limiting step in drug absorption. However, for low solubility drugs (BCS Class II) the rate at which the drug goes into solution is an important determinant of drug absorption from the gastrointestinal tract. Additionally, for BCS class II molecules with pH dependent solubility, there is a variable to drug dissolution and absorption due to the changes in the gastrointestinal pH and drug precipitation[116].

Cinnarizine, a piperazine derivative, is currently used for the treatment of cerebral thrombosis, cerebral arteriosclerosis, subarachnoid hemorrhage and other additional indications. An oral formulation of cinnarizine (Stugeron®) is available in clinical practice. However, this formulation exhibits variable dissolution and low bioavailability after oral administration as a consequence of its poor aqueous solubility and wettability[117,118]. Solid dispersion is a well known formulation development process for

improving the solubility and potentially oral bioavailability for such dissolution-rate limited drugs[119,65]. However, the tendency of the drug to precipitate is affected by the degree of supersaturation offered by the formulation. Crystallization of the drug to a less soluble and thermodynamically stable free form can rapidly occur in the microenvironment of the dissolving dosage form. The slower dissolution of the precipitated form can result in incomplete absorption and lower bioavailability. Incorporation of pH modifiers to such dosage forms has been shown to improve their dissolution behavior. The pH modifier is selected to manipulate the drug diffusion layer pH in order to enhance the solubility of the drug in the microenvironment of the dissolving dosage form[120]. This allows the drug to diffuse into the bulk medium and escape precipitation long enough to allow for absorption. In this study, previously developed solid dispersion systems of cinnarizine with acidic counterions such as maleic acid and succinic acid have been used to determine their dissolution enhancement potential for cinnarizine. The chosen dissolution medium was pH 6.8 + 0.1% sodium lauryl sulfate which being physiologically relevant and a non-sink condition for the 25 mg dose of cinnarizine, provided sufficient discriminatory power for the various formulations. An *in vitro* dissolution comparison is made between the marketed tablet formulation of cinnarizine (Stugeron® 25 mg) and the developed acidified solid dispersions. The nature of the dissolution assay (sink versus non-sink, and rate and extent of supersaturation) can impact the ability to effectively use the dissolution data in the assessment of *in vivo* performance[121]. Predictive computational model such as Advanced Compartmental and Transit (ACAT) Model in Gastroplus™ has been utilized to make successful predictions of several orally administered drugs[122,123,124]. Gastroplus™ uses

convolution algorithms to predict the *in vivo* plasma concentration-time profiles based on the dissolution data. In this assessment, Gastroplus™ has been used to compare the developed solid dispersions and the marketed tablet dosage form based on the observed *in vitro* dissolution data.

5.2 Materials and Methods

5.2.1 Materials

Cinnarizine ($C_{26}H_{28}N_2$; pk_a 1.9 and 7.5) was purchased from Sigma Aldrich (St. Louis, MO) and was used as the model compound due to its low aqueous solubility (2 µg/ml. Marketed product containing 25 mg cinnarizine, Stugeron® tablets was purchased from manufacturer Janssen Cilag, India. Binary solid dispersions containing cinnarizine free base and neutral polymer Kollidon® VA64 and ternary solid dispersion systems containing cinnarizine free base, neutral polymer and acidic counterion were manufactured as detailed in section 4.2. All materials were used as received.

5.2.2 *In Vitro* Dissolution Study

Dissolution studies were performed in 500 mL of pH 6.8 phosphate buffer + 0.1% sodium lauryl sulfate using USP basket apparatus (Varian™, Cary, NC). Basket speed was set to 100 rpm; and the dissolution study temperature was maintained at 37±0.5 ºC. Size 3, pink, opaque hard gelatin capsules were filled with solid dispersions containing

25 mg equivalents of cinnarizine. For the marketed tablet, USP paddle apparatus at 50 rpm paddle speed was used for dissolution testing under the same conditions. Due to the very low solubility of cinnarizine in pH 6.8 (0.008 mg/ml), there was no sink condition established for 25 mg dose of cinnarizine. This made the dissolution method discriminatory. pH of bulk media was checked before and after dissolution; bulk pH did not change at the end of dissolution. 10mL of aliquots were siphoned at pre-defined time-points (10, 20, 30 and 45 min), and passed through 0.45 micron PVDF filter. In order to avoid precipitation of cinnarizine prior to HPLC analysis, 600 µL of filtered aliquot was added to 400 µL of acetonitrile. All dissolution aliquots were analyzed using HPLC. Each dissolution study was performed in triplicates (n=3).

5.2.3 HPLC analysis

Concentrations of cinnarizine in the samples were determined using Waters 2695 Separations Module with a Waters 2487 dual λ absorbance detector HPLC system at a wavelength of 254 nm using a Waters Xterra MS C8, 3.5 µm, 4.6 x 50 mm column (Waters Corporation, USA). All measurements were performed at an injection volume of 10 µL using a mobile phase mixture of acetonitrile (50%) in water (50%) with 0.1% TFA pumped at a flow rate of 1ml/min, and at temperature of 30 ºC using a column oven. These conditions resulted in an elution time of around 1.5 min for cinnarizine. Calibration curves were constructed using standard solutions of known concentrations. Chromeleon™ software was used to integrate the peak areas.

5.2.4 Gastroplus™ Simulations

Gastroplus™ (version 7.0, Simulations Plus, Inc., Lancaster, CA, USA) was used to estimate absorption and pharmacokinetics (PK) for the formulated solid dispersions of cinnarizine and its commercial tablet dosage that were tested using the *in vitro* dissolution measurements. The program requires insertion of relevant physicochemical, physiological and pharmacokinetic input data. The input values of physicochemical data including pK_a, pH-solubility profile, log D, bulk density, particle size distribution, cinnarizine dose were used by the software to calculate the drug concentration in each compartment. A summary of these and other model parameters is presented in Table 5.1. The rat permeability (P_{eff}) of 0.123 x 10^{-4} cm/s as reported by Katneni et al.[125] was converted to estimated human effective permeability within the program. The relevant elimination parameters were estimated by fitting the observed oral PK data for cinnarizine reported by Rodger HJ et. al[94], in a single compartment elimination model using PK Plus™ Module within Gastroplus™. Integral tablet dosage form model was selected in Gastroplus™.

5.2.5 Statistical Analysis

Dissolution data obtained were analyzed using descriptive statistics, single factor analysis of variance (ANOVA) and presented as mean value ± the standard deviation (SD) from three independent measurements in separate experiments. The comparison among groups

was performed by the independent sample Student's *t* – tests. The difference between variants is considered significant if $P < 0.05$.

5.3 Results and Discussion

5.3.1 *In vitro* dissolution studies

As shown in Fig.5.1, solid dispersion of CNZ-fb and polymer showed a higher dissolution rate of CNZ-fb (17.3% dissolved at 45 min) compared to the marketed tablet form (10.5% dissolved at 45 min). Such enhancement in dissolution rate is well documented when using solid dispersion as formulation technique[126], wherein the physical form of CNZ-fb is altered to amorphous state rather than the crystalline form which is found in the conventional tablet dosage form. As expected, the physical mixture of the crystalline CNZ-fb, polymer and maleic acid showed a slightly lower dissolution rate (7.1% dissolved at 45 min) compared to the reference marketed tablet. As shown in section 4, inclusion of acidic counterions during solid dispersion preparation has proven to be beneficial to enhance release rate of CNZ-fb from the formulation matrix in media that otherwise it has very low solubility. Solid dispersions with maleic acid and succinic acid as counterion showed a 4-fold and 5-fold increase respectively, in the dissolution rate of CNZ-fb compared to the reference tablet (Fig.5.1). This marked improvement in the dissolution of CNZ-fb can be attributed to a few different reasons. First, being the amorphous nature of CNZ-fb in the solid dispersions which showcases a higher solubility than its crystalline form. Second, the influence of micro-environmental pH in the drug diffusion layer during dissolution process. Water soluble acidic counterions such as

maleic and succinic acid are capable of reducing the pH of the dissolving layer to keep the solubility of CNZ-fb much higher than that it would be in the higher pH of the bulk dissolution media. Another mechanism for dissolution enhancement, as described in section 4.3, is the *in situ* salt formation of CNZ-fb with the acidic counterions occurring during the formation of solid dispersion by melt extrusion.

5.3.2 Gastroplus™ modeling

Human PK data for intravenous formulation of CNZ is not available[95]. Hence, human oral PK data for the mean plasma levels of CNZ (Table 5.2) when administered as a tablet was chosen as the reference for this purpose[94]. Additionally, with only intravenous PK data available in a dog model, the relative bioavailability of cinnarizine oral dose from in humans was assumed to be similar to that of dog model at 46.4%. Hence, for the cited oral dose of 75 mg, the absorbed dose was estimated to be 34.8 mg. PK parameters were obtained from the PKPlus module in Gastroplus™ using the mean plasma-concentration profile following oral administration of 75 mg CNZ tablets as shown in Table 5.3. One, two, three-compartment PK models were evaluated with the one-compartment model providing the best fit. A similar finding has been reported by Rodgers et. al[94], when they used a digital computer non-linear least squares program for the same set of oral plasma data. With the assumption of linear PK, this absorption model was subsequently used to predict trends observed in *in vivo* data with varying dose and compositionally different solid dispersion formulations. Firstly, the *in vitro* dissolution profile generated at a relevant physiological pH (pH =6.8) for 25 mg CNZ tablet (Stugeron®) was used to simulate and predict the oral plasma profile in humans as shown

in Fig.5.2. This is considered as the reference formulation which is used for comparison for the developed solid dispersion formulations of the same dose (i.e., 25 mg) of CNZ-fb. Subsequently, simulated *in vivo* plasma concentration-time profiles were generated for each formulation (solid dispersions with and without acidic counterions) using their respective *in vitro* dissolution profiles. The overlay of the predicted human plasma profiles comparing the developed solid dispersion formulations to the commercially available Stugeron® 25 mg CNZ tablet is shown in Fig.5.3. All the PK parameters are listed in Table 5.4 for comparison. The T_{max} is very similar for all the formulations indicating similar disintegration times for both the tablet and solid dispersion systems. It is quite interesting that the AUC for the predicted *in vivo* plasma profiles (Fig.5.3) follow the same rank order of the *in vitro* dissolution profiles (Fig.5.1): SD with succinic acid > SD with maleic acid > SD with no acidic counterion > Reference tablet > Physical mixture of the SD components. The *in vivo* AUC_{0-72} enhancement from the SDs with maleic acid and succinic acid as counterion in comparison to the reference tablet is 1.9 and 2.1 respectively. The *in vitro* differences between the SDs with the two different counterions translate into *in vivo* differences of similar magnitude with the SD of CNZ with the succinic acid providing the highest C_{max} and AUC for cinnarizine among all the tested formulations.

5.4 Conclusions

For BCS class II molecules such as CNZ-fb, the rate of dissolution of drug is the principal limitation to its oral absorption. Comparison of the developed solid dispersion formulations of CNZ-fb with maleic/succinic acid to its commercially available tablets

Stugeron® showed a marked improvement in the dissolution rate and improving its solubility in the physiologically relevant pH of 6.8. Using the oral human plasma profile for CNZ tablets reported by Rodger et.al.[94], an absorption model was created to simulate the generated *in vitro* dissolution profile for the different formulations to their predicted *in vivo* plasma profiles. CNZ solid dispersions with acidic counterions showed the most improvement both *in vitro* and *in vivo* compared when compared with the solid dispersion without the acidifier and the 25 mg marketed CNZ tablet. Based on the results obtained from Gastroplus™ predictions, it is expected that the designed solid dispersions with observed *in vitro* dissolution enhancement for CNZ may provide *in vivo* PK performance improvements over the presently marketed tablets.

Parameter	Value
pK_a	1.9, 7.5
logD	4.6 at pH 7.4
Solubility @pH (mg/mL)	0.0001174 @ pH = 7.3
Human P_{eff} (x 10^{-4} cm/s)	0.549
Mean particle radius (μm)	D50 = 25
Drug particle density (g/mL)	1.2
Mean precipitation time (sec)	90
Diffusion coefficient (x 10^{-5} cm^2/s)	0.6878
Dose (mg)	25
Dose volume (mL)	250
Oral formulation of Cinnarizine	25mg marketed tablet dosage form, 25mg oral solid dispersion capsule
Physiology	Human- physiological-fasted

Table 5.1 List of parameters (measured or optimized) for Gastroplus™ absorption model.

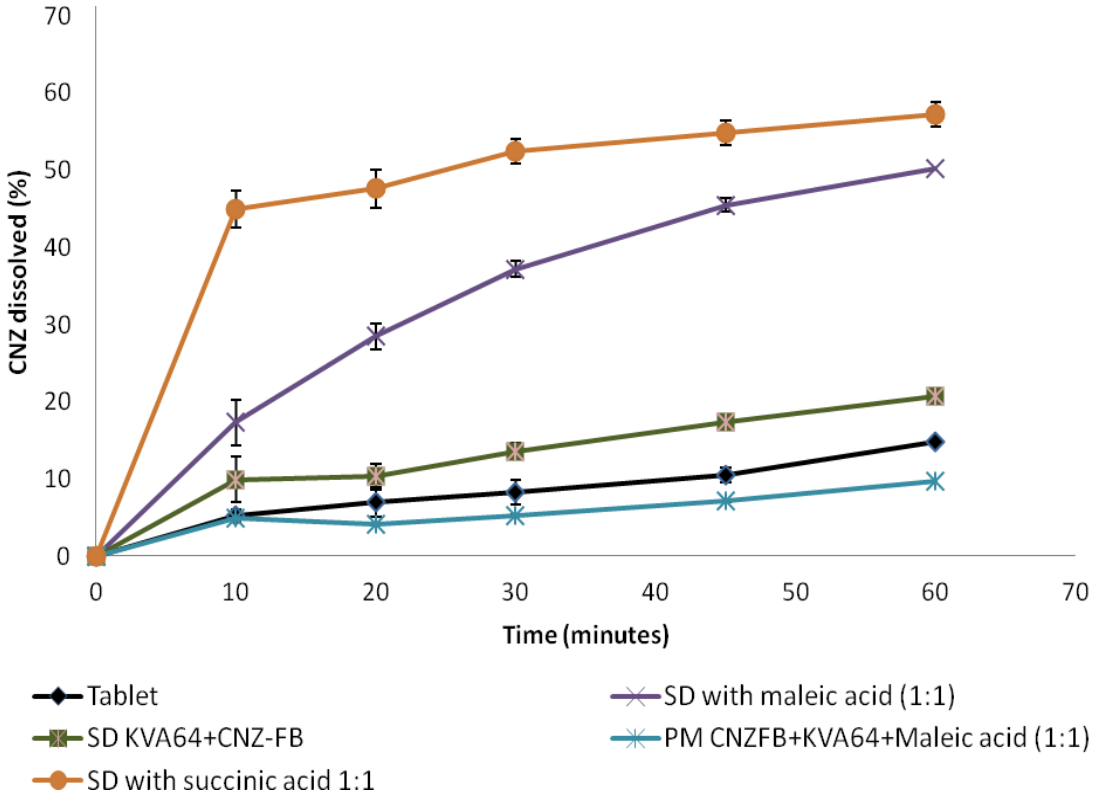

Figure 5.1 Comparison of dissolution rates of cinnarizine (CNZ) from capsules containing ternary solid dispersions with counterion 1 (i.e. maleic acid) and counterion 2 (i.e. succinic acid) in pH=6.8 phosphate buffer + 0.1% SLS. Dissolution profile for the marketed tablet (Stugeron®, 25mg cinnarizine) is generated in the same media for comparative evaluation of the developed solid dispersion formulations. Data points are expressed as mean± S.D (n=3).

Time (h)	Plasma concentration from tablets (ng/mL)
1	32 (20-300)
2	116 (60-560)
3	131 (70-410)
4	125 (70-290)
5	100 (50-200)
6	81 (40-160)
8	46 (30-110)
10	31 (10-70)

Table 5.2 Mean (range) plasma concentrations of cinnarizine after single oral dose of 75mg Stugeron® tablets to twelve subjects (95).

PK parameter	Value
CL [L/h/kg]	0.57505
Vc [L/Kg]	2.2134
T ½ [h]	2.67

Table 5.3 Optimized PK parameters from Gastroplus™ for oral mean plasma profile of cinnarizine tablet fitted to a one-compartment, open pharmacokinetic model.

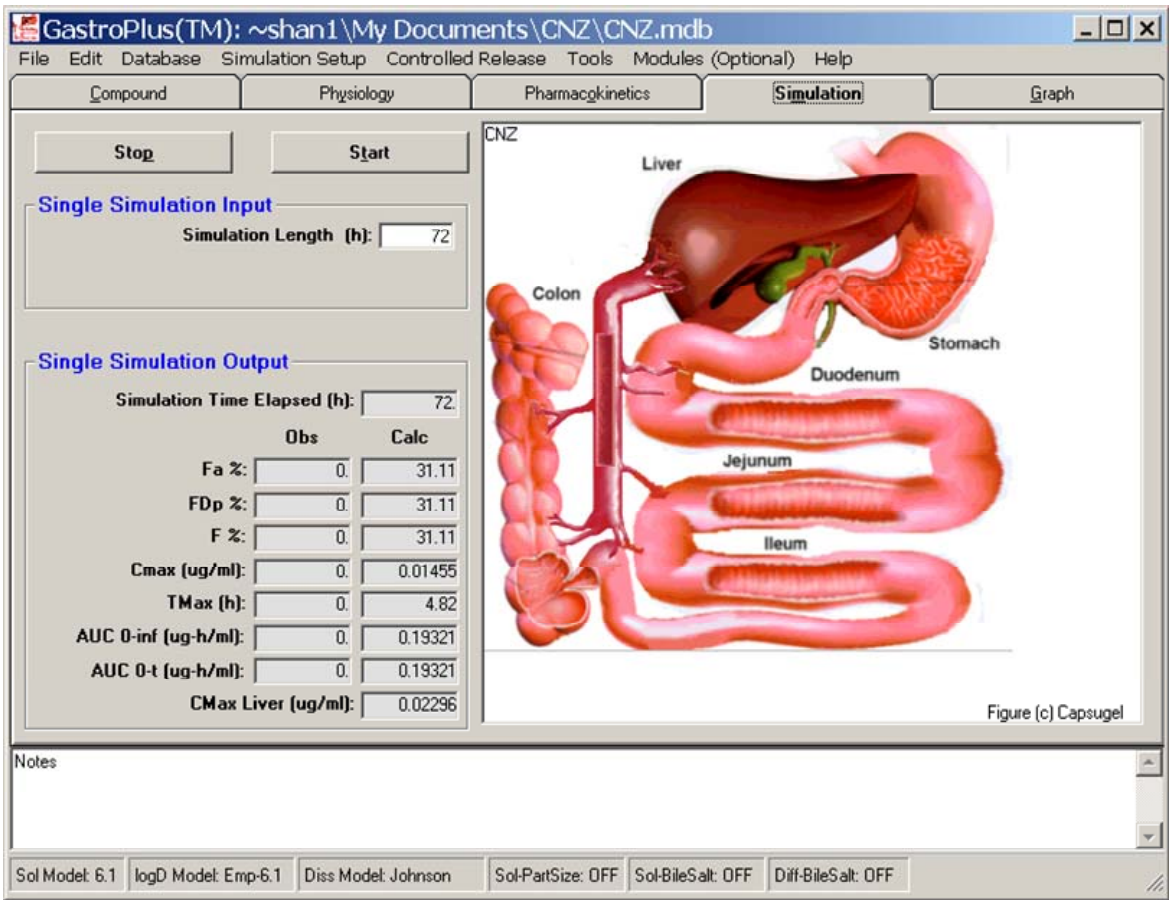

Figure 5.2 Illustration of the Gastroplus™ simulation for 25mg Stugeron® tablets using *in vitro* dissolution data predicting the *in vivo* PK parameters.

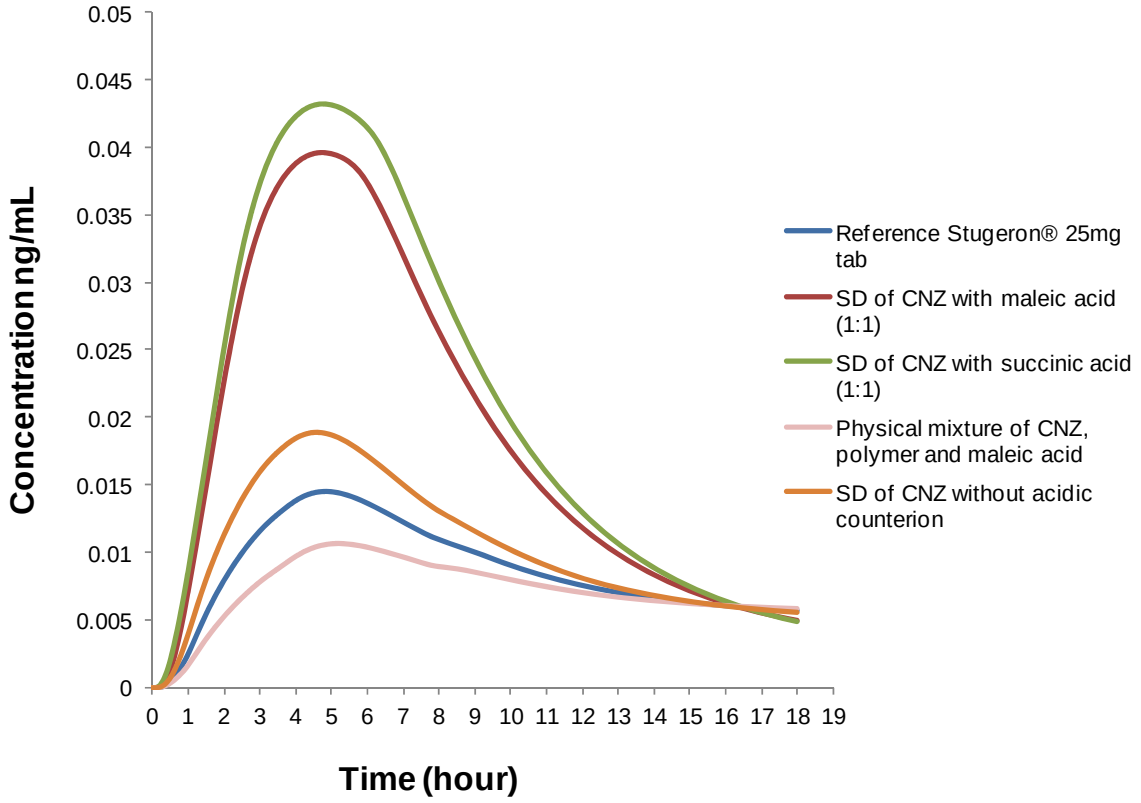

Figure 5.3 Comparison of the predicted *in vivo* human plasma profiles obtained from Gastroplus™ simulation for 25mg marketed tablet and developed solid dispersion (SD) formulations of 25mg cinnarizine with acidic counterions. Physical mixture of the components of solid dispersion is used as a negative control for the solid dispersion formulations.

Formulation	C_{max} (µg/mL)	T_{max} (h)	AUC_{0-72} (µg-h/mL)	Fraction absorbed (Fa) %
Reference Stugeron® 25mg tab	0.0145	4.82	0.1932	31.11
Physical mixture of CNZ-fb + polymer + maleic acid	0.0107	5.20	0.1671	26.91
SD of CNZ-fb (no acidic counterion)	0.0189	4.62	0.2223	35.79
SD of CNZ-fb with maleic acid (1:1)	0.0396	4.72	0.3704	59.65
SD of CNZ-fb with succinic acid (1:1)	0.0432	4.80	0.4053	65.26

Table 5.4 Comparison of pharmacokinetic parameters determined from the predicted *in vivo* human plasma profiles obtained from Gastroplus™ simulation for the reference 25mg marketed tablet and developed solid dispersion (SD) formulations of 25mg cinnarizine with acidic counterions.

6 EFFECT OF INCREASING SOLUBILITY, ACIDITY AND MOLECULAR WEIGHTS OF pH MODIFIERS IN SOLID DISPERSIONS PREPARED BY MELT EXTRUSION

6.1 Introduction

Formulation development for weakly acidic or basic drugs pose a major challenge due to their pH-dependent solubility which causes undesirable pharmacokinetic profiles which then leads to limited oral bioavailability[127]. The pH solubility profile for weakly ionizable basic drug is dependent upon its pk_a and can be generally described as follows: (i) Intrinsic solubility region (~pH > 7) where the drug is completely unionized and has the lowest solubility in this pH range. (ii) Ionizing region where the pH is around the pK_a of the drug and the ionized and unionized forms are present in equal concentrations. (iii) pH_{max} region wherein the drug has maximum solubility and as the pH is further decreased the drug is completely ionized. (iv) The salt plateau wherein the drug forms a salt with an oppositely charged counter ion and the salt solubility is dominant. Among the strategies to enhance the dissolution rate of such weakly acidic or basic drugs, is the inclusion of pH modifiers in matrix tablets and more recently in solid dispersion formulations[128,129]. The goal is to manipulate the pH within or in the vicinity of the dissolving dosage form, thus improving the dissolution behavior of the drug. The increase in solubility therefore obtained in the microenvironment of the diffusion layer helps to decrease the degree of supersaturation which prevents or slows down the rate of crystallization, providing an opportunity for the drug to diffuse to the bulk medium and escape precipitation. This improved *in vitro* dissolution behavior reflects in improved oral bioavailability for

weakly basic drugs[130,131]. However, the rationale for the choice of the pH modifier and the impact of the manufacturing process used for the formulations containing such pH modifiers has been limited, particularly for solid dispersions. Hot melt extrusion (HME) is considered an effective process in the pharmaceutical industry for the formation of molecular dispersions in order to improve the bioavailability of drugs that have poor water solubility[132]. The melt extrusion process offers various advantages over conventional approaches including being a solvent-free process over other methods such as solvent evaporation, spray drying, co-precipitation, supercritical fluid technologies and freeze drying. Heat sensitive compounds can be easily processed by HME due to short residence time and the flexibility to lower the processing temperatures by selecting an appropriate polymeric matrix.[133] Moreover, HME provides an opportunity to convert crystalline drug substances to amorphous state as well as a chance to dissolve the drug in the inert polymeric matrix through the formation of solid solutions[134]. Different case studies have been reported to increase the solubility of various poorly soluble drugs by HME including nifedipine, tolbutamide, lacipidine, itraconazole and nitrendipine[135,136,137,138,139].

We have demonstrated that inclusion of organic dicarboxylic acids such as maleic acid and succinic acid as a component of the solid dispersion system of a weak base cinnarizine (CNZ-fb) and Kollidon VA®64 (neutral polymer) helped to increase the dissolution rate of CNZ-fb. No plasticizer was needed for melt extrusion to form the amorphous solid dispersion. In addition to all the known mechanisms of a pH modifier it was shown that inter-molecular interactions occurring between CNZ-fb and the acidic counterion during the melt extrusion process helped to form an *in situ* salt which due to

its higher solubility also contributed to the dissolution enhancement. As a next step, the present study evaluates the effect of increasing solubility, acidity and molecular weight of pH modifiers when incorporated in the solid dispersions of CNZ-fb prepared using HME. The prepared ternary solid dispersions of drug, polymer and pH modifier were characterized for drug crystallinity and homogeneity. Dissolution studies were conducted in multiple pH media to obtain the release rate of CNZ-fb from solid dispersions containing organic acids such as maleic acid, citric acid, succinic acid and adipic acid and two anionic enteric coating polymers such as Eudragit® L100-55 and Hypromellose acetate succinate (HPMCAS). This was also an attempt to evaluate the impact of a pH modifier in developing a pH-independent solid dispersion formulation. In addition, a correlation between the microenvironmental pH of the different solid dispersions, the solubility, and acidity potential of the acidifier was investigated to understand the different mechanisms governing the dissolution enhancement of CNZ-fb.

6.2 Materials and Methods

6.2.1 Materials

Cinnarizine (1-(Diphenylmethyl)-4-(3-phenyl-2-propenyl)-piperazine; $C_{26}H_{28}N_2$; pK_a 1.9 and 7.5) was purchased from Sigma Aldrich (St. Louis, MO) and was used as the model compound due to its low aqueous solubility (2 µg/ml in purified water), and its demonstrated ability to form salts with selected organic acids. Maleic acid ($C_4H_4O_4$; pK_a 1.9 and 6.1), Succinic acid ($C_4H_6O_4$; pK_a 4.2), Citric acid ($C_6H_8O_7$; pK_a 3.13) and Adipic acid ($C_6H_{10}O_4$; pK_a 4.44) were purchased from Sigma Aldrich Chemical Co., (St. Louis, MO), and were used as acidic counterions. Kollidon® VA64, a water-soluble non-ionic

polymer with poly-vinylpyrrolidone-co-vinyl acetate backbone (M_w~55000 g/mol) was obtained from BASF Chemicals (Budd Lake, NJ). Eudragit® L100-55 an anionic coploymer was obtained from Evonik (Piscataway, NJ). AQOAT® LF (hypromellose acetate succinate, HPMCAS) was obtained from Shin-Etsu Chemical Company (Tokyo, Japan). Organic solvents used in salt synthesis were purchased from Sigma-Aldrich Co. LLC., (St. Louis, MO). All materials were used as received.

6.2.2 Thermogravimetric analysis (TGA)

Thermal stability of CNZ-fb and salts were assessed using a thermogravimetric analyzer (TGA) with a TA5300® controller. TGA analysis was carried out by heating samples at 10 ºC/min in an open pan under air from room temperature to 240 ºC. TGA helped to determine a maximum processing temperature for melt extrusion studies.

6.2.3 Preparation of Solid Dispersions with Melt extrusion

Solid dispersions (SDs) were manufactured as previously described in section 4.2.6 using a twin screw extruder. Briefly, physical mixtures of CNZ-fb (20% w/w) and Kollidon® VA64 (60% w/w), with organic acids or ionic polymers were prepared using blend/screen/blend process. Physical mixtures were fed manually into the extruder at a consistent rate. Screw speed was set at 150 rpm, and extrusion was conducted above the glass transition temperature (T_g) of the polymers used and melting point (T_m) of CNZ-fb (120 °C). Extrudates were allowed to cool to room temperature, milled, sieved through 0.5 mm screen, and placed in air-tight containers at 4 ºC until further analysis. Milled extrudes were assayed using HPLC method to assess thermal degradation, if any, from

melt extrusion for CNZ-fb. Drug-polymer miscibility and amorphous nature were evaluated using modulated DSC and XRD pattern.

6.2.4. Thermal analysis

Modulated Differential scanning calorimeter (mDSC) Q1000® TA Instruments (New Castle, DE) was used to assess structural properties of the salt and solid dispersion systems. High purity indium and sapphire were used frequently to calibrate the heat flow and heat capacity of the instrument. All systems were placed in standard aluminum pans and crimped with lids containing three pin-holes. Salts were heated at 10 °C/min to determine melting point, and solid dispersions were heated at 1 °C/min with modulation of 0.5 °C every 50 sec to determine glass transitions. Refrigerated Cooling System (RCS) was used for controlled cooling.

6.2.5 *In Vitro* Dissolution Study

Based on the generated pH solubility profile of CNZ-fb (section 4, Fig.4.10), the solubility of CNZ-fb in pH 4.5 and 6.8 is very poor, making these conditions non-sink and discriminatory for all formulations containing 25mg CNZ-fb. Dissolution studies for all SDs prepared using organic acids were conducted in both pH media. However, for the selected enteric coated polymers that show pH-dependent solubility and dissolve only at pH>5.5, the dissolution media for comparison was pH 6.8 phosphate buffer. Dissolution studies were performed in 500 mL of either pH 4.5 acetate buffer or pH 6.8 phosphate buffer + 0.1% sodium lauryl sulfate media using USP basket apparatus (Varian™, Cary, NC). Basket speed was set to 100 rpm; and the dissolution study temperature was

maintained at 37±0.5 ºC. Size 3, pink, opaque hard gelatin capsules were filled with SDs containing 25 mg equivalents of CNZ free base. pH of bulk media was checked before and after dissolution.10 mL aliquots was siphoned at pre-defined time-points (10, 20, 30 and 45 min), and passed through 0.45 µm PVDF filter. In order to avoid precipitation of CNZ to its crystalline form in the sample vial prior to HPLC analysis, 600 µL of filtered aliquot will be added to 400 µL of acetonitrile. All dissolution aliquots were analyzed using HPLC. Each dissolution study was performed in triplicate.

6.2.6 HPLC analysis

Concentrations of CNZ-fb in the samples were determined using Waters 2695 Separations Module with a Waters 2487 dual λ absorbance detector HPLC system at a wavelength of 254 nm using a Waters Xterra MS C8, 3.5 µm, 4.6 x 50 mm column (Waters Corporation, Milford, MA). All measurements were performed at an injection volume of 10 µL using a mobile phase mixture of acetonitrile (50%) in water (50%) with 0.1% TFA pumped at a flow rate of 1 mL/min, and at temperature of 30 ºC using a column oven. Calibration curves were constructed using standard solutions of CNZ-fb with known concentrations. Chromeleon™ software (Dionex Corporation, Sunnyvale, CA) was used to integrate the peak areas.

6.2.7 Determination of Solid Surface pH: Slurry pH Method

Slurries of all the SD formulations were prepared in polypropylene centrifuge tubes (Corning, Inc., Corning, NY). A known amount of solid, approximately 20–40% (w/w) in excess of its solubility, was added to deionized water and mixed for 15 min on a vortex.

The suspension pH was measured by potentiometry using an Accumet® Research AR15 pH meter equipped with an Accumet® glass electrode (Fisher Scientific, Pittsburgh, PA). The pH measured was used to approximate the pH at the surface of the solid as the diffusion layer pH approaches zero ($pH_{h=0}$) [140].

6.2.8 Statistical Analysis

Data obtained was analyzed using descriptive statistics, single factor analysis of variance (ANOVA) and presented as mean value ± SD. The differences between variants were considered significant as the value for *P* was less than 0.05.

6.3 Results and Discussion

6.3.1 Solid dispersion formation and solid state characterization

The model drug CNZ-fb is characterized as a weak base (pK_a ~7.5) with pH dependent solubility. From the pH solubility profile for CNZ-fb (Fig.4.10), pH 3 was the pH of maximum solubility. Below pH 3, CNZ-fb is protonated and ionized, resulting in formation of a soluble compound. As listed in Table 6.1, the pH modifiers selected are based on increasing solubility, pK_a and molecular weight to determine the critical parameter for enhancing the dissolution rate of CNZ-fb. In addition to the organic small molecule acids, enteric polymers with different functional backbone and large differences in their molecular weights were selected for comparison. Table 6.2 shows the compositions of the different solid dispersions manufactured using HME. A 1:1w/w drug to pH modifier ratio was kept constant in the polymeric matrix.

For melt extrusion using a twin screw extruder, chemical decomposition of the drug or polymers can occur due to number of factors including higher processing temperatures, longer residence time. TGA thermograms were utilized in order to select the processing temperatures for melt extrusion. CNZ-fb melted at 120 ºC, with decomposition initiating at 171.5 ºC, as indicated by the weight loss (Fig 6.1,a). For the neutral polymer, Kollidon®VA64 the onset temperature for decomposition is around 175°C and the weight loss is significantly greater after 200°C as seen from the derivative weight plot (Fig 6.1,b). For Eudragit®L100-55 there is about 3.5% weight loss from room temperature to 105°C with decomposition starting around 115°C. HPMCAS has its decomposition temperature at 175°C. With the CNZ-fb melting point being 120°C, it is essential to choose a processing temperature higher than 120°C to ensure the drug is completely melted and transformed to amorphous state. The processing conditions for the various formulation mixtures are listed in Table 6.3. The content of CNZ-fb as deducted from HPLC measurements was found to be > 97% in all solid dispersion formulations suggesting no significant degradation of the drug in the different polymeric matrices.

6.3.2 Thermal analysis

Modulated DSC profiles for CNZ-fb only and the various solid dispersion systems were evaluated for their extent of miscibility. CNZ-fb alone (Fig.6.2) showed a Tg of 8.9 ºC with ΔCp of 0.3456J/(g.ºC) followed by an exothermic re-crystallization (at 60ºC) suggesting a high propensity for CNZ-fb re-crystallization. On the other hand, solid dispersions of Kollidon® VA64 and CNZ-fb however, showed no such CNZ-fb re-crystallization exotherm peak suggesting polymer's ability to inhibit drug re-

crystallization during heating, likely due to a drug-polymer homogeneous mix. Moreover, single Tg was noticed at 74.5°C for solid dispersion versus Tg at 108.5°C for Kollidon® VA64 alone (Fig.6.2). A lower single Tg for the drug-polymer system compared to polymer Tg suggest drug's plasticizing effect on polymer due to solid-state miscibility.

Phase transitions were very different when a ternary component *i.e*., organic acid was added to drug-polymer solid dispersion. Fig.6.3 shows the magnitude of such difference. While all SDs showed a single Tg, citric acid containing solid dispersion showed the least plasticizing effect, as inferred by its higher Tg at 91.5°C. Adipic acid system on the other hand showed Tg at 46.5°C, thereby exhibiting a greater plasticizing effect. Succinic acid and maleic acid systems were in between with Tg at 55.3°C and 62.1°C, respectively.

In order to rule-out the possibility that a difference in Tg of solid dispersions was not because of differences in Tg of acids alone, the Tg values of acids were examined *via* heat-cool-reheat cycle in DSC pans (Table 6.4). Adipic acid on its own did not form an amorphous phase. However, it showed greatest miscibility when present in solid dispersion. Tg values of succinic and citric acids were comparable around 17°C, yet succinic acid showed significantly higher miscibility than citric acid did. Maleic acid had a Tg of -13°C, but its solid dispersion showed Tg greater than that of succinic acid system. These findings lead us to believe that the acids tested in our study seem to impact the solid-state of ternary solid dispersion systems. Although adipic, succinic, maleic, and citric acids are all small organic acids containing carboxylic functional groups, our hypothesis is that they seem to exhibit varying levels of intermolecular bonding and degrees of entropy mixing with drug and polymer that translate into

difference in Tg values. Fig.6.4 shows DSC profiles of CNZ-fb, Kollidon® VA64, and either of the two polymeric acids Eudragit®L100-55 or HPMC acetate succinate at 20% level. All three systems demonstrated Tg that were in the same vicinity. Eudragit®L100-55 solid dispersion system showed Tg at 74.4°C which was similar to that from binary system of CNZ-fb and Kollidon®VA64. HPMCAS dispersion showed Tg at 80.7°C. These findings confirm CNZ-fb mixing with Eudragit or HPMCAS systems, as inferred by the reduction in Tg values compared with Tg of neat Eudragit (110°C) or HPMCAS (118°C). In a study done by Fieldstein et al.,[141] the authors looked at the impact of hydrogen bonding degree which varied based on the number of hydroxyl groups. They concluded that the extent of miscibility was proportional to the number of hydroxyl groups which overcame the miscibility barriers between polyethylene glycol and poly(*N*-vinyl pyrrolidone) with the addition of plasticizer. Similarly, in our study, mixing between the drug and the two polymers may have been favored by the intermolecular interaction between drug and polymeric acidic groups which may have been strong enough to overcome entropy barriers for mixing.

As shown in Fig.6.5 and Fig.6.6, XRPD patterns confirms the lack of crystallinity for all the solid dispersions prepared using hot melt extrusion.

6.3.3 *In vitro* dissolution studies

The release rate of CNZ-fb from its different solid dispersions in pH 4.5 and pH 6.8 dissolution media is shown in Fig.6.7, 6.8 and 6.9. The dissolution rate of pure CNZ-fb was also investigated in both dissolution media to signify the dissolution enhancement achieved with the extruded solid dispersions. As seen in Figure 6.7, CNZ-fb had a poor

release rate (3% @ 45mins) due to its poor solubility in pH 4.5. The SD of CNZ-fb and polymer helped to improve the dissolution rate (18.8%@45mins) compared to any physical mixture of drug and polymer (2.4%@45mins). A simple physical mixture of drug, polymer with acidifier as maleic acid was not efficient to improve the dissolution rate of CNZ-fb (11%@45mins). The addition of the different types of organic acids at 20%w/w as an internal buffer system in the SD prepared using melt extrusion showed dissolution enhancement for CNZ-fb. As seen from Fig. 6.8, the impact of the acidifier type in the SD on the % of CNZ-fb released after 45mins of dissolution in pH 4.5 media can be ranked as SD (adipic acid) > SD (succinic acid) > SD (citric acid) > SD (maleic acid) with SD of CNZ-fb with adipic acid showing the highest dissolution rate (64.6% @ 45mins). The dissolution rate of CNZ-fb was also evaluated in pH 6.8 media for all the SDs. Since the solubility of CNZ-fb is negligible (< 0.001mg/ml), 0.1% SLS was added to pH 6.8 phosphate buffer. The use of surfactants in the dissolution media for sparingly soluble drugs is physiologically relevant and well-documented[142,143]. SLS containing fasted state gastric simulated fluid has 0.25% (8.67mM) SLS is commonly used as FaSSGF. The dissolution media provided sufficient discriminatory power between all the formulations and was still a non-sink condition thus avoiding any CNZ-fb solubility overestimation. CNZ-fb in pH 6.8 + 0.1% SLS had a release rate of 4.1% @ 45mins (Fig.6.9). From Fig.6.6, the rank order in the decreasing order of dissolution rate of CNZ-fb was SD (adipic acid) > SD (succinic acid) > SD (maleic acid) > SD (citric acid) with SD of CNZ-fb and adipic acid again showing the highest dissolution rate (61.2% @ 45mins). SD of CNZ-fb and succinic acid also increased the dissolution rate of CNZ-fb significantly in both media (54.9% @ 45mins in pH 6.8 + 0.1% SLS media, 56.5% @

45mins in pH 4.5 media). The SD of CNZ-fb and citric acid had variable dissolution rate between pH 4.5 8 (49.2% @ 45 mins) and pH 6.8 (37.7% @ 45 mins). For the SD of CNZ-fb and maleic acid the dissolution rate was quite similar irrespective of the dissolution media pH (45.5% @ 45mins in pH 4.5 and 40.5% @ 45mins in pH 6.8). In cases where the SD contained an ionic polymer instead of an organic acid as the pH modifying component (Fig.6.10), the SD of CNZ-fb with Eudragit®L100-55 showed a higher dissolution rate (46.4% @ 45mins) versus the SD of CNZ-fb and HPMCAS (17.7% @ 45mins). Polymeric carriers such as Eudragit®L100-55 and HPMCAS have been characterized as polymers facilitating supersaturation of poorly water-soluble drugs[144]. However, in this study, the SD system with Eudragit®L100-55 had a much superior dissolution for CNZ-fb than the SD with HPMCAS.

6.3.3 Mechanisms of dissolution enhancement

The observed differences in the CNZ-fb dissolution rates for the SDs with the selected organic acids could be due to (1) the acid's microenvironmental pH modulation capacity in the SD (2) solubility of the acid (3) acidity of the acidifier. Previous reports have demonstrated that, it is not the solubility under a bulk pH condition; rather it is the solubility under pH condition at the solid surface in the diffusion layer that controls dissolution rates of pH-dependent soluble drugs[145,146]. In the present study, among all the SDs with the selected organic acids, the SD of CNZ-fb and adipic acid showed the highest dissolution rate irrespective of the bulk pH of the dissolution media making it a pH-independent formulation. As a further investigation, the solid surface pH was measured for the various SD formulations using the slurry pH method. As seen in Table

6.5, CNZ-fb alone has a slurry pH of 6.3 indicating its weakly basic nature. A SD of CNZ-fb + polymer had a solid surface pH of 5.4. On inclusion of acidifier in the SD, the ternary SD systems showed a decrease in the solid surface pH compared to the drug alone indicating the acidifier's ability to lower the diffusion layer pH in the dissolving layer of the dosage form. The rank order of the measured solid surface pH for the formulations were SD with maleic acid < SD with citric acid < SD with succinic acid < SD with adipic acid < SD with no acid. In addition to the pH lowering effects in the microenvironment, adipic acid and succinic acid have lower aqueous solubility compared to citric and maleic acid (Table 6.1). Due to lower aqueous solubility, the pH modifier as adipic acid in the dosage form maintains the low solid surface pH of the dissolving dosage form for a prolonged period hence keeping the drug in a solubilized form capable of diffusing out to the bulk medium and escape precipitation long enough to allow for absorption. On the other hand, maleic acid has a higher solubility (788g/L) and hence leaches out to the solid surface thereby lowering the surface pH to a larger extent (pH of 1.9). We believe this finding supports the theory that the dissolution rate of the acidifier is an important parameter in modulating drug release of weakly basic drugs like CNZ. A similar observation was noted by Streubel et al.[147] in their evaluation of the effect of incorporating various acids into matrix systems on release of verapamil in phosphate buffers at pH 6.8 and 7.4. The acids tested (fumaric, sorbic, adipic) had relatively low pKa (<5) and relatively low aqueous solubility (<2%). Fumaric acid was the most effective in enhancing the drug release.

From our previous study, we demonstrated that CNZ-fb forms *in situ* complex with maleic and succinic acid. While it is difficult to isolate the salt form of the selected acidic

counterions (adipic acid, citric acid), it is reasonable to believe that the dissolution rate of the *in situ* complex may have an impact on the dissolution rate of CNZ from the SD system. As adipic acid and succinic acid have the potential to lower the solid surface pH to below the pHmax of CNZ-fb wherein CNZ is ionized and can form acid-base *in situ* complex during extrusion process which modifies the dissolution rates. Such acid-base interaction for polyelectrolyte complexes during the fusion process has been recently observed by Brietkr J et al[114].

In measuring the slurry pH, it was intriguing to note the difference between the pKa of the acid and its slurry pH. As seen from Table 6.5, there is a difference of 1.4 unit for adipic acid and 0.8 unit for maleic acid. Such a difference being greater in the SD with adipic acid among all the other acids potentially indicates the role of the greater acidic strength of adipic acid in increasing the dissolution rate of CNZ-fb.

The mechanism of carboxylic acid polymer dissolution is different than that of non-ionic polymers as it involves an additional ionization step that stabilizes the polymer chain.[148] Among the ionic polymers tested, both polymers showed their effectiveness in maintaining their structural integrity in acidic dissolution media. However in pH 6.8 media, SD with Eudragit®L100-55 was able to increase the dissolution rate of CNZ-fb to a far greater extent than the SD with HPMCAS (Fig.6.10). This could be attributed to their polymeric backbone structures which show differences in the percentage of free carboxyl groups present in Eudragit®L100-55 (46-50%) compared to HPMCAS (14-18%) which also reflects in their slurry pH measurements of 4.8 and 5.21 respectively (Table 6.5).

6.4 Conclusions

SD prepared using different organic acids showed a different degree of dissolution enhancement for CNZ-fb. All SD could be processed without a plasticizer and were amorphous in nature. Among the selected organic acids, adipic acid when included in the SD matrix showed the highest dissolution rate of about 15-fold compared to CNZ-fb due to several factors such as lower water solubility of the acid, lowering of the solid surface pH to below the pH_{max} of the drug wherein it is ionized, possibility of acid-base interactions occurring during the fusion process and the amorphous nature of the SD system. Using enteric polymers as pH modifying components of SD, it was observed that Eudragit®L100-55 showed a greater extent of improved dissolution of CNZ-fb compared to a SD matrix with HPMCAS. Thus, pH-independent SD systems were developed for a weakly basic drug such as CNZ-fb by incorporating acidic pH modifiers in the SD matrix prepared using HME.

Organic acids	Class	Molecular weight	pKa (s)	Solubility in water (g/L)	Melting Point/ Glass Transition temperature (ºC)
Maleic	Unsaturated dicarboxylic acid	116.07	1.92, 6.23	788	131
Succinic	Saturated dicarboxylic acid	118.09	4.21, 5.64	58	186
Citric	Hydroxy tricarboxylic acid	192.12	3.13, 4.76, 6.40	730	153
Adipic	Saturated dicarboxylic acid	146.14	4.44, 5.44	14.4	152.1
Ionic Polymers					
HPMC acetate succinate (LF grade)	Cellulosic polymer with acetyl and succinoyl groups	18,000	n/a	Insoluble in water, dissolves when pH>5.5	118
Eudragit L100-55	Anionic copolymer based on methacrylic acid and ethyl acrylate	320,000	n/a	Insoluble in water, dissolves when pH>5.5	110

Table 6.1 Characteristics of organic acids and ionic polymers used as pH modifying component of solid dispersion of CNZ-fb and water soluble polymer.

Solid Dispersion	Components (%w/w)							
	CNZ -fb	**Kollidon ®VA64**	**Maleic acid**	**Succinic acid**	**Citric acid**	**Adipic acid**	**Eudragit ® L100-55**	**HPMC -AS**
1	20	60						
2	20	60	20					
3	20	60		20				
4	20	60			20			
5	20	60				20		
6	20	60					20	
7	20	60						20

Table 6.2 List of compositions of the solid dispersions prepared using HME.

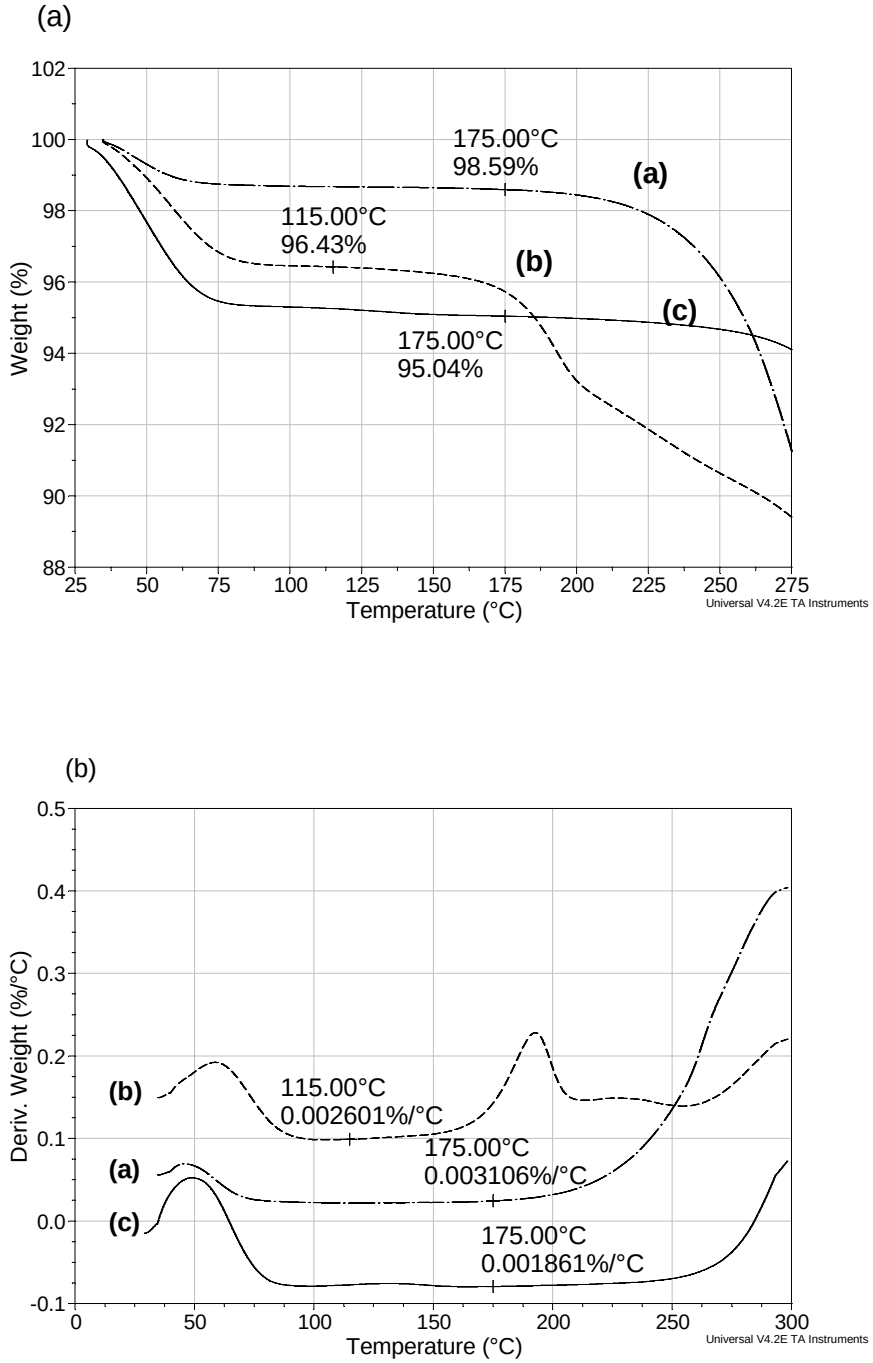

Figure 6.1 Overlay of thermogravimetric analysis of the polymers used in the solid dispersion formulation HPMCAS (a), Eudragit L100-55 (b), and Kollidon® VA64 (c) indicating the onset for decomposition temperature.

Formulation	Extrusion temperature (°C)	Torque generated (Ncm)	CNZ-fb Assay (%)
SD (no acid)	125	25	98.5%
SD of maleic acid	125	10	98.8%
SD of succinic acid	140	5	98.9%
SD of citric acid	140	50	97.5%
SD of adipic acid	140	5	98.2%
SD of Eudragit® L100-55	125	20	99.0%
SD of HPMCAS	140	40	97.9%

Table 6.3 HME processing conditions using a twin screw extruder at a constant screw speed of 150 revolutions per minute and resulting potency values from the solid dispersions prepared using HPLC analysis.

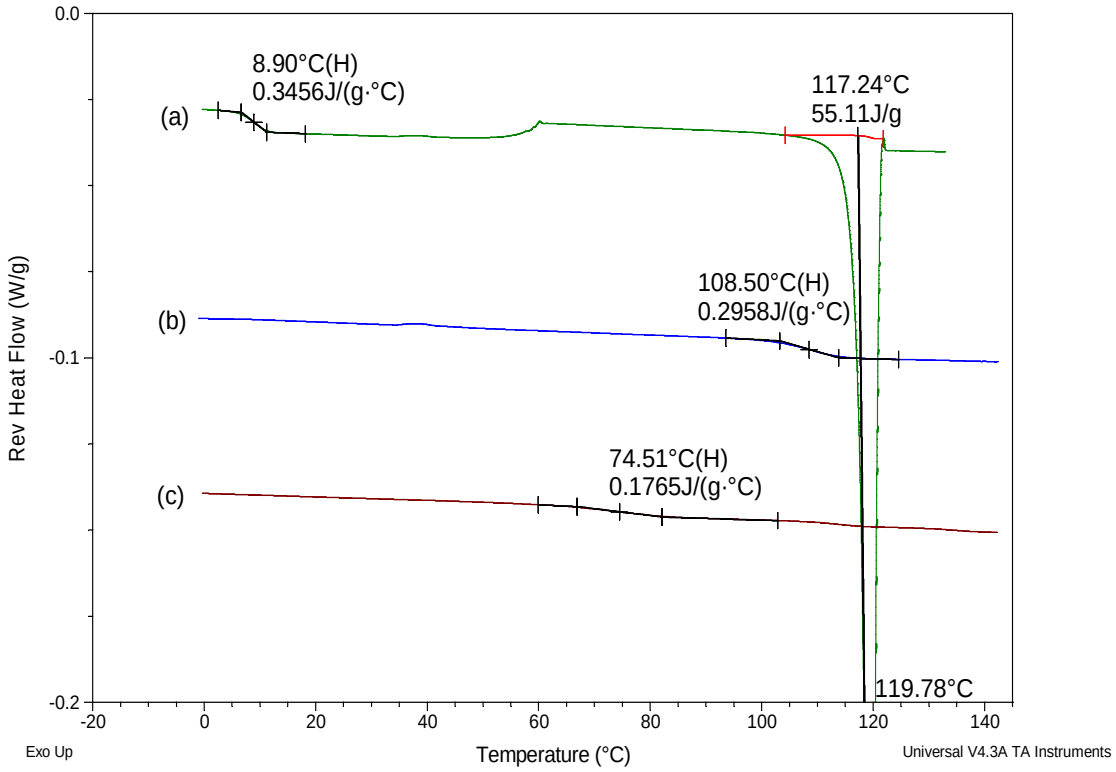

Fig.6.2 Modulated DSC overlays of the solid dispersion systems (a) cinnarizine free base (CNZ-fb) (b) Kollidon®VA64 polymer (c) SD of CNZ-fb and Kollidon®VA64 polymer and showing amorphous nature with shifts in Tg (glass transition temperatures).

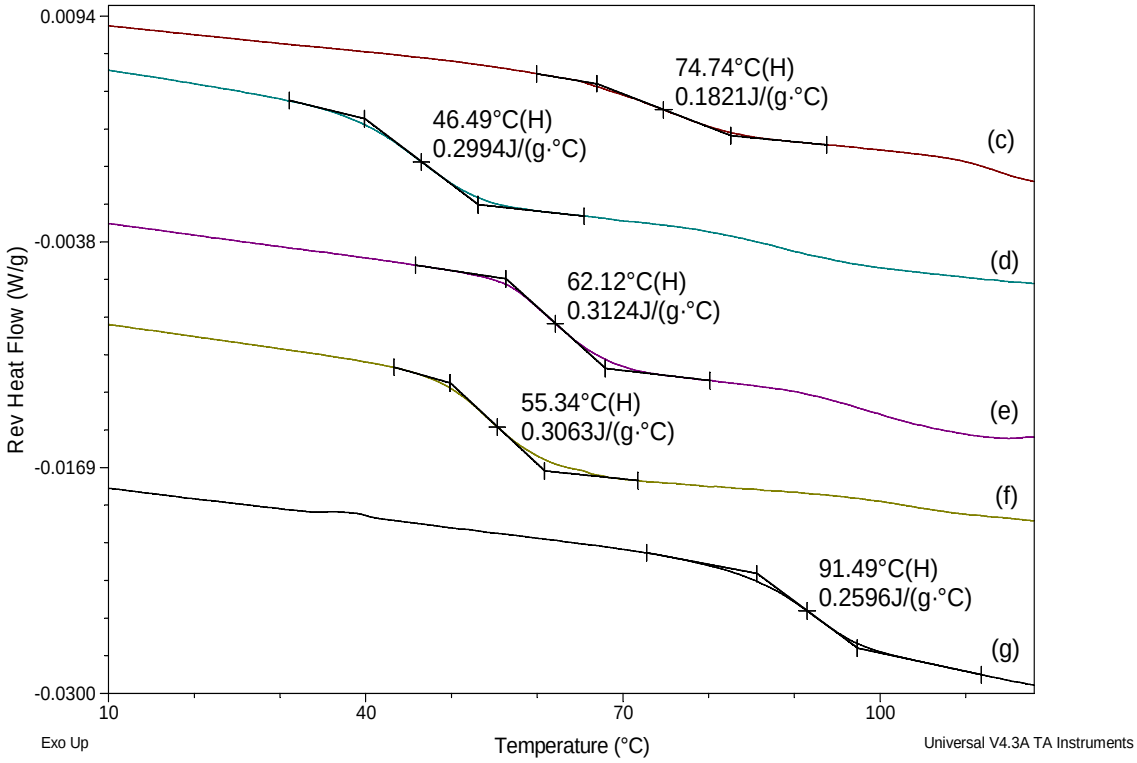

Fig.6.3 Modulated DSC overlays of the solid dispersion systems (c) SD of CNZ-fb and Kollidon®VA64 polymer (d) SD of CNZ-fb + adipic acid + polymer (e) SD of CNZ-fb + maleic acid + polymer (f) SD of CNZ-fb + succinic acid + polymer (g) SD of CNZ-fb + citric acid + polymer, showing amorphous nature with shifts in Tg (glass transition temperatures).

Component	Tg (°C)	ΔCp (J/g.°C)
CNZ-fb	8.79	0.3668
Succinic acid	16.8	0.0307
Adipic acid	-	-
Maleic acid	-13.2	0.2881
Citric acid	17.3	0.7374
Kollidon®VA64	108.4	0.3037
Eudragit®L100-55	110	0.2209
HPMCAS	118	0.2472

Table 6.4 HME processing conditions using a twin screw extruder at a constant screw speed of 150 revolutions per minute and resulting potency values from the solid dispersions prepared using HPLC analysis.

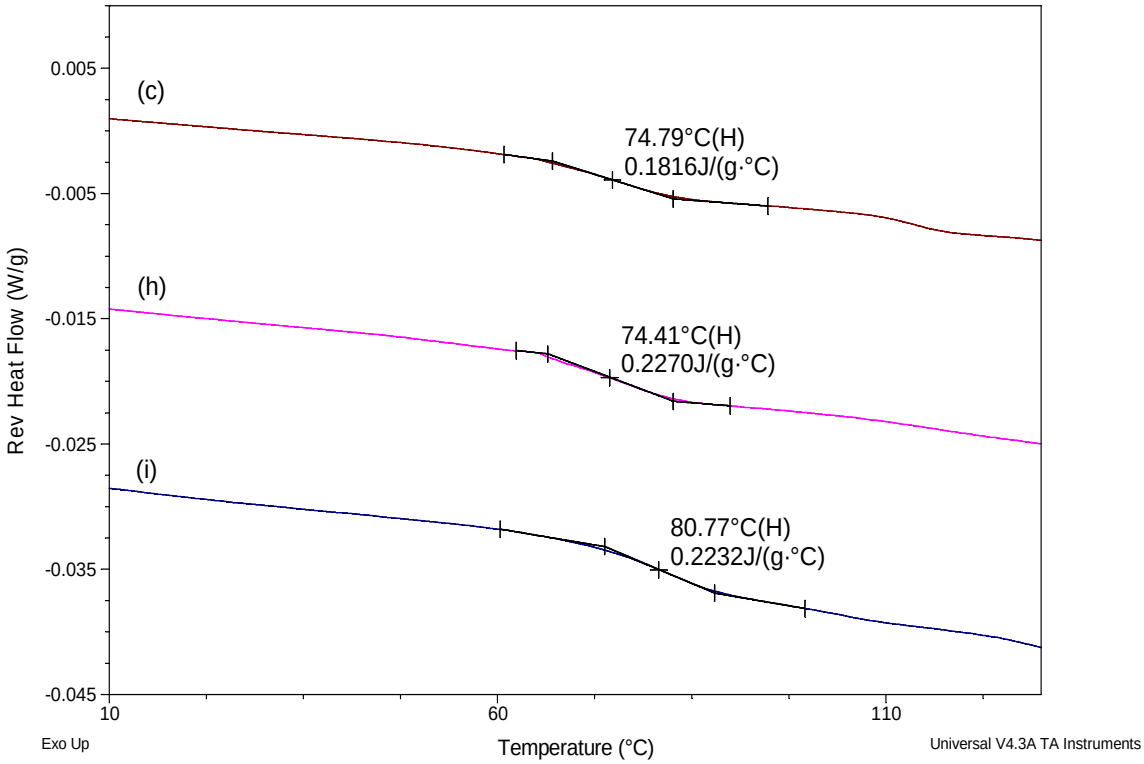

Fig.6.4 Modulated DSC overlays of the solid dispersion systems (c) SD of CNZ-fb and Kollidon®VA64 polymer (h) SD of CNZ-fb + Eudragit®L100-55 + polymer (i) SD of CNZ-fb + HPMCAS + polymer, showing amorphous nature with shifts in Tg (glass transition temperatures).

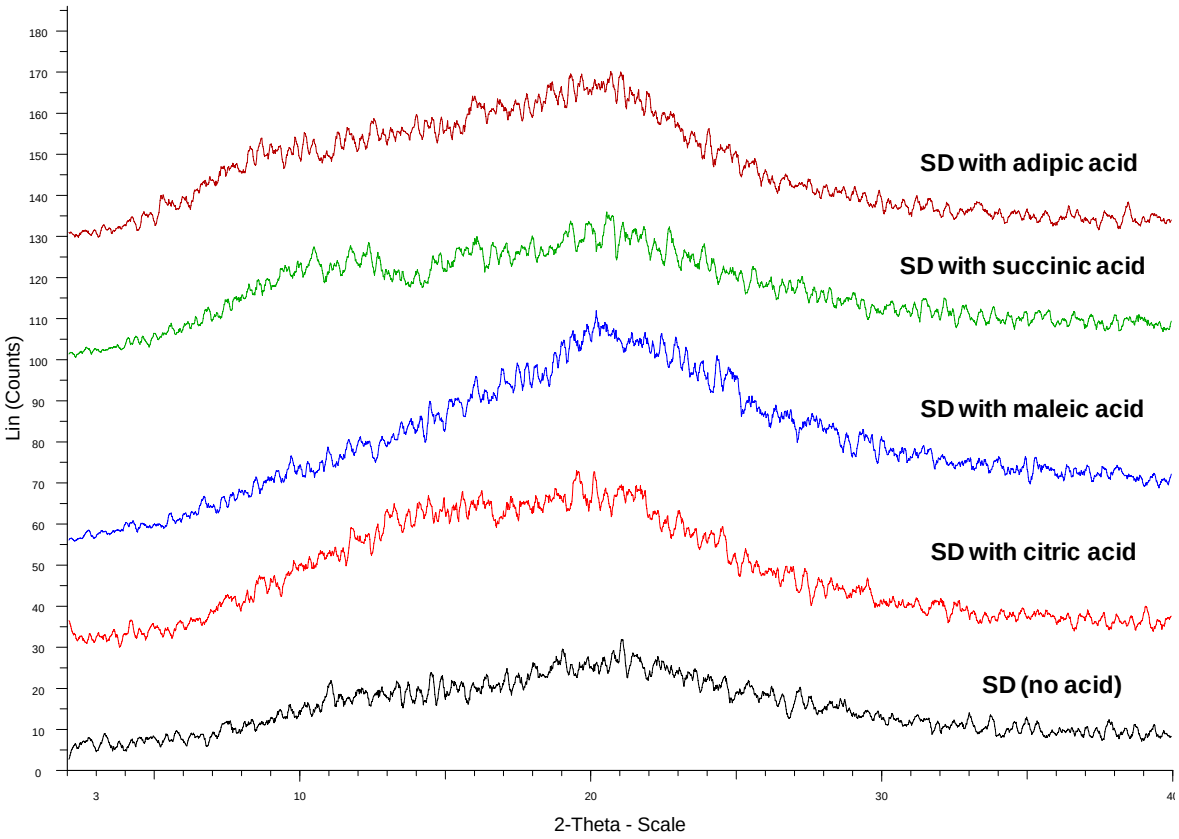

Figure 6.5 X-ray powder diffraction of the solid dispersions of CNZ-fb, Kollidon®VA64 with or without acidic counterion prepared using HME showing the amorphous nature of the dispersions.

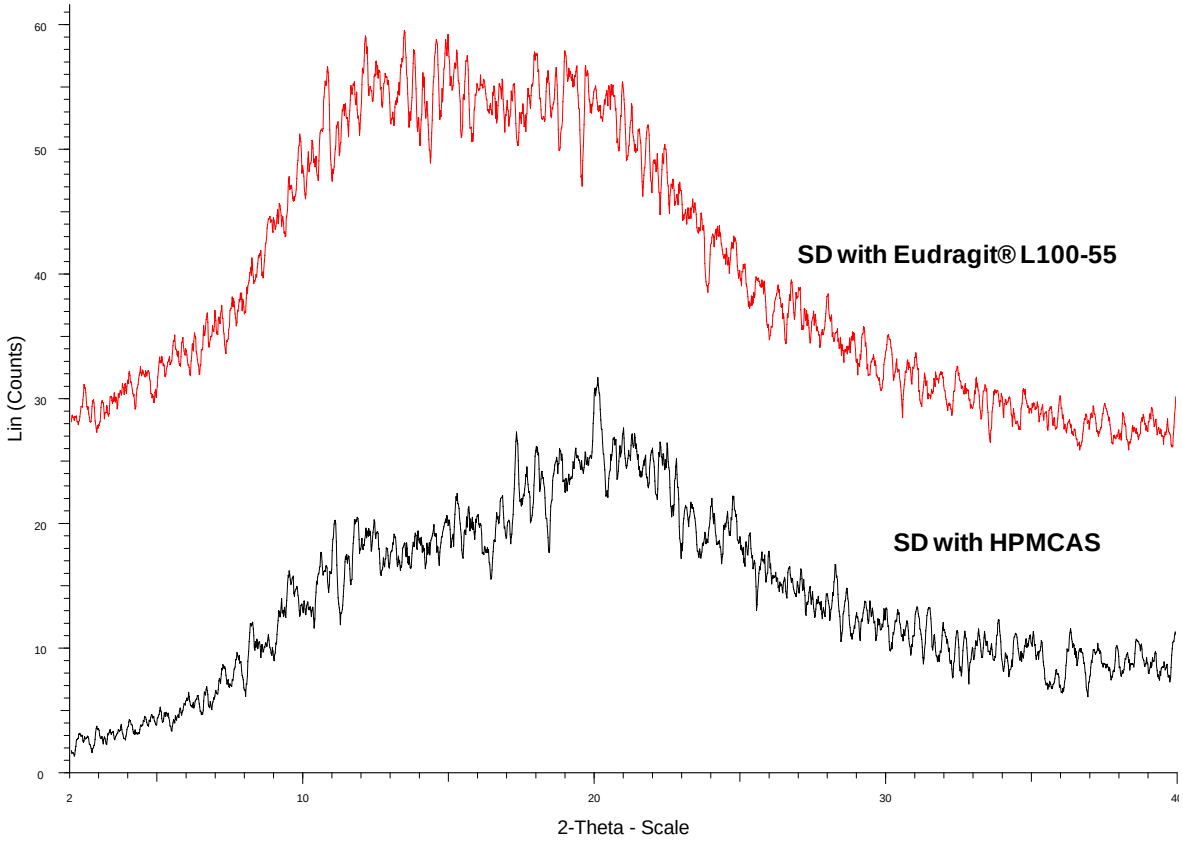

Figure 6.6 X-ray powder diffraction of the solid dispersions of CNZ-fb, Kollidon®VA64 with ionic polymer as the pH modifier, prepared using HME showing the amorphous nature of the dispersions.

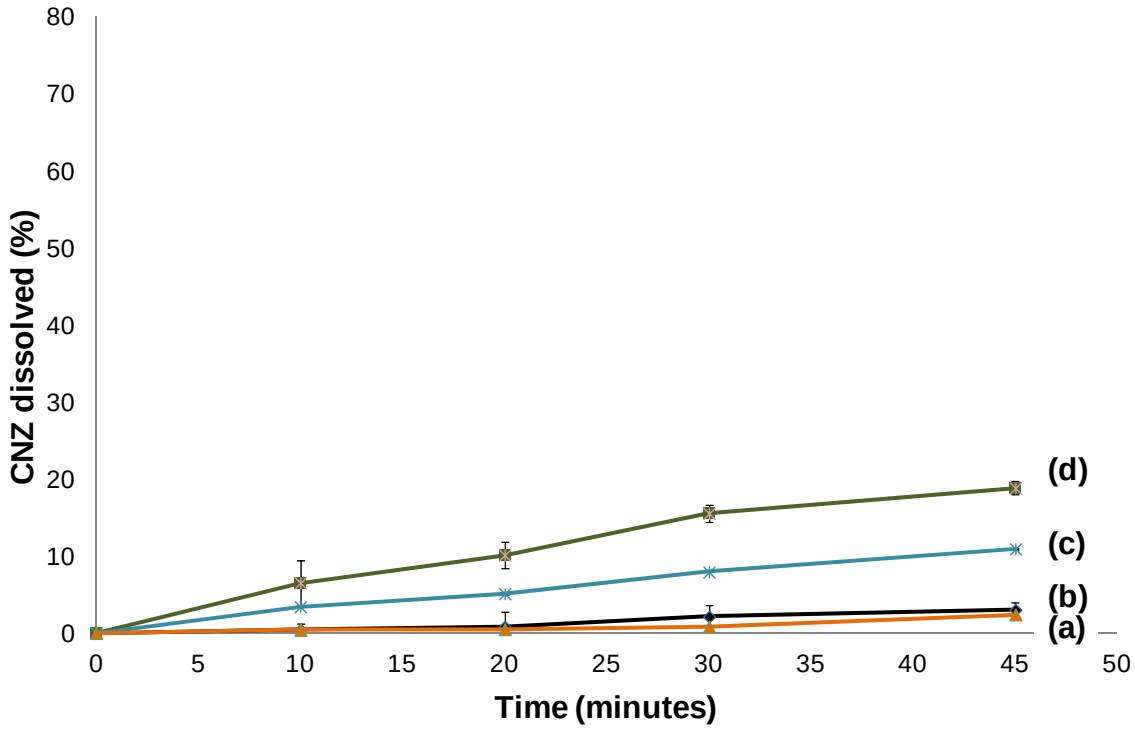

Figure 6.7 Comparison of dissolution rates for capsules containing equivalent to 25 mg CNZ-fb in pH 4.5 acetate buffer using USP Apparatus 1. **(a)** CNZ-fb, **(b)** physical mixture of CNZ-fb+ polymer, **(c)** physical mixture of CNZ-fb+ maleic acid + polymer, **(d)** SD of CNZ-fb + polymer, **(e)** SD of CNZ-fb + maleic acid + polymer. Data points are expressed as mean± S.D (n=3).

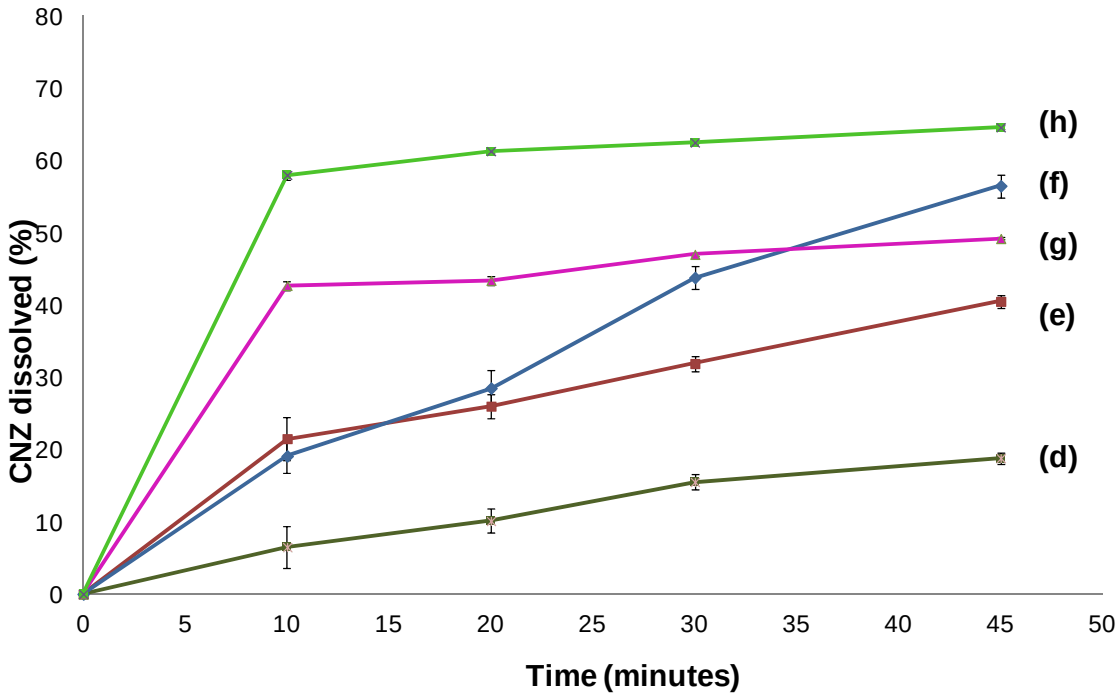

Figure 6.8 Comparison of dissolution rates for capsules containing equivalent to 25 mg CNZ-fb in pH 4.5 acetate buffer using USP Apparatus 1. **(d)** SD of CNZ-fb + polymer, **(e)** SD of CNZ-fb + maleic acid + polymer, **(f)** SD of CNZ-fb + succinic acid + polymer, **(g)** SD of CNZ-fb + citric acid + polymer, **(h)** SD of CNZ-fb + adipic acid + polymer. Data points are expressed as mean± S.D (n=3).

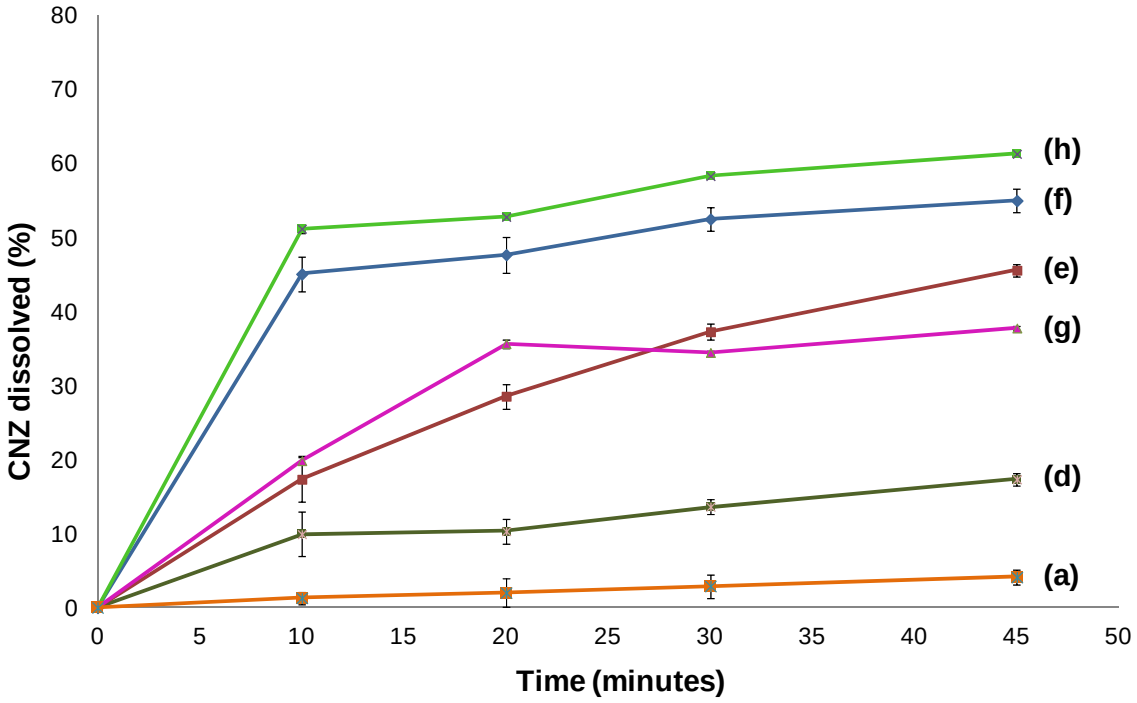

Figure 6.9 Comparison of dissolution rates for capsules containing equivalent to 25 mg CNZ-fb in pH 6.8 phosphate buffer + 0.1% SLS using USP Apparatus 1. **(a)** CNZ-fb, **(d)** SD of CNZ-fb + polymer, **(e)** SD of CNZ-fb + maleic acid + polymer, **(f)** SD of CNZ-fb + succinic acid + polymer, **(g)** SD of CNZ-fb + citric acid + polymer, **(h)** SD of CNZ-fb + adipic acid + polymer. Data points are expressed as mean± S.D (n=3).

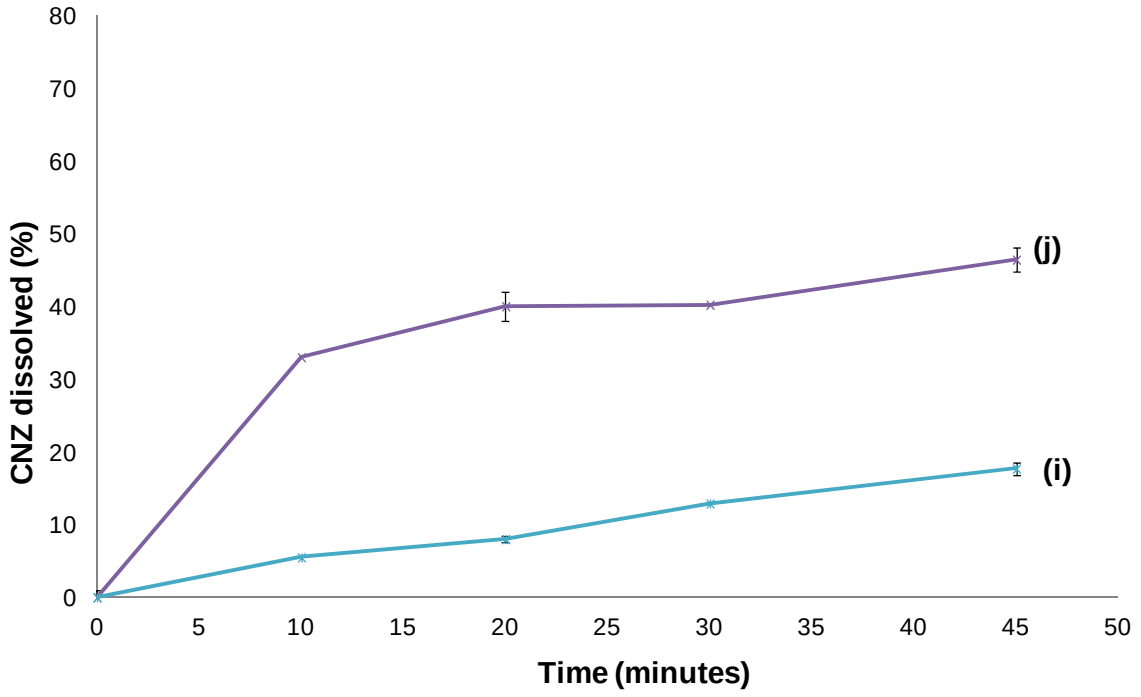

Figure 6.10 Comparison of dissolution rates for capsules containing equivalent to 25 mg CNZ-fb in pH 6.8 phosphate buffer + 0.1% SLS using USP Apparatus 1. **(i)** SD of CNZ-fb + HPMCAS + polymer, **(j)** SD of CNZ-fb + Eudragit® L100-55 + polymer. Data points are expressed as mean± S.D (n=3).

Composition	% release of CNZ @ 45mins in pH 6.8 media	Measured pH at solid surface ($pH_{h=0}$)	pK_a(s) of the acidic components
CNZ-fb alone	4.1	6.3	7.5
SD (no acid)	17.3	5.40	-
SD with maleic acid	45.5	1.90	1.92, 6.23
SD with succinic acid	54.9	2.56	4.21, 5.64
SD with citric acid	37.7	2.54	3.13, 4.76, 6.40
SD with adipic acid	64.6	3.02	4.44, 5.44
SD with Eudragit® L100-55	46.4	4.80	-
SD with HPMCAS	17.7	5.21	-

Table 6.5 Correlation of dissolution of CNZ-fb to the solid surface pH measured using 10% slurry pH method for SD with organic acids or ionic polymers.

7 OVERALL CONCLUSION

This study systematically offers the benefits of adding organic acids as acidic counterions to a solid dispersion matrix of a weakly basic drug during melt extrusion, should a classical salt formation technique fail. In general, this approach would be applicable to molecules:

- that have functional groups that demonstrate salt forming ability
- can form miscible systems in a solid dispersion matrix of drug, neutral polymer and salt forming counterions
- are not thermolabile hence can be processed using melt extrusion technology

Thus, this developed formulation approach of forming *in situ* salt solid dispersions using melt extrusion can be used as a platform technology in drug product development for ionic compounds that show dissolution limited absorption.

8 REFERENCES

1. www.fda.gov/downloads/drugs/development approval process/how drugs are developed and approved/drug and biologic approval reports/ UCM242695.

2. Hans MM, Oprea TI. 2004. Pursuing the leadlikenes concept in pharmaceutical research. Curr Opin Chem Biol 8:255-263.

3. Alanine A, Nettekoven M, Roberts E, Thomas AW. 2003. Lead generation – enhancing the success of drug discovery by investing in hi to lead process. Comg Chem High Throughput Screen 6:51-66.

4. Kola I, Landis J. 2004. Can the pharmaceutical industry reduce attrition rates? Nat Rev Drug Discov 3:711-715.

5. Pace SN, Pace GW, Parikh I, Mishra AK. 1999. Novel injectable formulations of insoluble drugs. Pharm Technol 23:116-134.

6. Caldwell GW, Ritchie DM, Masucci JA, Hageman W, Yan Z. 2001. The new pre-preclinical : Compound optimization in early and late phase drug discovery. Curr Top Med Chem 1:353-366.

7. Kerns EH, Di L. 2003. Pharmaceutical profiling in drug discovery. Drug Discov Today 8:316-323.

8. Lipinski CA. 2000. Drug-like properties and the causes of poor solubility and poor permeability. J Pharmaco Toxico Methods 44:235-249.

9. Liu R. 2008. Water-insoluble drug formulation. 2nd edition, CRC press, Boca Raton.

10. Nelson E. 1957. Solution rate of theophylline salts and effects from oral administration. J Am Pharm Assoc Sci. Ed. 46:607-614

11. Serajuddin ATM. 2007. Salt formation to improve drug solubility. Adv. Drug Deliv Rev 59:603-616.

12. Agharkar S, Lindenbaum S, Higuchi T. 1976. Enhancement of solubility of drug salts by hydrophilic counterions: Properties of organic salts of an antimalarial drug. J Pharm Sci 65:747-749.

13. Miller LC, Heller WH. 1975. Physical and chemical considerations in the choice of drug products. On Drugs of Choice. 1974-1975, edited by W.C. Modell, 20-29. St. Louis, MO: Mosby.

14. Berge SM, Bighley LD, Monkhouse DC. 1977. Pharmaceutical salts. J Pharm Sci. 66:1-19.

15. Fiese EF, Hagen TA. 1986. Preformulation. In The Theory and Practice of Industrial Pharmacy, edited by L. Lachman, H.A. Lieberman, and J. L. Kanig, 171-196. Philadelphia, PA: Lea & Febiger.

16. Bowker MJ, Stahl H. 2008. Preparation of water-soluble compounds through salt formation. In Pharmaceutical and Chemical Means to Solubility and Formulation Problems. 749-766, edited by Michael Bowker. Elsevier Ltd.

17. Shozo M, Midori O, Tanekazu N. 1980. Unusual solubility and dissolution behavior of pharmaceutical hydrochloride salts in chloride-containing media. Int J Pharm 6: 77-85.

18. Serajuddin AT. 1999. Solid dispersion of poorly water-soluble drugs: early promises, subsequent problems, and recent breakthroughs. J Pharm Sci 88:1058-1066.

19. Joshi HN, Tejwani RW, Davidovich M, Sahasrabudhe VP, Jemal M, Varia SA, Serajuddin ATM. 2004. Bioavailability enhancement of a poorly water-soluble drug by solid dispersion in polyethylene glycol-polysorbate 80 mixture. Int J Pharm 269: 251-258.

20. Franco M, Trapani G, Latrofa A. 2001. Dissolution properties and anticonvulsant activity of phenytoin-polyethylene glycol 6000 and polyvinylpyrrolidone K-30 solid dispersions. Int J Pharm 225:63-73.

21. Chutimaworapan S, Ritthidej GC, Yonemochi E. 2000. Effect of water-soluble carriers on dissolution characteristics of nifedipine solid dispersions. Drug Dev Ind Pharm 26:1141- 1150.

22. Tran PHL, Tran TTD, Lee KH, Kim DJ, Lee BJ. 2010. Dissolution-modulating mechanism of pH modifiers in solid dispersion containing weakly acidic or basic drugs with poor water solubility. Expert Opin Drug Deliv 7:647-661.

23. Noyes AA, Whitney WR. 1897. The rate of solution of solid substances in their own solutions. J Am Chem Soc 19:930-934.

24. Rabinow BE. 2004. Nanosuspensions in drug delivery. Nat Rev Drug Discov 3:785-796.

25. Stella V. 1975. Pro-drugs: an overview and definition. In Pro-drugs as Novel Drug Delivery Systems, edited by T.Higuchi and V.Stella, 1-115. Washington, D.C. : American Chemical Society.

26. Nelson E. 1958. Comparative dissolution rates of weak acids and their sodium salts. J Pharm Sci 47:297-299.

27. Pudipeddi M, Serajuddin ATM, Grant DJW, Stahl PH. 2002. Solubility and Dissolution of weak acids, bases, and salts. Handbook of Pharmaceutical Salts-Properties, Selection and Use, Wiley-VCH, Zurich : 19-41.

28. Dittert LW, Higuchi T, Reese DS. 1964. J Pharm Sci 53:1325-1328.

29. Connors KA. 1982. A Textbook of Pharmaceutical Analysis, John Wiley & Sons, New York.

30. Sugano K, Okazaki A, Sugimoto S, Tavornvipas S, Omura A, Mano T. 2007. Drug Metab Pharmacokinet 22:225-254.

31. Kearney AS, Mehta SC, Radebaugh GW.1992. Pharm Res 9:1092-1095.

32. Dalhlan R, McDonald C, Sunderland VB. 1987. , J Pharm Pharmacol 39: 246-251.

33. B. D. Anderson, R. A. Conradi, J. Pharm. Sci. 1985, 74, 815-820.

34. Kramer SF, Flynn GL. 1972. Solubility of organic hydrochlorides. J Pharm Sci 61: 1896-1904.

35. Chowhan ZT. 1978. pH-solubility profiles of organic carboxylic acids and their salts. J Pharm Sci 67:1257-1260.

36. Serajuddin ATM, Rosoff M. 1984. pH-solubility profile of papaverine hydrochloride and its relationship to the dissolution rate of sustained release pellets. J Pharm Sci 73:1203-1208.

37. Ledwidge MT, Corrigan OI. 1998. Effects of surface active characteristics and solid state forms on the pH-solubility profiles of drug-salt systems. Int J Pharm 174:187-200.

38. Pudipeddi M, Serajuddin ATM. 2002. Salt-selection strategies. Handbook of Pharmaceutical Salts-Properties, Selection and Use, Wiley-VCH, Zurich : 19-41.

39. Sekiguchi K, Obi N. 1961. Studies on absorption of eutectic mixture. I. A comparison of the behavior of eutectic mixture of sulfathiazole and that of ordinary sulfathiazole in man. Chem Pharm Bull 9:866-872.

40. Sekiguchi K, Obi N, Ueda Y. 1964. Studies on absorption of eutectic mixture. II. Absorption of fused conglomerates of chloramphenicol and urea in rabbits. Chem Pharm Bull 12: 134-144.

41. Goldberg AH, Gibaldi M, Kanig JL. 1966. Increasing dissolution rates and gastrointestinal absorption of drugs via solid solutions and eutectic mixtures. I. Experimental evaluation of eutectic mixture: Urea-acetoaminophen system. J Pharm Sci 55:482-487.

42. Goldberg AH, Gibaldi M, Kanig JL. 1966. Increasing dissolution rates and gastrointestinal absorption of drugs via solid solutions and eutectic mixtures. II. Experimental evaluation of eutectic mixture: griseofulvin-succinic acid system. J Pharm Sci 55:487-492.

43. Chiou L, Riegelman S. 1971. Pharmaceutical applications of solid dispersion systems. J Pharm Sci 60:1281-1302.

44. Crowley MM, Zhang F, Repka MA, Thumma S, Upadhye SB, Battu SK, McGinity JW, Martin C. 2007. Pharmaceutical applications of hot melt extrusion: Part I. Drug Dev Ind Pharm 33:909-926.

45. Prodduturi S, Urman KL, Otaigbe JU. 2007. Stabilization of hot-melt extrusion formulations containing solid solutions using polymer blends. AAPS Pharm Sci Tech 8(2):Article 50.

46. Liu J, Zhang F, McGinity JW. 2001. Properties of lipophilic matrix tablets containing phenylpropanolamine hydrochloride prepared by hot-melt extrusion. Eur J Pharm Biopharm 52(2):181-90.

47. Ndindayino F, Vervaet C, Van den Mooter G. 2002. Direct compression and moulding properties of co-extruded isomalt/drug mixtures. Int J Pharm 235:159-68.

48. Bialleck S, Rein H. 2011. Preparation of starch-based pellets by hot-melt extrusion. Eur J Pharm Biopharm 79:440-8.

49. Repka MA, Gerding TG, Repka SL. 1999. Influence of plasticizers and drugs on the physical-mechanical properties of hydroxypropylcellulose films prepared by hot melt extrusion. Drug Dev Ind Pharm 25:625-33.

50. De Brabander C, Vervaet C, Fiermans L. 2000. Matrix mini-tablets based on starch/microcrystalline wax mixtures. Int J Pharm 199:195-203.

51. Schilling SU, Bruce CD, Shah NH. 2008. Citric acid monohydrate as a release-modifying agent in melt extruded matrix tablets. Int J Pharm 361:158-68.

52. Thumma S, Majumdar S, ElSohly MA. 2008. Chemical stability and bioadhesive properties of an ester prodrug of Delta 9-tetrahydrocannabinol in poly(ethylene oxide) matrices: effect of formulation additives. Int J Pharm 362:126-32.

53. Ghebremeskel AN, Vemavarapu C, Lodaya M. 2006. Use of surfactants as plasticizers in preparing solid dispersions of poorly soluble API: stability testing of selected solid dispersions. Pharm Res 23:1928-36.

54. Wu C, McGinity JW. 2003. Influence of methylparaben as a solid-state plasticizer on the physicochemical properties of Eudragit RS PO hot-melt extrudates. Eur J Pharm Biopharm 56:95-100.

55. Repka MA, Shah S, Lu J, Maddineni S, Morott J, Patwardhan K, Mohammed NN. 2012. Melt extrusion: process to product. Expert Opin Drug Deliv 9:105-125.

56. Vasanthavada M, Wang Y, Haefele T, Lakshman JP, Mone M, Tong W, Joshi YM, Serajuddin AT. 2011. Application of melt granulation technology using twin-screw extruder in development of high-dose modified-release tablet formulation. J Pharm Sci 100:1923-1934.

57. Stanley TH, Egan TD, Van Alken H. 2008. A tribute to Dr. Paul A.J. Janssen: Entrepreneur Extraordinaire, Innovative Scientist, and Significant Contributor to Anethesiology. Anesthetic Pharmacol 106:451-462.

58. Masso JFM, Obeso JA, Carrera N, Martinez-Lage JM. 1987. Aggravation of Parkinson's disease by cinnarizine. J Neurol Neurosurg Psychiatry 50:804-805.

59. Okoro EO, Marwood JF. 1997. Effects of 5HT2 receptor antagonists on responses to potassium depolarization in rat solated aorta. Clin Exp Pharmacol Physiol 24:34-39.

60. Godfraind T. 1987. Classification of calcium antagonists. Am J Cardiol 59:11B-23B.

61. Tokumura T, Tsushima Y, Tatsuishi K. 1987. Enhancement of the oral bioavailability of cinnarizine in oleic acid in beagle dogs. J Pharm Sci 76:286-288.

62. Basu B, Bagdiya A, Makwana S, Vipul V, Batt D, Dharamsi A. 2011. Formulation and evaluation of fast dissolving tablets of cinnarizine using superdisintegrant blends and subliming material. J Adv Pharm Technol Res 2:266-273.

63. Vithlani S, Sarraf S, Chaw CS. 2011. Formulation and in vitro evaluation of self-emulsifying formulations of cinnarizine. Drug Dev Ind Pharm 12:1-7.

64. Alhnan MA, Murdan S, Basit AW. 2011. Encapsulation of poorly soluble basic drugs into enteric microparticles : a novel approach to enhance their oral bioavailability. Int J Pharm 416:55-60.

65. Gines JM, Veiga MD, Arias MJ, Rabasco AM. 1995. Elaboration and thermal study of interactions between cinnarizine and gelucire®53/10 physical mixtures and solid dispersions. Int J Pharm 126:287-291.

66. Dressman JB, Thelen K, Willmann S. 2011. An update on computational oral absorption simulation. Expert Opin Drug Metab Toxicol 7:1345-1364.

67. Kesisoglou F, Wu Y. 2008.Understanding the effect of API properties on bioavailability through absorption modeling. The AAPS J 10(4):516-525.

68. Teorell T. Kinetics of distribution of substances administered to the body. 1937.Arch Int Pharmacodyn Ther 57:205-40.

69. Kramer J, Grady LT, Gajendran J. 2005. Pharmaceutical dissolution testing. USA:

70. Gibaldi M, Perrier D. Pharmacokinetics. New York: 1975.

71. Dressman JB, Amidon GL, Fleisher D. 1985. Absorption potential: estimating the fraction absorbed for orally administered compounds. J Pharm Sci 74:588-9.

72. Dressman JB, Fleisher D. 1986. Mixing-tank model for predicting dissolution rate control of oral absorption. J Pharm Sci 75:109-16.

73. Wagner JG, Nelson E. 1964. Kinetic analysis of blood levels and urinary excretion in the absorptive phase after single doses of drug. J Pharm Sci 53:1392-403.

74. Loo JCK, Riegelman S. 1968. New method for calculating the intrinsic absorption rate of drugs. J Pharm Sci 57:918-28.

75. Wagner JG. 1975. Fundamentals of clinical pharmacokinetics. Hamilton, IL.

76. Dressman JB, Berardi RR, Elta TM, 1992. Absorption of flurbiprofen in the fed and fasted states. Pharm Res ;9:901-7.

77. Levy G. 1964.Effect of dosage form on drug absorption a frequent variable in clinical pharmacology. Arch Int Pharmacodyn Ther 152:59-68.

78. United States Pharmacopeial Convention. The United States Pharmacopeia (USP); 2010.

79. Mauger DT, Chinchilli VM. 1997. In vitro-in vivo relationships for oral extended-release products. J Biopharm Stat 7:565-78.

80. Yu LX, Amidon GL. 1999. A compartmental absorption and transit model for estimating oral drug absorption. Int J Pharm 186:119-125.

81. Yu LX, Amidon GL. 1998. Saturable small intestinal drug absorption in humans: modeling and interpretation of cefatrizine data. Eur J Pharm Biopharm 45:199–203.

82. Yu LX. 1999. An integrated model for determining causes of poor oral drug absorption. Pharm Res. 16:1883–7.

83. Kortejarvi H, Urtti A, Yliperttula M. 2007. Pharmacokinetic simulation of biowaiver criteria: the effects of gastric emptying, dissolution, absorption and elimination rates. Eur J Pharm Sci 30:155–66.

84. Yu LX, Lipka E, Crison JR, Amidon GL. 1996. Transport approaches to the biopharmaceutical design of oral drug delivery systems : Prediction of intestinal absorption. Adv Drug Deliv Rev 19:359-376.

85. Agoram B, Woltosz WS, Bolger MB. 2001. Predicting the impact of physiological and biochemical processes on oral drug bioavailability. Adv Drug Deliv Rev 50 (suppl 1):S41-67.

86. Huang W, Lee SL, Yu LX. 2009. Mechanistic approaches to predicting oral drug absorption. The AAPS J 11:217-224.

87. Tubic-Grozdanis M, Bolger MB, Langguth P. 2008. Application of gastrointestinal simulation for extensions for biowaivers of highly permeable compounds. AAPS J 10:213–26.

88. Congressional Budget Office Study. October 2006. Research and development in pharmaceutical industry: 7-17.

89. The Long view-R&D productivity. September 30, 2010. Bernstein Research

90. Stahl PH. 2002. Appendix. Handbook of Pharmaceutical Salts-Properties, Selection and Use, Wiley-VCH, Zurich : 329-350.

91. Li S, Doyle P, Metz S, Royce AE, Serajuddin ATM.2005. Effect of chloride ion on dissolution of different salt forms of haloperidol, a model basic drug. J Pharm Sci 94:2224-2231.

92. Yoo SU, Krill SL, Wang Z, Telang C. 2009. Miscibility/stability considerations in binary solid dispersion systems composed of functional excipients towards the design of multi-component amorphous systems. J Pharm Sci 98:4711-4723.

93. Tran TTD, Tran PHL, Choi HG, Han HK, Lee BJ. 2010. The role of acidifiers in solid dispersions and physical mixtures. Int J Pharm 384:60-66.

94. Morrison PJ, Bradbrook ID, Rodgers HJ. 1979. Plasma cinnarizine levels resulting from oral administration as capsule or tablet formulation investigated by gas-liquid chromatography. Br J Clin Pharmac 7:349-352.

95. Li BQ, Yang GQ, Fang SH, Gao JY, Gu FM, Dong X, Zhang JX, Wang Y. 2010. Effect of route of administration on the pharmacokinetics and toxicokinetics of cinnarizine in dogs. Eur J Pharm Sci 40:197-201.

96. Tarsa PB, Towler CS, Woollam G, Berghausen J. 2010. The influence of aqueous content in small scale screening – Improving hit rate for the weakly basic, low solubility drugs. Eur J Pharm Sci 41:23-30.

97. Reilly J, Wright P, Larrow J, Mann T, Twomey J, Grondine M, Dodd S, Daniel CC, Bilotta J, Shah L, Towler C. 2012. Counterion quantification for discovery chemistry and pre-formulation salt screening. J Liq Chromatogr Relat Technol 35: 1001-1010.

98. Li S, Wong S, Sethia S, Almoazen H, Joshi YM, Serajuddin AT.2005. Investigation of solubility and dissolution of a free base and two different salt forms as a function of pH. Pharm Res 22:628-635.

99. Zannou E, Ji Q, Joshi YM, Serajuddin AT.2007. Stabilization of the maleate salt of a basic drug by adjustment of microenvironmental pH in solid dosage form. Int J Pharm 337:210-218.

100. Tatavarti AS, Hoag SW. 2006.Microenvironmental pH modulation based release enhancement of a weakly basic drug from hydrophilic matrices. J Pharm Sci 95:1459-1468.

101. Doherty C, York P. 1989. Microenvironmental pH control of drug dissolution. Int J Pharm 50: 223-232.

102. Gabr K. 1992. Effect of organic acids on the release patterns of weakly basic drugs from inert sustained release matrix tablets. Eur J Pharm Biopharm 38:199-202.

103. Hancock BC, Zografi G. 1997. Charateristics and significance of amorphous state in pharmaceutical system. J Pharm Sci 86: 1-12.

104. Pudipeddi M, Zannou EA, Vasanthavada M, Dontabhaktuni A, Royce AE, Joshi YM, Serajuddin ATM. 2007. Measurement of surface pH of pharmaceutical solids: A critical evaluation of indicator dye-sorption method and its comparison with slurry pH method. J Pharm Sci 97:1831-1842.

105. Siepe S, Lueckel B, Kramer A, Ries A, Gurny R. 2006. Strategies for the design of hydrophilic matrix tablets with controlled microenvironmental pH. Int J Pharm 316:14-20.

106. Pignatello R, Spadaro D, Vandelli MA, Forni F, Puglisi G. 2004. Characterization of the mechanism of interaction in Ibuprofen-EudragitRL100® coevaporates. Drug Dev Ind Pharm 30:277-288.

107. Fini A, Cavallari C, Ospitali F. 2008. Raman and thermal analysis of indomethacin/PVP solid dispersion enteric microparticles. Eur J Pharm Biopharm 70 (1): 409-420.

108. Strachan CJ, Rades T, Gordon KC, Rantanen J. 2007. Raman Spectroscopy for quantitative analysis of pharmaceutical solids. J Pharm Pharmacol 59:179–192.

109. Taylor LS, Langkilde FW, Zografi G. 2001. Fourier transformation raman spectroscopy study for the interaction of water vapour with amorphous polymers. J Pharm Sci 90:888-901.

110. Pignatello R, Spadaro D, Vandelli MA, Forni F, Puglisi G. 2004. Characterization of the mechanism of interaction in Ibuprofen-EudragitRL100® coevaporates. Drug Dev Ind Pharm 30:277-288.

111. Fini A, Cavallari C, Ospitali F. 2008. Raman and thermal analysis of indomethacin/PVP solid dispersion enteric microparticles. Eur J Pharm Biopharm 70 (1): 409-420.

112. Strachan CJ, Rades T, Gordon KC, Rantanen J. 2007. Raman Spectroscopy for quantitative analysis of pharmaceutical solids. J Pharm Pharmacol 59:179–192.

113 . Breitenbach J, Schrof W, Neumann J. 1999. Confocal Raman-spectroscopy: analytical approach to solid dispersions and mapping of drugs. Pharm Res 16: 1109-1113.

114. Kindermann C, Matthée K, Strohmeyer J, Sievert F, Breitkr J. 2011. Tailor-made release triggering from hot-melt extruded complexes of basic polyelectrolyte and poorly water-soluble drugs. Eur J Pharm Biopharm 79 (2): 372-381.

115. Martinez MN, Amidon GL. 2002. A mechanistic approach to understanding the factors affecting drug absorption: A review of fundamentals. J Clin Pharmacol 42:620-643.

116. Gu CH, Rao D, Gandhi RB, Hilden J, Raghavan K. 2005. Using a novel multicomponent dissolution system to predict the effect of gastric pH on oral absorption of weak bases with poor intrinsic solubility. J Pharm Sci 94:199-208.

117. Ogata H, Aoyagi N, Kaniwa N, Ejima A, Sekine N, Kitamura M, Inoue Y. 1986. Gastric acidity dependent bioavailability of cinnarizine from two commercial capsules in healthy volunteers. Int J Pharm 29:113-120.

118. Hundt HKL, Brown LW, Clark EC. 1980. Determination of cinnarizine in plasma by high-performance liquid chromatography. J Chromatogr 183:378-382.

119. Kalava BS, Demirel MY, Yazan Y. 2005. Physicochemical characetrization and dissolution properties of cinnarizine solid dispersions. Turkish J Pharm Sci 2:51-62.

120. Serajuddin ATM, Jarowski CI. 1985. Effect of diffusion layer pH and solubility on the dissolution rate of pharmaceutical bases and their hydrochloride salts. Part 1. Phenazopyridine. J Pharm Sci 74:142-147.

121. Dressman JB, Amidon GL, Reppas C, Shah VP. 1998. Dissolution testing as a prognostic tool for oral drug absorption: Immediate release dosage forms. Pharm Res 15:11-22.

122. Kuentz M, Nick S, Parrott N. 2006. A strategy for preclinical formulation development using Gastroplus as pharmacokinetic simulation tool and a statistical screening design applied to a dog study. Eur J Pharm Sci 27:91-99.

123. Parrott N, Lave T. 2002. Prediction of intestinal absorption: comparative assessment of Gastroplus and Idea. Eur J Pharm Sci 17:51-61.

124. Okumu A, DiMaso M, Lobenburg R. 2008. Computer simulations using Gastroplus™ to justify a biowaiver for etoricoxib solid oral drug products. Eur J Pharm Biopharm 72:91-98.

125. Katneni K, Charman SA, Porter CJH. 2006. Permeability assessment of poorly water-soluble compounds under solubilizing condiitons: The reciprocal permeability approach. J Pharm Sci 95(10): 2170-2185.

126. Dressman J, Leuner C. 2000. Improving drug solubility for oral delivery using solid dispersions. Eur J Pharm Biopharm 50: 47-60.

127. Guo F, Zhong H, He J, Xie B, Liu F, Xu H, Liu M, Xu C. 2011. Self-microemulsifying drug delivery system for improved oral bioavailability of dipyridamole: preparation and evaluation. Arch Pharm Res 34(7): 1113-1123.

128. Tran TTD, Tran PHL, Lee BJ. 2009. Dissolution-modulating mechanism of alkalizers and polymers in a nanoemulsifying solid dispersion containing ionizable and poorly water-soluble drug. Eur J Pharm and Biopharm 72: 83-90.

129. Bassi P, Kaur G. 2010. pH modulation: mechanism to obtain pH-independent drug release. Expert Opin Drug Deliv 7(7): 845-857.

130. Doherty C, York P. 1989. In vitro pH dissolution dependence and in vivo bioavailability of frusemide-PVP solid dispersions. J Pharm Pharmacol 41: 73-78.

131. Badaway SIF, Gray D, Zhao F, Sun D, Schuster A, Hussain MA. 2006. Formulation of solid dosage forms to overcome gastric pH interaction of factor Xa inhibitor, BMS-561389. Pharm Res 23:989-996.

132. Brientenbach J. 2002. Melt extrusion: from process to drug delivery technology. Eur J Pharm Biopharm 54: 107-117.

133. Lakshman JP, Cao Y, Kowalski J, Serajuddin ATM. 2008. Application of melt extrusion in the development of a physically and chemically stable high-energy amorphous solid dispersion of a poorly water-soluble drug. Mol Pharm 5(6): 994-1002.

134. Repka MA, Battu SK, Upadhye SB, Thumma S, Crowley MM, Zhang F et al. 2007. Pharmaceutical applications of hot-melt extrusion: Part II. Drug Dev Ind Pharm 33: 1043-1057.

135. Forster A, Hempenstall J, Rades T. 2001. Characterization of glass solutions of poorly water-soluble drugs produced by melt extrusion with hydrophilic amorphous polymers. J Pharm Pharmacol 53: 303-315.

136. Forster A, Hempenstall J, Rades T. 2001. Selection of excipients for melt extrusion for two poorly water-soluble drugs by solubility parameter calculation and thermal analysis. Int J Pharm 226: 147-161.

137. Rambali B, verreck G, Baert L, Massart DL. 2003. Itraconazole formulation studies of the melt extrusion process with mixture design. Drug Dev Ind Pharm 29: 641-652.

138. Six K, Daems T, de Hoon J, Van Hecken A, Depre M, Bouche MP et al. 2005. Clinical study of solid dispersions of itraconazole prepared by hot-stage extrusion. Eur J Pharm Sci 24: 179-186.

139. Wang L, Cui FD, Hayase T, Sunada H. 2005. Preparation and evaluation of solid dispersion for nitrendipine-carbopol and nitrendipine-HPMCP systems using a twin screw extruder. Chem Pharm Bull 53: 1240-1245.

140. Serajuddin ATM and Jarowski CI. 1985. Effect of diffusion layer pH and solubility on the dissolution rate of pharmaceutical acids and sodium salts II: salicyclic acid, theophylline and benzoic acid. J Pharm Sci 74: 148-154.

141. Feldstein MM, Shandryuk GA, Plate NA. 2001. Relation of glass transition temperature to the hydrogen-bonding degree and energy in poly(N-vinyl pyrrolidone) blends with hydroxyl-containing plasticizers. Part 1. Effects of hydroxyl group number in plasticizer molecule. Polymer 42: 971-979.

142. Shah VP, Konecny JJ, Everett RL, McCullough B, Noorizadeh AC, Skelley JP. 1989. In vitro dissolution profile of water-insoluble drug dosage forms in presence of surfactants. Pharm Res 6: 612-618.

143. Aburub A, Risley DS, Mishra D. 2007. A critical evaluation of fasted state simulating gastric fluid (FaSSGF) that contains sodium lauryl sulfate and proposal of a modified recipe. Int J Pharm 347: 16-22.

144. Curatolo W, Nightangle JA, Herbig SM. 2009. Utility of hydroxypropylmethylcellulose acetate succinate (HPMCAS) for initiation and maintenance of drug supersaturation in the GI Milieu. Pharm Res 26(6): 1419-1431.

145. Mooney KG, Mintun MA, Himmelstein KJ, Stella VJ. 1981. Dissolution kinetics of carboxylic acids. Part I. Effect of pH under unbuffered conditions. Part 2. Effect of buffers. J Pharm Sci 70: 13-22.

146. Serajuddin ATM and Jarowski CI. 1985. Effect of diffusion layer pH and solubility on the dissolution rate of pharmaceutical bases and their hydrochloride salts. Part 1.Phenazopyridine. J Pharm Sci 74: 148-154.

147. Streubel A, Siepmann J, Dashevsky A, Bodmeier R. 2000. pH-independent release of weakly basic drug from water-insoluble and –soluble matrix tablets. J Control Release 67: 101-110.

148. Nguyen DA and Fogler HS. 2005. Facilitate diffusion in the dissolution of carboxylic acid polymers. 51: 415-425.

CURRICULUM VITA

ANASUYA A. GHOSH

EDUCATION

October 2012	Ph.D., Pharmaceutical Science, Rutgers, The State University of New Jersey
May 2001	M.S., Pharmacology and Toxicology, The University of Rhode Island
May 1998	B.S., Pharmacy, The University of Mumbai, India

PROFESSIONAL EXPERIENCE

Sep.2001~present	Senior Scientist, Pharmaceutical Development, Novartis Pharmaceuticals Corporation, NJ, USA
Sep.1999~Aug.2001	Teaching Assistant, Department of Biomedical Sciences, The University of Rhode Island, RI, USA
Sep.1998~Jun.1999	Research Associate, Novartis Enterprises Pvt. Ltd., Mumbai, India

PUBLICATIONS

1. **Ghosh A**, Vasanthavada M, Minko T. Effect of increasing solubility, acidity and molecular weight of pH modifiers in solid dispersions prepared using melt extrusion. *Drug Development and Industrial Pharmacy*. Manuscript prepared for submission.

2. **Ghosh A**, Minko T. Gastroplus™ predictions of *in vivo* pharmacokinetic performance of cinnarizine from *in vitro* dissolution studies for designed solid dispersions and its marketed product. Manuscript prepared for submission.

3. **Ghosh A**, Vasanthavada M, Minko T. A comparative evaluation of dissolution enhancement of a weakly basic drug from its salt solid dispersion and amorphous dispersions containing acidic counterions. *Journal of Pharmaceutical Sciences*. Submitted.

4. King RS, **Ghosh AA**, Wu J. Inhibition of SULT1A1 by meclofenamic acid, nimesulide, and aspirin. *Current Drug Metabolism* 7(7): 745-753, Oct. (2006).

5. Li P, **Ghosh A**, Wagner RF, Krill S, Joshi YM, Serajuddin AT. Effect of combined use of non-ionic surfactants on formation of oil-in-water microemulsions. *International Journal of Pharmaceutics* 288: 27-34 (2005).

PATENTS

1. Patent published WO 2005/004900. Orally dosed pharmaceutical compositions comprising a delivery agent in micronized form.

2. Patent published WO 2012/048235. Vitamin E formulations of Sulfamide NS3 inhibitors.

3. Patent published WO 20080234179. Orally dosed pharmaceutical compositions comprising a delivery agent in micronized form.

4. Patent filed 50446. Pharmaceutical compositions manufactured with external spray lubrication. September 2006.